University of Tennessee, Knoxville

TRACE: Tennessee Research and Creative Exchange

Doctoral Dissertations

Graduate School

8-2004

Investigation of Fiber Splitting in Side-by-side Bicomponent Meltblown Nonwoven Webs through Post Treatment

Yanbo Liu
University of Tennessee, Knoxville

Follow this and additional works at: https://trace.tennessee.edu/utk_graddiss

Part of the Other Materials Science and Engineering Commons

Recommended Citation

Liu, Yanbo, "Investigation of Fiber Splitting in Side-by-side Bicomponent Meltblown Nonwoven Webs through Post Treatment. " PhD diss., University of Tennessee, 2004.
https://trace.tennessee.edu/utk_graddiss/4560

This Dissertation is brought to you for free and open access by the Graduate School at TRACE: Tennessee Research and Creative Exchange. It has been accepted for inclusion in Doctoral Dissertations by an authorized administrator of TRACE: Tennessee Research and Creative Exchange. For more information, please contact trace@utk.edu.

To the Graduate Council:

I am submitting herewith a dissertation written by Yanbo Liu entitled "Investigation of Fiber Splitting in Side-by-side Bicomponent Meltblown Nonwoven Webs through Post Treatment." I have examined the final electronic copy of this dissertation for form and content and recommend that it be accepted in partial fulfillment of the requirements for the degree of Doctor of Philosophy, with a major in Materials Science and Engineering.

Dong Zhang, Major Professor

We have read this dissertation and recommend its acceptance:

Christine (Qin) Sun, Larry C. Wadsworth, Randall R. Bresee, Gajanan S. Bhat, Kevin M. Kit

Accepted for the Council:

Carolyn R. Hodges

Vice Provost and Dean of the Graduate School

(Original signatures are on file with official student records.)

To the Graduate Council:

I am submitting herewith a dissertation written by Yanbo Liu entitled "Investigation of Fiber Splitting in Side-by-side Bicomponent Meltblown Nonwoven Webs through Post Treatment". I have examined the final paper copy of this dissertation for form and content and recommend that it be accepted in partial fulfillment of the requirements for the degree of Doctor of Philosophy, with a major in Materials Science and Engineering.

Dong Zhang
Major Professor

We have read this dissertation
and recommend its acceptance:

Christine(Qin) Sun

Larry C. Wadsworth

Randall R. Bresee

Gajanan S. Bhat

Kevin M. Kit

Accepted for the Council:

Vice Chancellor and
Dean of Graduate Studies

INVESTIGATION OF FIBER SPLITTING IN SIDE-BY-SIDE BICOMPONENT MELTBLOWN NONWOVEN WEBS THROUGH POST TREATMENT

A Dissertation

Presented for the

Doctor of Philosophy

Degree

The University of Tennessee, Knoxville

Yanbo Liu

August 2004

ACKNOWLEDGEMENTS

I would like to sincerely thank my advisors Dr. Dong Zhang and Dr. Christine(Qin) Sun for their precious guidance and good suggestions about my research work and dissertation. I am grateful for my committee members for their kind help and suggestions about my dissertation, including Dr. Larry C. Wadsworth, Dr. Gajanan S. Bhat, Dr. Randall R. Bresee and Dr. Kevin M. Kit.

I am thankful for all the people in TANDEC (Textiles and Nonwovens Development Center), for their kind help in both my study and my personal life here, especially Mr. Van Brantley, who always helped me when I need help in my test work.

Great thanks would be given to my friends for their kind help and care. I especially thank my family members for their great support and encouragements to me; their good understanding, selfless assistance and true care are the power source for me to study in UTK and eventually complete my Ph. D degree. Particular thanks are given to my sweet daughter, Peipei, for her healthily growing up in China in the absence of her mom.

At last, I am sincerely grateful for the financial support from Reifenhäuser GmbH & Co., Germany.

ABSTRACT

Finer fibers are increasingly desirable in the nonwoven industry in many applications due to increased specific surface area, increased surface adsorption ability, and improved filtration efficiency. Splitting bicomponent (Bico) fibers to produce finer fibrous nonwoven webs has become one of the hot topics in nonwoven industries.

Investigation of Bico fiber splitting mechanism and hence finding proper ways to achieve fiber splitting in S/S Bico MB nonwoven webs are the key issues in this research. Based on the fiber splitting mechanism, incompatible polymer pairs were chosen and appropriate post-treating methods as well as the post-treating agents were selected to facilitate fiber splitting in S/S Bico MB nonwoven webs.

Several post treatments were used to split side-by-side meltblown nonwoven fibers in this research, including hydroentanglement, heat-stretching, NaOH and benzoic acid treatment. In each post treatment method, fiber splitting was examined with SEM and/or laser-source microscope. Fiber diameter, web structure and web properties were examined before and after the fiber splitting inducing treatment.

Hydroentangling has been applied to S/S Bico MB nonwoven webs with Bico pairs of PA6/PE, PA6/PP and PA6/PET. Fiber diameter, web structure and web properties were examined based on the corresponding test standards. Fiber splitting phenomenon

and web morphology were observed with SEM, and web structure was evaluated using WebPro technology.

Heat-stretching post treatment was applied to S/S Bico MB nonwoven webs with Bico pairs of PA6/PE and PA6/PP. The fiber splitting phenomenon was observed using SEM; fiber diameter and web properties in MD and CD were examined, especially the change in flexural rigidity and elasticity of the heat-stretched webs.

The S/S Bico MB nonwoven webs of 25PE/75PET, and 50PBT/50PP were treated with sodium hydroxide at a bath ratio of 1/20 and temperature of 100 °C using different concentrations of NaOH at different treating times. The fiber splitting phenomenon was investigated using SEM in this research.

Benzoic acid (BA) has been employed to split S/S Bico MB webs composed of 50PET/50PA6 and 50PP/50PA6. The degree of fiber splitting was evaluated using both *fiber splitting ratio* and *initial dye adsorption ratio (initial dyeing ratio)* in this research. Web properties were examined to characterize the change after benzoic acid treatment. The fiber splitting mechanism during BA treatment was discussed as well, and it was concluded that the BA method could be an efficient way to split S/S Bico MB fibers, compared to the foresaid three methods.

TABLE OF CONTENTS

CHAPTER

1 INTRODUCTION 1

1.1 Research Background 1

1.1.1 Concept of Nonwovens 1

1.1.2 Meltblowing Technology 1

1.1.3 Bicomponent Meltblowing Technology 3

1.1.4 Fine Microfibers and Their Advantages 6

1.1.5 Production Methods of Fine Fibers 9

1.1.6 Difficulties and Possibilities in Splitting S/S Bico MB NW Webs 10

1.1.7 Market /Applications for MB Nonwovens Containing Finer Fibers 11

1.1.7.1 Market for Traditional MB Nonwoven Webs 11

1.1.7.2 Applications of MB Nonwovens Containing Finer Fibers 12

1.2 Mechanism of Bicomponent Fiber Splitting 14

1.2.1 Diffusion Theory 15

1.2.2 Weak Boundary Theory 23

1.3 Review of Fiber Splitting Techniques 25

1.3.1 Pre-requirements for Fiber Splitting in Multi/Bicomponent Fibers 25

1.3.1.1 Definition of Fiber Splitting 25

1.3.1.2 Splittable Nonwoven Bicomponent Filaments 26

1.3.1.3 Selection of Incompatible Polymers as Bico Pair 28

1.3.1.3.1 Desirable Polymer Pairs Suitable for Splittable Bico Filaments 29

1.3.1.3.2 Cross-sectional Shape of the Splittable Fibers 30

1.3.2 Fiber-splitting Inducing Pre-treatments 31

1.3.3 Fiber Splitting-inducing Post-treatments 32

1.3.3.1 Hydroentanglement Treatment 32

1.3.3.2 Heat Treatment 34

1.3.3.3 Chemical Post-treatment 35

1.3.3.4 Hot Aqueous Medium Treatment 36

1.4 Research Objective 37

1.5 Summary 39

2 PRELIMINARY STUDY ON FIBER SPLITTING IN S/S BICO MB NONWOVEN WEBS THROUGH HYDROENTANGLEMENT 41

2.1 Introduction 41

2.2 Experiments 43

2.3 Results and Analysis 45

2.3.1 Fiber Configuration, Web Structure and Appearance 45

2.3.2 Fiber Diameter, Basis Weight, Thickness and Flexural Rigidity 52

2.3.3 Web Uniformity 57

2.3.4 Air Permeability and Hydrostatic Head 58

2.3.5 Tensile Properties 58

2.4 Summary 62

3 PRELIMINARY STUDY ON FIBER SPLITTING IN S/S BICO MB NW WEBS THROUGH HEAT-STRETCHING TREATMENT 67

3.1 Introduction 67

3.2 Experiments 68

3.3 Results and analysis 71

3.3.1 Changes in Fiber Diameter after Heat Stretching Treatment 71

3.3.2 Changes in Web Thickness after Heat Stretching Treatment 77

3.3.3 Changes in Basis Weight after Heat Stretching Treatment 79

3.3.4 Changes in Air Permeability after Heat Stretching Treatment 81

3.3.5 Changes in Bending Stiffness after Heat Stretching Treatment 81

3.3.6 Changes in Peak Load after Heat Stretching Treatment 84

3.3.7 Changes in Breaking Elongation after Heat Stretching Treatment 86

3.3.8 Changes in Tenacity after Heat Stretching Treatment 90

3.3.9 Changes in Elasticity after Heat Stretching Treatment 90

3.3.10 Changes in Web Structure after Heat Stretching Treatment 97

3.4 Summary 97

4 PRELIMINARY STUDY OF FIBER SPLITTING IN S/S BICO MB NONWOVEN WEBS USING NaOH TREATMENT 101

4.1 Introduction 101

4.2 Fiber Splitting in 25PE/75PET S/S Bico MB Web 102

4.2.1 Experiments of NaOH Treatment 102

4.2.2 Results and Analysis 102

4.3 Fiber Splitting in 50PBT/50PP S/S Bico MB Web 104

4.3.1 Experiments and Results 104

4.3.2 Changes in Web Structure and Property after NaOH Treatment 109

4.4 Summary 114

5 FUNDAMENTAL STUDY OF FIBER SPLITTING IN S/S BICO MB NONWOVEN WEBS THROUGH BENZOIC ACID TREATMENT 116

5.1 Selection of S/S MB Samples and Post-treating Agent Suitable for Fiber Splitting 116

5.1.1 Selection of 50PA6/50PET Bico MB Webs for the Investigation of Fiber Splitting 117

5.1.2 Selection of Benzoic Acid as the Fiber-splitting Inducing Agent 117

5.2 Selection of Methods for Evaluating the Degree of Fiber Splitting 119

5.2.1 Fiber Splitting Ratio 119

5.2.2 Initial Dye Adsorption Ratio 121

5.3 Investigation of Fiber Splitting in 50PET/50PA6 S/S MB Web with Benzoic Acid Solution 125

5.3.1 Experimental Design 125

5.3.2 Experiments for Fiber Splitting 126

5.3.2.1 Fiber Splitting Ratio Based on the SEM Photos 127

5.3.2.2 Initial Dye Adsorption Ratio 128

5.3.3 Results and Analysis 129

5.3.3.1 Observation of Fiber Splitting with SEM/Microscopic Technique 129

5.3.3.1.1 Longitudinal View of Split Fibers in SEM Photo 129

5.3.3.1.2 Cross-sectional View of Split Fibers in SEM / Microscopic Photos131

5.3.3.2 Determination of Fiber Splitting Ratio and the Change in (Specific) Surface Area 134

5.3.3.3 Initial Dye Adsorption Ratio 138

5.3.3.4 Comparison of the two Evaluation Methods for the Degree of Fiber Splitting.... 140

5.3.3.5 Change in Structure and Property of 50PA6/50PET S/S MB NW Webs

after BA Treatment 141

5.4 Investigation of Fiber Splitting in 50PP/50PA6 S/S MB Web with Benzoic Acid Solution 144

5.4.1 Preliminary Experiments for Optimal Fiber Splitting Conditions 145

5.4.2 Experimental Results 147

5.4.2.1 SEM Photos Showing Fiber Splitting after Control Treatments 149

5.4.2.2 Initial Dye Adsorption Ratio 150

5.4.2.3 Fiber Diameter 154

5.4.2.4 Barrier Property 156

5.4.2.5 Web Structure 157

5.4.2.6 Mechanical Properties 158

5.4.2.7 The Role that Water Played in BA Treatment for Fiber Splitting 160

5.4.2.8 Changes in the Internal Structure after the Treatments 161

5.5 Summary 165

6 CONCLUSION 168

7 FUTURE WORK 173

LIST OF REFERENCES 176

LIST OF TABLES

Table 1.1 The conversions between denier and diameter 7

Table 1.2 Solubility parameter $(cal/cm^3)^{1/2}$ of some polymers and solvents 22

Table 2.1 Meltblown processing conditions and sample description 44

Table 2.2 Water jet settings for hydro-entanglement 45

Table 3.1 Production conditions of the samples used for heat stretching treatments 68

Table 3.2 Fiber diameter before and after HST treatment 73

Table 3.3 Significance tests results for change in fiber diameter after HST treatment.. 76

Table 4.1 Diameter change after NaOH treatment of 25PE/75PET MB web..... 103

Table 4.2 Results of NaOH treatment of 50PBT/50PP MB web at different time 105

Table 4.3 NaOH treating conditions for 50PBT/50PP MB sample 110

Table 4.4 Parameters and results of significant test for diameter change..... 112

Table 5.1 Experimental factors and levels..... 125

Table 5.2 Orthogonal experimental table of BA treatment 126

Table 5.3 Orthogonal analysis table of fiber splitting ratio 133

Table 5.4 Increasing ratio of initial dyeing ratio for 50PA6/50PET webs 139

Table 5.5 Increasing ratio of initial dyeing ratio for 50PA6/50PET webs 139

Table 5.6 Conditions for the preliminary experiments using benzoic treatment 145

Table 5.7 The experimental design table for 50PP/50PA6 sample 147

Table 5.8 The peak value of absorbance of dye solution..... 152

Table 5.9 Dye adsorption ratio/dyeing ratio (%) of 50/PP/50PA6 S/S MB webs..... 153

Table 5.10 Increasing ratio (%) of dye adsorption ratio 153

LIST OF FIGURES

Figure 1.1 Schematic of meltblowing process 3

Figure 1.2 Cross-sectional conformations of different types of bicomponent fibers..... 4

Figure 1.3 Synthetic microfibers versus natural fibers 8

Figure 1.4 The comparison of patents in nonwoven industry..... 12

Figure 1.5 Maturity positions of nonwoven technologies 13

Figure 1.6 Illustration of diffusion theory of polymer adhesion..... 16

Figure 1.7 Adhesive bond strength vs. Solubility Parameter..... 23

Figure 1.8 Illustration of weak boundary layer between polymers 24

Figure 2.1 Hydroentanglement process 41

Figure 2.2 Sample 6 (75PA6/25PP) before treatment..... 46

Figure 2.3 Sample 6 (75PA6/25PP) after treatment-1 46

Figure 2.4 Sample 6 (75PA6/25PP) after treatment-2 47

Figure 2.5 Sample 6 (75PA6/25PP) after treatment-3 47

Figure 2.6 Sample 4 (25PA6/75PP) before treatment..... 48

Figure 2.7 Sample 4 (25PA6/75PP) after treatment-1 48

Figure 2.8 Sample 4 (25PA6/75PP) after treatment-2 49

Figure 2.9 Sample 4 (25PA6/75PP) after treatment-3 49

Figure 2.10 Sample 7 (50PA6/50PET) before treatments..... 50

Figure 2.11 Sample 7 (50PA6/50PET) after treatment-1 50

Figure 2.12 Sample 7(50PA6/50PET) after treatment-2 51

Figure 2.13 Sample 7 (50PA6/50PET) after treatment-3 51

Figure 2.14 Change in fiber diameter after hydroentanglement 53

Figure 2.15 Change in web thickness after hydroentanglement..... 54

Figure 2.16 Change in basis weight after hydroentanglement..... 55

Figure 2.17 Change in flexural rigidity after hydroentanglement 56

Figure 2.18 Change in total web uniformity of sample 7 after treatment-1 58

Figure 2.19 Change in air permeability after hydroentanglement 59

Figure 2.20 Change in hydrohead after hydroentanglement..... 60

Figure 2.21 Change in peak load after hydroentanglement 61

Figure 2.22 Change in tenacity after hydroentanglement..... 63

Figure 2.23 Change in extension @ break after hydroentanglement..... 64

Figure 3.1 Schematic of heat-stretching apparatus..... 69

Figure 3.2 Change in fiber diameter after heat stretching treatment.....72

Figure 3.3 Change in thickness after heat stretching treatment..... 78

Figure 3.4 Change in basis weight after heat stretching treatment 80

Figure 3.5 Change in air permeability after heat stretching treatment. 82

Figure 3.6 Change in bending stiffness (MD) after heat stretching treatment..... 83

Figure 3.7 Change in bending stiffness (CD) after heat stretching treatment..... 85

Figure 3.8 Change in MD peak load after heat stretching treatment 87

Figure 3.9 Change in CD peak load after heat stretching treatment..... 88

Figure 3.10 Change in MD Elongation at break after heat stretching treatment 89

Figure 3.11 Change in CD elongation at break after heat stretching treatment 91

Figure 3.12 Change in MD tenacity after heat stretching treatment..... 92

Figure 3.13 Change in CD tenacity after heat stretching treatment..... 93

Figure 3.14 Illustration for elastic recovery test for HST treated sample..... 94

Figure 3.15 Elastic Recovery (%) from the strain of 50% elongation at break..... 96

Figure 3.16 Fibers are randomly distributed in the web of sample 3 (75PP/25PA) before heat stretching treatment 98

Figure 3.17 Fibers aligned along machine direction in the web of sample 3 (75PP/25PA) 98

Figure 3.18 SEM photo of sample 1 (75PE/25PA) before heat stretching treatment 99

Figure 3.19 SEM photo of sample 1 (75PE/25PA) after heat stretching treatment 99

Figure 4.1 50PBT/50PP MB web after treating with 16.7% NaOH for 3 min 107

Figure 4.2 50PBT/50PP MB web after treating with 16.7% NaOH for 15 min 107

Figure 4.3 50PBT/50PP MB web after treating with 16.7% NaOH for 30 min 108

Figure 4.4 50PBT/50PP MB web after treating with 16.7% NaOH for 45 min 108

Figure 4.5 Changes in web stiffness, peak load, tenacity, thickness and fiber diameter among the original, control and treated samples 111

Figure 4.6 Changes in web elongation @ peak, hydrohead, air perm and basis weight among the original, control and treated samples 111

Figure 5.1 Illustration of Bico fiber splitting 120

Figure 5.2 Before treatment 129

Figure 5.3 After Experiment 9 130

Figure 5.4 SEM photo of the fiber cross-sections of benzoic acid treated web (50PET/50PA6) 132

Figure 5.5 Microscopic picture of the same sample in Figure 5.4 132

Figure 5.6 Splitting ratio vs. experiment No. 135

Figure 5.7 Visual analysis diagram of orthogonal experiment data 136

Figure 5.8 Initial dyeing ratios at different time (40°C) 139

Figure 5.9 Changes in fiber diameter, web thickness, tenacity, peak load and flexural rigidity 142

Figure 5.10 Change in shrinkage, basis weight, air perm, hydro head and breaking elongation 142

Figure 5.11 Fiber splitting in the preliminary Experiments 1 and 10. 146

Figure 5.12 SEM photos of the control samples 148

Figure 5.13 Typical curve of the Absorbance vs. wave length 151

Figure 5.14 The results of peak load, bending stiffness, thickness, shrinkage ratio and fiber diameter before and after different treatments. 155

Figure 5.15 The results of breaking tenacity, breaking elongation, air permeability, hydrohead and basis weight, before and after different treatments 155

Figure 5.16 DSC curves of the original, Experiment-1 and Control samples. 162

Figure 5.17 (left) γ form of PA6; (right) α form of PA6 163

Figure 7.1 Machine modification at TANDEC, UTK in the future 173

LIST OF SYMBOLS AND/OR ABRREVIATIONS

NOMENCLATURE

˚C — Celsius degree

cal — calorie

cm — centimeter

den — denier

˚F—Fahrenheit degree

g — gram

h — hour

J — Joule

kg — kilogram

L — liter

M — meter

mg — milligram

min — minute

ml — milliliter

mm — millimeter

in — inch

µm — micrometer

ABREVIATION

Air perm—Air permeability

BA—Benzoic acid

Bico—Bicomponent

CD—Cross machine direction

DCD—Distance between collector and die

HE—Hydroentanglement, hydroentangling, hydroentangled

HST—Heat-stretch, heat-stretching, heat-stretched

Hydrohead—Hydrostatic head

MB—Meltblowing, meltblown, meltblow

MD—Machine direction

MSE—Materials Science and Engineering

NW—Nonwoven

SB—Spunbonding, spunbonded, spunbond

SEM—Scanning Electron Microscopy

S/S—Side-by-side

TANDEC—Textile and Nonwovens Development Center

Temp—Temperature

UTK—the University of Tennessee at Knoxville

1 INTRODUCTION

1.1 Research Background

1.1.1 Concept of Nonwovens

Since the concept of *nonwovens* came to the textile world in 1942, the nonwoven industry has advanced continuously and rapidly. According to the definition of nonwoven from EDANA (European Disposables and Nonwovens Association) [1], "*Nonwoven* is a manufactured sheet, web or batt of directionally or randomly oriented fibers, bonded by friction, and/or cohesion and/or adhesion, excluding paper or products which are woven, knitted, tufted stitchbonded incorporating binding yarns or filaments, or felted by wetmilling, whether or not additionally needled. The fibers may be of natural or man-made origin. They may be staple or continuous or be formed in situ". A great deal of research work [2-35] has been conducted since the nonwoven production lines were set up at TANDEC several years ago.

1.1.2 Meltblowing Technology

As one of the nonwoven technologies, meltblowing technology came into the nonwoven world several years later after nonwoven technologies occurred in the textile industry. The concept of meltblowing technology was first introduced to the nonwoven world in 1954 through a Naval Research Laboratory project initiated by Wente [36, 37].

Since then, the meltblowing process and a variety of meltblown products have been developed, commercialized and put into use.

A recent market study has shown more than 60 meltblowing lines in production nationwide by 2000 [36, 37], including Kimberly-Clark and 3M Co.; also, using polyolefins, polyamides and polyesters has become common in the industry.

Meltblowing is one of the most popular processes to make super fine fibers on the micron level. The meltblowing process converts thermoplastic resins to nonwoven fabrics in only one integrated process. A typical meltblowing process consists of the following elements: extruder, metering pumps, die assembly, web formation, and winding. The main parameters influencing a meltblowing process include polymer throughput, polymer temperature, air throughput, air temperature, and the distance between collector and die (DCD) etc.

Meltbown fibers are produced by extruding molten thermoplastic resins/polymers through the die holes in a spinneret; while high velocity hot air attenuates the molten filaments into microfibers. Thereafter, the high velocity hot air carries the meltblown fibers and then deposits them on a collector to form a web. Meltblown fibers are generally smaller than 10 microns in diameter, usually from 1 to 5 μm, and are generally self-bonding when deposited onto a collector. The schematic of a typical meltblowing process is shown in Figure 1.1.

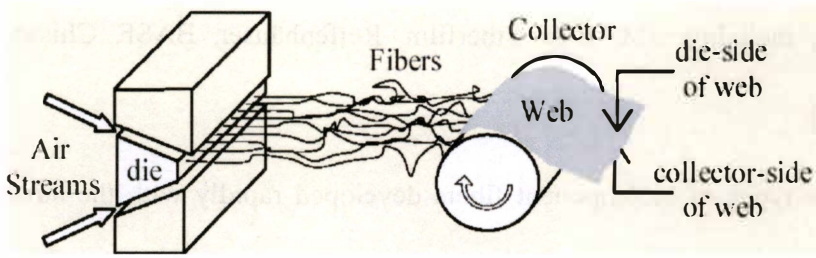

Figure 1.1 Schematic of meltblowing process

(Courtesy of Dr. Bresee, from Reference [31])

The number of fibers per unit weight is greatly increased in a meltblown nonwoven web composed of microfibers. Further, the amount of fiber surface exposed is also substantially greater than that exposed in conventional webs. These characteristics can have a significant impact in a variety of product applications.

1.1.3 Bicomponent Meltblowing Technology

Bicomponent fibers are typically formed by simultaneously and continuously extruding two polymer components from two separate extruders through the same spinning orifices of a spinneret to form unitary filament strands. Instead of being homogeneously blended, the two components have a distinct interface along the fiber axis, and the two parts may have different configurations or patterns [38].

There are many manufacturers in the world that produce a variety of bicomponent fibers nowadays. After the original endeavors by Buntin to obtain Bico MB web in the early 1970's, many companies were active in developing Bico MB

technologies, including 3M, Biax Fiberfilm, Reifenhäuser, BASF, Chisso, Hills, and Nordson [39].

New types of bicomponent fibers developed rapidly with the advancement of modern science and technology. The following categories of bicomponent fibers are commercially available now [40-47].

(1). Side-by-side

(2). Sheath/core, including concentric and eccentric types

(3). Islands-in-the-sea

(4). Citrus, wedge, or segmented pie

(5). Hollow or non-hollow

(6). Regularly round cross-section

(7). Irregularly non-round cross-section, including flat ribbon, multilobal, triangle, paralleled strip, and so forth.

Some typical types of bicomponent fibers are shown in Figure 1.2.

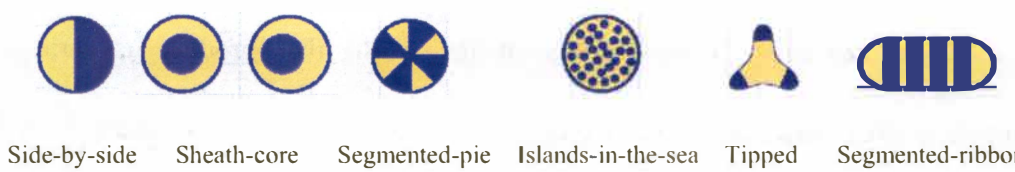

Figure 1.2 Cross-sectional conformations of different types of bicomponent fibers

Each kind of bicomponent fiber has special features and applications. Side-by-side fiber is mainly used to produce a self-crimping effect based on the different physical or chemical properties of the two components in the same fiber. Side-by-side bicomponent fibers are produced, as the name implies, by simultaneously spinning two fiber components together so that they are joined longitudinally. The two components may differ in chemical composition or differ in some properties such as molecular weight or degree of crystallization, which provides differential expansion or shrinkage. Bicomponent fibers may combine advantages of the two components, such as, strength, hydrophilicity, or low cost.

Bicomponent fibers can be used to produce finer microfibers through fiber splitting techniques or one component dissolving techniques.

Meltblown nonwoven webs containing side-by-side bicomponent fibers may impart bulk, resiliency, and soft hand due to the helical crimping of the bicomponent fibers. However, they may not have the strength of nonwoven fabrics composed of sheath/core bicomponent fibers. Bouchillon [48] points out that with these side-by-side fibers, "the bulk, resiliency, and stretch/recovery properties are desirable for many nonwoven applications, including: shoe components, apparel, toys, sleeping bags, pillows, furniture, and automotive." Additives can also be used to impart various properties to fabrics made from side-by-side fibers.

The Bico MB line from Reifenhäuser, Germany, was set up in TANDEC (Textile and Nonwoven Development Center), UTK (The University of Tennessee at Knoxville) in 1999. Since then, a great deal of research work has been done on the investigation of S/S Bico MB nonwoven webs and their fibers, most of which was focused on the characterization of Bico MB webs, product development and optimization of the processing conditions of the new Reicofil® Bico MB line by Zhang, Sun et al [10-22, 49]. A process model has been accomplished using the SRM (Surface Response Methodology) theory in 2001 by Zhang and Sun et al [19].

1.1.4 Fine Microfibers and Their Advantages

Due to the fact that the fiber cross section is not perfectly round, the diameter cannot always correctly reflect fiber fineness/thickness. The most accepted definition for microfibers seems to be a fiber with less than one denier [50-52]. One denier is the weight in gram of a fiber/yarn with 9000 meter length. The conversion between fiber diameter and denier depends on the density of the fiber, based on Equation 1.1:

$$Denier(linear\ density) = \frac{9 \times 10^{-3} \pi}{4} \rho D^2 \quad \text{..... Equation 1.1}$$

where ρ is the fiber density (g/cm^3), and D is the diameter of the fiber in micron (μm).

The most frequently used conversions between denier and diameter are listed in Table 1.1, based on the density of the fiber.

Table 1.1 The conversions between denier and diameter

LDPE		HDPE		PP		PA6		PET	
Density 0.92 g/cm^3 [53]		Density 0.95 g/cm^3 [53]		Density 0.91 g/cm^3 [53]		Density 1.14 g/cm^3 [53]		Density 1.39 g/cm^3 [53]	
Denier (den)	Diameter (μm)	Denier (den)	Diameter (μm)	Denier (den)	Diameter (μm)	Denier (den)	Diameter (μm)	Denier (den)	Diameter (μm)
0.001	0.39	**0.001**	0.39	**0.001**	0.39	**0.001**	0.35	**0.001**	0.32
1	12.40	**1**	12.21	**1**	12.47	**1**	11.14	**1**	10.09
10	39.22	**10**	38.60	**10**	39.44	**10**	35.24	**10**	31.91
0.006	**1**	0.007	**1**	0.006	**1**	0.008	**1**	0.010	**1**
0.16	**5**	0.17	**5**	0.16	**5**	0.20	**5**	0.25	**5**
2.6	**20**	0.001	**20**	2.6	**20**	3.2	**20**	3.9	**20**

Fineness of microfibers is compared with that of natural fibers in Figure 1.3. Fineness of the split polyester microfiber is only about 1/100th of a typical human hair.

Meltblown fibers are typically fine denier filaments with relatively low molecular weight and low orientation, which can have fineness ranging from 0.001denier to 10 deniers [45].

Fine fibers have increased specific surface area; the corresponding web will have increased absorbency and smaller pore size, which will facilitate filtration efficiency. Also, better capillary action can result from the increased filament surface area and may open more markets for bicomponent meltblown nonwoven webs.

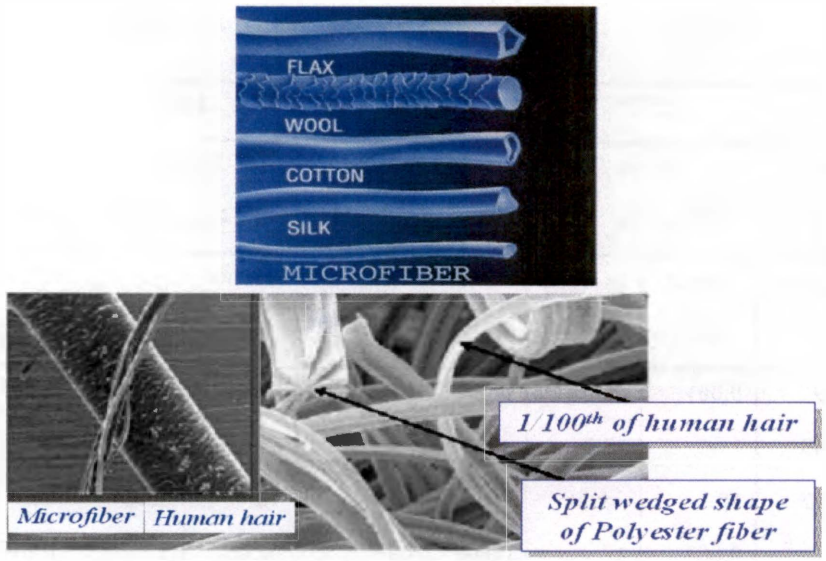

Figure 1.3 Synthetic microfibers versus natural fibers

(Revised from References [54, 55])

In addition, the nonwoven webs composed of fine denier fibers have good web uniformity, uniform fiber coverage, good barrier properties and high fiber surface area, and possibly desirable strength, hand and softness, wiping property, as well as certain levels of loft.

Meltblown nonwoven fabrics with finer fibers are desirable mainly for the application in filtration, absorbency industries and other applications. Extremely fine fibers are beneficial in the filtration of extremely small particulates. These fine denier fibers may be used to produce fabrics having smaller pore sizes, thus allowing smaller particulates to be filtered from a fluid stream. In addition, fine denier fibers can provide a greater surface area per unit weight of fiber, and hence can have greater absorbency.

In a word, the fine Bico meltblown fibers provide softness, bulkiness, filtration efficiency, adsorption and durability. They can be used as disposables in various application fields.

1.1.5 Production Methods of Fine Fibers

Fine fiber production can be carried out in three different ways:

1. Producing directly from fiber spinning by decreasing the polymer throughput or die hole size;

2. Dissolving one component of the two components in the bicomponent fibers. The island-in-the-sea, segmented pie, side-by-side or sheath-core Bico fibers, produced from two or more resins having different solubility can be made into ultrafine fibers by removing the matrix parts of the fibers using suitable solvents;

3. Splitting fibers, to get finer individual filaments after the two components separate from each other completely or partially. The two components can be physically split apart in the case of side-by-side, citrus, segmented pie type bicomponent fibers, etc., by pre-treatment and/or post-treatment.

Nowadays, fiber splitting has become a new avenue to produce finer fibers with increased specific surface area. Many efforts have been made to achieve fiber splitting in

Bico nonwoven webs, and fiber splitting were commercially achieved in spunbonded webs and carded webs having S/S, segmented pie, island-in-the-sea type of configurations.

1.1.6 Difficulties and Possibilities in Splitting S/S Bico MB NW Webs

Several technologies have been employed by some researchers to split Bico SB or carded nonwoven fibers, including the application of hydrophilic additives, post treatments such as hot aqueous medium treatment, hydroentanglement, alkaline or acid treatment, and heat treatment. Splitting SB fibers and carded NW fibers have been achieved. However, known split fiber production processes may not be suitable for splitting meltblown fibers.

As we know, typical MB fibers have lower molecular weight, lower orientation, lower crystallinity and lower fiber strength compared to traditional melt-spun fibers and spunbonded fibers. Therefore, MB fibers and their webs may not have enough strength to bear the post treatment for fiber splitting; in addition, the adhesion between the two components in Bico MB fibers seems too strong to allow them separate easily.

Generally, meltbown fibers with low tenacity may not be entangled easily using conventional nonwoven web formation technologies, such as hydroentangling and needle punching. Therefore, more efforts are needed to achieve fiber splitting in bicomponent meltblown nonwoven webs, especially in S/S bicomponent fiber web. A S/S Bico fiber

has less open ends than the Bico fibers having segmented pie shape cross-section, and thus it is hard for the two components to separate. Efforts should be concentrated on the selection of post-treatment techniques and treating conditions. Splitting S/S Bico MB fibers is so hard compared to splitting other type of fibers, a better understanding of fiber splitting mechanisms will be an important issue which can guide the selections of appropriate methods for fiber splitting.

1.1.7 Market /Applications for MB Nonwovens Containing Finer Fibers

1.1.7.1 Market for Traditional MB Nonwoven Webs

Basic end uses of meltblown webs are listed below:

(1) Filters for air or liquid;

(2) Absorbent products, including oil adsorbents;

(3) Medical and protective apparels;

(4) Wipes;

(5) Battery separators.

Growth of MB products over the past years has advanced worldwide, and the total market-growing ratio has been estimated to range from 10% to 12% per year [37]. MB NWs now play a key role in the nonwovens business, as shown in Figure 1.4 [56].

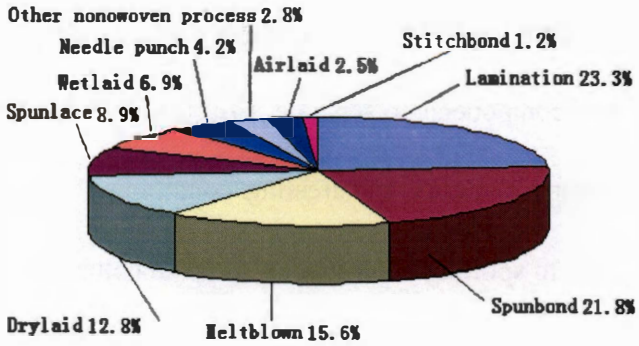

Figure 1.4 The *comparison of patents in nonwoven industry (Redrawn after Reference [56])*

Meltblowing technology is in the growth region of the development trend of nonwoven technologies, and has not matured yet, as shown in Figure 1.5. Since this technology is still in the rapid growth phase of the technology cycle, it has great potential to develop rapidly in the future [56].

The annual meltblowing growth in 10 years between 1991 and 2001 was 13.0%; and the expected growth from 2001 to 2006 is 9.0% [57]. As one of nonwoven technologies, meltblowing technology will grow towards maturity gradually, with the development and advancement of total nonwoven technologies.

1.1.7.2 Applications of MB Nonwovens Containing Finer Fibers

In recent years, filters made of meltblown nonwoven webs are widely used to control particulates because nonwoven filters are safe, reliable, efficient, and economical.

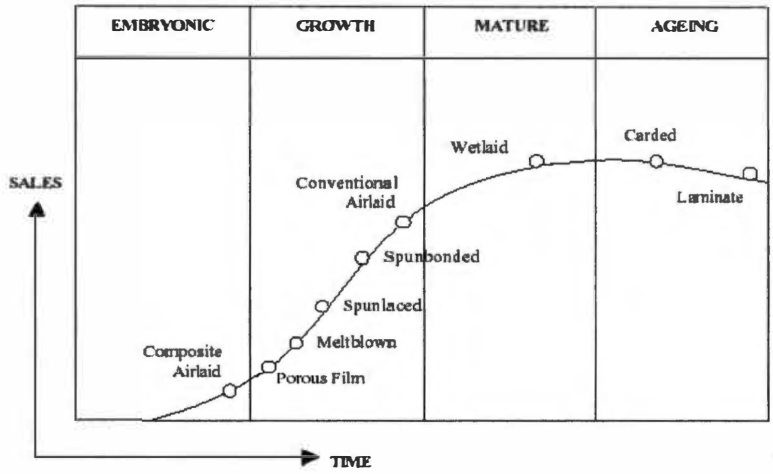

Figure 1.5 Maturity positions of nonwoven technologies

(Source: Nonwovens World, June/July 1999)

MB webs composed of finer microfibers have increased specific surface area compared to the conventional textile fibers, which may enhance the MB applications in absorbency, and adsorption fields; also the reduced pore size and increased web uniformity may make the MB webs containing finer fibers find more market share in filtration industry.

Moreover, the MB webs comprising finer fibers may improve fiber coverage, strength, texture, and filtration properties. In addition to applications in filtration industry, they can be used as disposable articles, protective garments, sterilization wraps, wiper cloth and covers for absorbent articles. They also can form laminates with other fabrics, e.g., the spunbond nonwoven web, to combine the strength and textual properties of the spunbond web and the breathable barrier properties of the microfiber web.

Fiber splitting in side-by-side meltblown nonwoven webs may result in finer fibers and increased specific surface area, the resultant split fibers will have irregular cross-sectional configurations, and the corresponding meltblown webs are expected to enhance their applications in filtration, absorbency and other related industries. Accordingly, the split side-by-side bicomponent meltblown nonwoven fabrics should find their ways to the increasing meltblown nonwoven markets in the world.

1.2 Mechanism of Bicomponent Fiber Splitting

The fiber splitting process is actually the opposite of polymer adhesion, meaning that, the materials and conditions which are not beneficial for polymer adhesion will facilitate fiber splitting. Therefore, the mechanisms in polymer adhesion can be used to explain the mechanisms of fiber splitting. The weaker the polymer adhesion is, the easier the corresponding fiber splitting will be.

Adhesion between two solid materials can be defined as the state when two parts are held together by intimate interfacial contact such that mechanical force or work can be transferred across the interface [58].

According to Mittal [59], adhesion is related to energetic quantities, from a molecular or microscopic point of view; it is the sum of all intermolecular interactions at the interface.

There are five main theories of adhesion between two non-reacting polymers [60], namely adsorption, electrostatic, mechanical keying, diffusion and weak boundary theory. The diffusion theory and weak boundary theory, which are most frequently used to explain the adhesion between the two components of a Bico fiber, will be addressed below.

1.2.1 Diffusion Theory

According to the diffusion theory [60], adhesion is due to intermolecular diffusion and entanglements of the molecules across their interface. The macromolecular chains or chain segments are supposed to be sufficiently mobile and mutually soluble at temperatures above T_g so that molecular chains of the two polymers can get enough energy to diffuse each other and get entangled. However, an interface will exist between the two polymers if the two polymers are incompatible. The illustration of the diffusion theory of polymer adhesion is shown in Figure 1.6.

Generally, the two components in Bico fibers are chemically incompatible, so there will be an interface between the two categories of molecular chains. Diffusion cannot occur to the polymer system if the two polymers are not or only slightly soluble, are highly cross-linked or crystalline, or are placed in contact at temperatures far below their glass transition temperature.

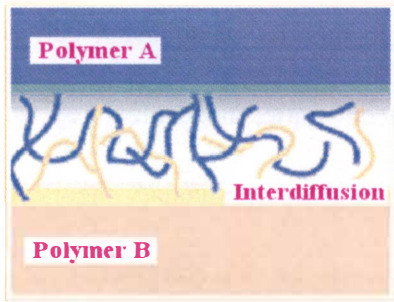

Figure 1.6 Illustration of diffusion theory of polymer adhesion (Revised after [61]*)*

Adhesion strength depends on diffusion factors such as pressure, contact time, temperature, and the nature and molecular weight of polymers [60]. Bond strength increases with longer contact time, higher bonding temperature, higher bonding pressure, lower molecular weight, higher chain flexibility, absence of bulky short side groups, lower degree of cross-linking, and the similarity of the solubility parameters of the two polymers. Polarity generally increases adhesion.

Voyutskii [62-64] has performed studies to investigate the effects of bonding conditions and molecular structures on adhesion strength, including both autohesive and adhesive bonding. The conclusions from Voyutskii and other researchers were summarized as below.

Bonding pressure

Voyutskii shows that both adhesive and autohesive strengths increase with increasing applied pressure during bonding.

Bonding time

Vasenin's Kinetic Theory [65, 66] predicts a $t^{1/4}$ dependence of adhesive strength which has been experimentally confirmed. However, Vasenin's theory has time limitation when used to explain the kinetic process of interdiffusion.

The ratio of adhesive strength development in many systems obeys Equation 1.2 [67-69]. Generally speaking, failure stresses vary as the jointing time $t^{1/4}$, and failure energies vary as $t^{1/2}$.

$$\sigma_f \sim at^b \quad \text{.....Equation 1.2}$$

where a is a constant and b is usually 1/4 or 1/2.

Temperature

Autohesive bond strength of rubbers increases with increasing bonding temperature [70, 71], as show in Equation 1.3,

$$\sigma_t = \sigma_{t_0} \exp(-E_a/RT) \quad \text{.....Equation 1.3}$$

where E_a is activation energy, σ_t is adhesive bond strength at time t, σ_{t_0} is adhesive bond strength at t = 0, R is the gas constant, and T is absolute temperature.

Molecular Weight

Increased molecular weight increases the cohesive strength of materials, and hence should facilitate high adhesion strength. Increased viscosity, however, usually retards not only wetting but diffusion. Thereafter, the influence of molecular weight on

bond strength will vary with polymer properties. For instance, autohesive strength of polyisobutylene increases with decreasing molecular weight [72].

Molecular Structure

Increased chain rigidity decreases adhesion strength at most times. However, chain rigidity not only increases the cohesive strength of the polymer, but also increases viscosity and retards diffusion of the molecules. Therefore, the effect of chain rigidity on adhesion is variable, depending on the specific polymer system. But adhesion strength usually tends to decrease with increasing chain rigidity [73, 74], due to decreased chain mobility and polymer solubility.

For instance, incorporation of rigid side groups such as methyl, t-butyl, and phenyl groups into a polymer generally lowers its adhesion [63, 64]. Cross-linked polymers are generally rather difficult to adhere to, due to decreased molecular diffusivity.

Solubility parameter

Solubility parameter is defined [75] as Equation 1.4:

$$\textit{Solubility parameter } \delta = \sqrt{\frac{E_{coh}}{V}} \quad \text{.....} \textit{Equation 1.4}$$

where E_{coh} is cohesive energy, the energy needed to remove a molecule from its nearest neighbors, and V is molar volume.

Generally, the more incompatible the two polymer components of the Bico fiber,

the easier the fiber splitting during the post treatment, the difference in the solution parameters of the two polymers is an indicator of the incompatibility of the two polymers.

According to the Second Law of thermodynamics, the possibility of mixing two polymers depends on the change in the Gribb's free energy of the mixing system ΔG_m [76, 77], as shown in Equation 1.5:

$$\Delta G_m = \Delta H_m - T\Delta S_m \quad \text{Equation 1.5}$$

$$\Delta H_m = V\varphi_1\varphi_2(\delta_1 - \delta_2)^2 \quad \text{Equation 1.6}$$

where ΔH_m is change in enthalpy of the mixing system;

ΔS_m is change in entropy of the mixing system, $\Delta S_m > 0$, because any dissolving processes always result in the increase in the mobility of the solute;

T is absolute temperature when mixing;

V is total volume of the solution;

φ_1 and φ_2 are volume fractions of the solvent and solute, respectively;

δ_1 and δ_2 are solubility parameters of the two polymers (or solute and solvent), respectively.

The enthalpy term ΔH_m is essentially independent of molecular weight and is a measure of the energy change associated with intermolecular interactions, and the entropy term ΔS_m is associated with the change in molecular arrangements. Magnitude of

the entropy change is essentially an inverse function of molecular weight of the polymers being mixed and is likely to be small. ΔH_m is thus the parameter determining the miscibility of polymers.

The essential condition for the dissolving/mixing/blending process to initiate spontaneously is $\Delta G_m < 0$. When $\delta_1 \approx \delta_2$, $(\delta_1 - \delta_2)^2 \approx 0$, namely, $\Delta H_m \rightarrow 0$, $\Delta G_m < 0$. Therefore, if the difference in the solution parameters of the two polymers (or the solute and solvent) is very small, the mixing/blending of the two polymers can proceed spontaneously, i.e., the produced bicomponent fiber will have strong strength of the interfacial adhesion. Conversely, if the difference in the solution parameters of the two polymers is great enough, the mixing/blending of the two polymers will encounter difficulties, and the resultant bicomponent fibers will have weak adhesion at the interface of the two polymers, and fiber splitting along the weak interface will be possible. Two identical or similar polymers can be chemically compatible; the two polymers having different chemical characteristics may not match well and will have a tendency for fiber splitting.

When the difference in solubility parameter between the two polymers is great, solubility between the solute and solvent will decrease, i.e., it will be difficult for the solvent to dissolve the solute (polymer). Usually, when $|\delta_1 - \delta_2| > 2.0$, it is not easy for the dissolving process to start [76], because $\Delta H_m >> 0$ and it will be easy for $\Delta G_m > 0$

(usually ΔS_m is > 0 but it will be small), so the two components of the bicomponent fiber will tend to separate.

Selection of the solvent, i.e., the post treating agent, is quite important, based on the analysis above. The solvent should have a similar solubility parameter to one of the two components in the Bico fibers, so that this component can be swollen by the solvent, and hence the internal stress can built up gradually and finally cause the Bico fibers to split.

Generally speaking, non-polar material has a smaller δ value, while polar material has a greater δ value. Usually, polar polymer will dissolve easily in polar solvent and non-polar polymer will mix easily in non-polar polymer.

The solubility parameters of frequently used polymers and their solvents are listed in Table 1.2 [76, 78].

To summarize, the possibility of fiber splitting will increase with shorter contact time, lower bonding temperature, lower bonding pressure, higher molecular weight, lower chain flexibility, existence of bulky short side groups, and higher degree of cross-linking as well as greater difference in solubility parameter between the two polymers.

Table 1.2 Solubility parameter $(cal/cm^3)^{1/2}$ of some polymers and solvents

Polymer	Solvent	
$\delta_{PE} = 7.9$	$\delta_{ether} = 7.4$	$\delta_{ethanol} = 12.7$
$\delta_{PP} = 8.3$	$\delta_{ethyl\ acetate} = 9.1$	$\delta_{formic\ acid} = 13.5$
$\delta_{PET} = 10.7$	$\delta_{acetone} = 9.8$	$\delta_{methyl\ alcohol} = 14.5$
$\delta_{PA6} = 13.0$	$\delta_{pyridine} = 10.9$	$\delta_{water} = 23.4$

In addition, adhesion between two incompatible polymers depends on the entanglement between the two kinds of polymer chains. If the two polymers are essentially insoluble to each other and the interface between them is very narrow, low adhesion can be expected and the subsequent fiber splitting will be easy.

The solubility parameter can be considered as the index reflecting the compatibility/incompatibility between two polymers, as illustrated in Figure 1.7. The polymer composite will cohesively fail (failure occurs at bulk polymers) only when the two polymers match each other, i.e., they have similar solubility parameters, and hence the polymer composite has a strong interface, it is not easy for the polymer composite break at their interface. If the two polymers have significant difference in solubility parameter, however, they do not match each other, and the polymer composite will have a weak interface between the two polymers. The polymer composite will tend to fail at its interface. This is desirable for fiber splitting in bicomponent fibers.

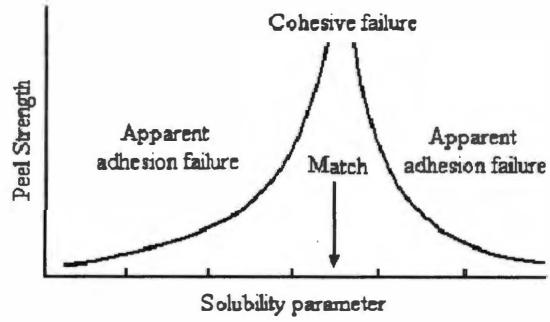

Figure 1.7 Adhesive bond strength vs. Solubility Parameter

(Redrawn after Reference [75])

1.2.2 Weak Boundary Theory

According to this theory, fracture always takes place at the weakest link. Weak locations may be intrinsic defects such as bubbles, voids, crevices, or microcracks in interface region. Weak adhesive spots may also be created during service due to stress or corrosion which arises from permeated grease, gas, water, ions, low-molecular weight foreign matter, etc. The weak spots are flaws where neither molecular contact nor chemical bonding exists. The weak boundary theory is a theory of debonding rather than bonding or adhesion [79-81].

A weak boundary layer is a non-adhesion layer [60, 82] existing on the interface between two polymers, as illustrated in Figure 1.8, due to the existence of regions of low cohesive strength on the interface. According to *Weak boundary layer theory*, the interfacial failure is actually separation of the two polymers in a weak boundary layer,

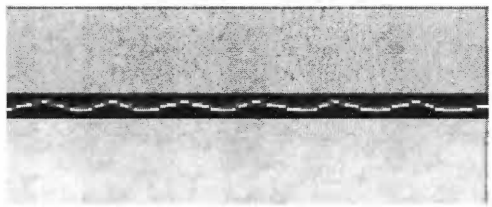

Figure 1.8 Illustration of weak boundary layer between polymers (Taken from Reference [75]

i.e., a thin layer with mechanical strength much weaker than that of each polymer phase.

Weak boundary layers are possibly originated from the following sources: (1) impurities arising from the polymerization process; (2) migration of cohesively weak low-molecular-weight fractions of a polymer; (3) additives, such as antioxidants and slip/lubricants agents; (4) external processing aids, e. g., mold release agents; (5) contamination after processing, e. g., adsorption of oily contaminants from the environment; and (6) damaged surface of the polymer.

As known in the art, an adhesive bond will break at its weakest part; therefore, if there is a cohesively weak layer on the interface, the adhesive bond within this weak boundary layer may break at low applied stress. Therefore, the formation of the weak boundary layer will facilitate fiber splitting. Certain hydrophilic additives or lubricants may be added to the bicomponent polymers to form a weak boundary layer before the production of MB webs, or some chemical solutions can be employed to promote splitting the Bico fibers after the MB webs are produced.

Based on the weak boundary theory, hydrophilic additives or lubricants, etc., can be meltblown together with one or both of the two polymers. The weak boundary layer formed at the interface of the two components will promote fiber splitting in a subsequent aqueous treatment.

1.3 Review of Fiber Splitting Techniques

A number of processes are known for separating multicomponent fibers into fine denier filaments. The particular process employed depends on the specific combination of components comprising the fiber, as well as their configuration. One common process by which to divide a multicomponent fiber involves mechanically working with the fiber by means such as drawing on godet rolls, needle punching or hydroentangling.

1.3.1 Pre-requirements for Fiber Splitting in Multi/Bicomponent Fibers

1.3.1.1 Definition of Fiber Splitting

Bicomponent fibers may be split into fine fibers comprised of the respective components, if the composite fiber is formed from incompatible polymers. The single Bico composite filament thus becomes two individual component microfilaments following splitting. This phenomenon is called fiber splitting. (U.S. Patent 5,783,503 and 5,759,926).

Fiber splitting (or dissociating, dividing) indicates that, at least one of the fiber components is separated completely or partially from the original multicomponent fiber; partial splitting means dissociation of some individual segments from the fiber, or dissociation of pairs or groups of segments, which remain together in these pairs or groups, from other individual segments, or pairs or groups from segments from the original fiber [45].

Splitting fibers to make finer fibers began with the production of superfine melt spun fibers. The technology was first developed commercially in Japan in the mid to late 1960's for synthetic suede fabrics, by dissolving the co-PET sea part in the island-in-the-sea Bico fibers comprising PET and co-PET [83].

Since that time, other forms of synthetic splittable fibers have been produced, including segmented pie type of fiber cross-sections. The fibers were again spun from two dissimilar polymers. The segments alternate between polymer types. The number of fiber segments ranges from 2 to 64 or more in a round fiber cross-section.

1.3.1.2 Splittable Nonwoven Bicomponent Filaments

Splittable composite fibers, comprised of two components with low solubility to each other, can be converted into a web by a dry or wet method, and then subjected to a splitting process with a mechanical impact such as hydroentanglement (JP Patent Publication No. Sho 48-28005, Hei 5-321018 and Hei 6-63129).

Splittable Bico fibers are the Bico filaments that will split lengthwise into finer filaments of the individual thermoplastic polymer segments when subjected to a stimulus. Therefore, the splittable fibers should first of all have the potential splittability, and contain at least two incompatible polymers arranged in distinct segments across the cross-section of each filament. The incompatible segments are continuous along the length of the each filament. In a mechanically splittable Bico fiber, each of polymer components forms a portion of the outer peripheral surface of the fiber to form distinct unocclusive cross-sectional segments along the length of the fiber so that the components are not physically impeded from being separated from each other [45]. Therefore there are special requirements for the polymer composition and cross-sectional shape to the splittable bicomponent meltblown fibers.

In the splittable fiber, the two components in the bicomponent fiber should have dissociable/immiscible/incompatible properties, different solubility and/or other distinct physical properties [38], so that the components may dissociate/separate/split into respective individual filaments later on when being subject to the fiber-splitting induced treatment. In addition, the melt rheologies of the two components must be taken into consideration, such that one component does not totally encapsulate the other during melt spinning, thus precluding later splitting.

The components of the fiber are mutually incompatible, indicating that, they do not substantially mix together or enter into chemical reactions with each other. When spun into a composite fiber, the components exhibit a distinct phase boundary between them so that substantially no blend polymers are formed, preventing dissociation. The components must differ from each other significantly to ensure minimal interfilamentary bonding. They should be selected from different chemical families, having extremely different chemistries [43].

A balance of the adhesion and incompatibility between the components of the Bico fiber should be well maintained. The components should adhere sufficiently to each other to allow the unsplit multicomponent fiber to form nonwoven webs without any appreciable separation of the components until desired. On the other hand, the polymers should be sufficiently incompatible so that adhesion between the components is sufficiently weak, thereby allowing subsequent separation upon the application of sufficient external force from the subsequent post-treatment [42, 45].

1.3.1.3 Selection of Incompatible Polymers as Bico Pair

Incompatible polymer composition indicates the polymer pair that does not form a miscible blend, i.e., immiscible, when melt blended. Difference in the polymer solubility parameter (δ) may be used to select suitably incompatible polymers. The least difference in δ values of two polymers is desired to be greater than 0.5 to 2 $(cal/cm^3)^{1/2}$

[40]. There is no limitation to the upper limit of the difference in the two δ values, as long as the filaments do not split prematurely so as to interfere with spinning, and there is adequate control over the splitting (which means, that the greater the difference in δ value between the two polymers, the more splittability of the Bico filaments, as long as the processability of the polymers are assured). The higher the difference, the more spontaneous the splitting of the fiber becomes [44].

1.3.1.3.1 Desirable Polymer Pairs Suitable for Splittable Bico Filaments

The chemically incompatible polymer pairs include polyolefin/polyamide, polyolefin/polyester, polyamide/polyester [40], [44].

The two chemically incompatible components can be physically incompatible as well. Splittable polymer pairs include, hydrophobic/hydrophilic; elastic/inelastic; heat shrinkable/non-heat shrinkable [40] or one component is composed of linear molecules, while the other contains grafts or branches in its molecules to decrease the affinity of the two components, in order to facilitate the subsequent fiber splitting [43].

The composition of the two components by weight percent is preferably around 50/50 for the splittable Bico fibers [41]. In the previous research work of our group, the Bico ratios by weight of the two components were selected as 25/75, 50/50 and 75/25 [8-12, 14-16, 21, 22, 84].

1.3.1.3.2 Cross-sectional Shape of the Splittable Fibers

In the splittable Bico fibers, the fiber components are arranged so as to form distinct unocclusive cross-sectional segments along the length of the fiber so that none of the components is physically impeded from being separated, i.e., one component does not encapsulate, or only partially encapsulates, other components; or in other words, at least a portion of the polymer components forms an exposed surface of the multicomponent fiber [45].

The splittable bicomponent fibers can have the following cross-sectional configurations: side-by-side; segmented pie/wedge; segmented ribbon; segmented round; segmented oval; segmented rectangular; segmented ribbon; segmented multilobal; the fiber may be hollow or non-hollow; conventional round or irregular non-round shape. Side-by-side bicomponent fiber has the cross-sectional conformation which is difficult to split the two components apart, especially for side-by-side meltblown nonwoven fiber, because it has the biggest interface between the two polymer parts.

It is advised that the foresaid possibility of fiber splitting only demonstrated the theoretical potential of fiber splitting in nonwoven webs composed of splittable fibers, which are only the essential condition for fiber splitting later on, but not the sufficient condition. Some adequate post-treatments or even pre-treatments are still needed to facilitate the separation of the components in the multi/bi-component fiber(s) and achieve fiber splitting eventually.

1.3.2 Fiber-splitting Inducing Pre-treatments

The incompatible polymers, ready to separate with poor affinity, may be combined with suitable lubricant or slip agent, which can be added in melt-spinning process to facilitate later fiber splitting [38, 44]. Hydrophilic modifiers may be incorporated into one or both polymers to facilitate fiber splitting when the fiber is subject to subsequent fiber-splitting inducing treatment. The hydrophilic component polymer may be naturally hydrophilic, e.g., polyamide or polyurea. (US Patent 4,767,825 to Pazos et al), or hydrophilically modified, e.g., polyolefin, polyester, or polyamide, etc.

When a hydrophobic or insufficiently hydrophilic polymer is used as the hydrophilic component of the splittable conjugate fiber, the polymer must be hydrophilically or wettably modified by adding a hydrophilic agent or hydrophilic modifier, which includes various surfactants.

The amount of surfactants required varied depending on the hydrophilicity needed for the modified polymer, the surfactant type and the polymer type. In general, more hydrophilic components in the filament will result in more fiber splitting. Therefore, hydrophilic surfactants may be added as much as possible as long as no adverse influence occurs to the processability of the polymer composition. The weight percentage of the hydrophilic additive is generally from 0.1% to 5%, desirably from 0.3% to 4%.

The hydrophilic surfactants may be thoroughly blended (compounded) and melt extruded with the polymer compositions in the extruders and then spun into fibers.

1.3.3 Fiber Splitting-inducing Post-treatments

A separate splitting step is needed for fiber splitting in meltblown web. The splittable fibers may be dissociated by sufficient flex or mechanical actions such as hydroentangling, carding, crimping, drawing, etc [45].

The bicomponent fibers can be divided into microfilaments either prior to, during, or following fabric formation, e.g., dry-laid nonwoven process, may be bonded and split by hydroentangling [45] or other splitting-inducing process.

The individual segments of each filament may split apart from each other when the splittable bicomponent fiber is subject to a fibrillation-inducing treatment, resulting in finer individual filaments formed from the segments. The splitting-inducing treatments include contacting the Bico nonwoven filaments with a hot aqueous medium, mechanical agitation and spontaneous splitting caused by differential shrinkage of the two components (U.S. Patent 5,759,926 to Pike et al). Also, sodium hydroxide has been utilized to split Bico fibers composed of PET polymer.

1.3.3.1 Hydroentanglement Treatment

Hydroentangling creates fibrous nonwoven webs using fine, high pressure, columnar jets which rearrange and intertwine the fibers thereby providing strength and

integrity to the web. It is similar to the mechanical needling except that penetration of the water jets, as opposed to needles, is utilized to accomplish entanglement of the fibers. The web to be bonded may be supported by an apertured mesh screen or forming wire, during the processing. After hydroentangling treatment, the nonwoven web is entangled to a unitary web with the incompatible components being separated into individual filaments.

One or both of the web sides can be treated. Greater separation of the components can be achieved by subjecting both of the sides of the nonwoven webs to the treatment for two or more times, at lower impact energy.

A nonwoven fabric of ultrafine fibers has been produced by subjecting a web of splittable conjugate polyolefin fibers to a hydroentanglement processing [41, 43, 45, 46]. One of the two components may contain 1 to 7% by weight of hydrophilic component blended therein.

In addition, a spunbond nonwoven web [38] has been invented according to the Patent WO 9823804. The polymer pair is PA6 and PP with 1% TiO_2, with the fiber configuration being 16 segmented pie. After spinning, the web was subjected to drawing on a draw unit, and the unbonded web was thermally point bonded, and then went to hydroentangling.

1.3.3.2 Heat Treatment

If the bicomponent meltblown fabric is composed of two polymers significantly different in thermal shrinkage or stretchability, then heat treatment may induce fiber splitting. However it is a key issue to control the heat treating conditions such as temperature, time, stretching ratio, based on the breaking properties of the treated fabric.

Yu Jing-Peir et al [42] invented the thermally divisible bicomponent fibers having the first component including a low-shrinkage elastomeric polymer (e.g., polyurethane) and the second component including a high-shrinkage non-elastomeric polymer (e.g., polypropylene). The two components have solubility parameters sufficiently different so that the elastomeric and nonelasomeric components split upon thermal action.

The fibers are split by contacting the fibers with a heated gaseous medium, such as heated air, radiant or steam heat, although the presence of water is not required to achieve splitting. The following types of heating apparatus can be used, such as hot plates, heated rolls, hot baths (water or oil), microwave energy and so on [42].

High-shrinkage nonelastomeric polymers typically have limited power to cause separation, so a considerable amount of high-shrinkage component must be used in the bicomponent fiber to achieve even modest splitting. When elastomeric polymers shrink, they have more power than nonelastomeric polymers to cause separation of the fiber

segments [42].

A Japanese patent [47] released a method to produce nonwoven fabrics with thermally splittable fibers. The cross section shape of the fiber is 8 pie configuration, and the two components have different thermal shrinkage ratio and different melting temperatures. One of the two components contains 0.1-5% by weight of hydrophilic agent to improve the splittability, also impart the permanent hydrophilicity. More than 50% of the heat-splittable composite fibers split after thermal calendaring, especially when the additive is added to one of the components [47].

1.3.3.3 Chemical Post-treatment

Fibrillation of multicomponent fibers can be achieved by causing swelling and shrinkage of one of the components relative to the others. U.S. Patent No. 3,966,865 issued to Nishida et al disclosed a method of forming splittable fibers from multicomponent fibers, the composition of which is PA and one of PET, PP, PE or PAN. The PA component is swelled and shrunk by treatment with an aqueous solution of an alcohol, such as benzyl alcohol or phenylethyl alcohol, causing separation.

Fiber splitting using NaOH post treatment initiated in Japan and developed in Japan and other countries rapidly. Akita [85], Matsumoto [86], Ogawa [87], Hideyasu [88], and Koho [89] etc., investigated on Bico fiber splitting using NaOH solution. The treated fabrics/webs had suede-like hand, and the fabrics or webs were reduced in weight

by 22-41%. The concentration used for fiber splitting ranged from 20-35 g/L.

1.3.3.4 Hot Aqueous Medium Treatment

U.S. Patent No. 4,369,156 issued to Mathes et al disclosed a process for separating a multicomponent fiber of a copolyamide and polyester by treatment with liquid or vaporous water 10 ~ 20 °C below the soft point of the copolyamide. U.S. Patent with the Application Serial No. 08/484,365 filed on June 7, 1995 teaches a method of splitting fibers using a hot aqueous media.

Post treatment can be employed to induce fiber splitting using hot water or steam [40]. When a hydrophilic material is used as one of the incompatible polymers, splitting may be accomplished without mechanical agitation using an aqueous split-inducing medium (U.S. Patent 5,759,926). It may be a hot water medium with the temperature above 60 °C (better between 65°C and 100°C); steam or mixtures of steam and hot air with the temperature higher than 60°C but lower than the lower melting point of the two component polymers in order to prevent inadvertent melting of the polymer components during the fiber splitting process.

When an air and steam mixture medium is utilized, the temperature of the air, which is mixed with steam, can be adjusted to change the temperature of the split-inducing medium. The fiber splitting can be achieved in 1 to 30 seconds after contacting with the hot aqueous medium, and the degree of fiber splitting is desired to be

from about 25% to 100%.

Pike et al [44] invented splittable side-by-side meltblown nonwoven fabrics in combination with hydrophilic pretreatment and hot aqueous post-treatment, the resultant superfine microfiber webs nonwoven webs provide many good properties desirable for various applications for meltblown webs composed of superfine fibers.

The variables controlling the splitting process include: (1) Hydrophilicity of the components of the Bico fibers; (2) Temperature of the aqueous split-inducing medium; (3) Duration of exposure to the hot medium.

1.4 Research Objective

Fiber splitting in bicomponent spunbonding and carding nonwoven webs have been commercially achieved using different post-treatments. Fiber cross-sectional configurations with segmented pie shape or flat ribbon shape were used, combined with the application of hydrophilic additive(s) in the polymer resin to perform Bico fiber splitting in most of the previously used methods.

Because MB fibers have lower molecular orientation, lower crystallinity and hence less strength, it might be difficult to split Bico MB fibers through post treatment, compared to split Bico spunbonded fibers or carded fibers, because the MB fibers may lose their strength and hence cannot bear the subsequent fiber-splitting inducing post-treatment, i.e., the MB fibers may break before the two components separate.

Therefore, seeking the mechanisms of Bico fiber splitting to investigate theoretical possibility of Bico MB fiber splitting became a very important part of the fiber splitting research. In addition, the selection of polymer pairs and the selection of post treatment methods and post treating agents are crucial issues in the research of Bico MB fibers as well.

Fiber splitting in S/S Bico MB nonwoven webs may be practically achieved by swelling/separating the segments/components of the fibers by means of mechanical, chemical or thermal treatments, or the combined application of hydrophilic additive in the pre-treatment process and the hot aqueous medium in the post-treatment. Good understanding of the mechanism of polymer adhesion may be helpful in the achievement of fiber splitting. The objectives of this research are listed as below:

1. Understanding the mechanism of Bico fiber splitting and hence exploring the theoretical possibility of fiber splitting in S/S Bico MB webs;
2. Splitting S/S Bico MB nonwoven fibers using post treatments, including hydroentanglement, heat-stretching and chemical treatments such as NaOH treatment and benzoic acid treatment;
3. Selecting the Bico polymer pairs and post treatment methods favorable for fiber splitting in S/S Bico MB nonwoven webs, including the selection of post-treating chemical agent, sample processing conditions, etc.;

4. Exploring and optimizing the post-treating conditions based on the comprehensive considerations of degree of fiber splitting and web property deterioration;

5. Establishing an appropriate method to evaluate the degree of fiber splitting in S/S Bico MB nonwoven webs;

6. Analyzing changes in web structure and property before and after the post-treatments.

1.5 Summary

Technology and development of bicomponent meltblown nonwoven were addressed in this chapter. Basic concepts about nonwoven, meltblown nonwoven, Bico MB nonwoven and the developing trend of meltblown nonwoven were discussed as well. Bico MB nonwoven webs construct an important part of the MB nonwoven family owing to a combination of the features of two components. Crimping S/S Bico fibers give MB nonwoven webs bulk, resiliency and soft hand.

Meltblown technology is still in the immature phase and hence still has great potential for rapid development in the near future. Finer fibers are increasingly desirable in many applications such as absorbency and filtration industries due to increased specific surface area, and splitting Bico fibers is becoming an important technology to produce finer microfibers in the textile field. Commercial Bico fiber splitting has been

achieved in traditional meltspun fibers and spunbonded nonwoven webs, but it has not been investigated sufficiently in meltblown webs. Therefore, research on Bico fiber splitting in S/S MB nonwoven webs should be conducted for new product development.

There are more difficulties in splitting Bico MB fibers than splitting SB fibers and meltspun fibers. The investigation of Bico fiber splitting mechanism is thus an important part of this research. Polymer adhesion theory may be used to investigate Bico fiber splitting in MB nonwoven webs, since fiber splitting is actually an opposite process of polymer adhesion; the weaker the interfacial adhesion between the two components is, the easier the Bico fiber splitting will be. Among the main polymer adhesion theories, Diffusion Theory and Weak Boundary Theory may be used to explain Bico fiber splitting. Solubility parameter is an indicator for polymer compatibility or incompatibility. Greater difference in solubility parameter between the two components indicates greater incompatibility, and hence greater potential of subsequent Bico fiber splitting.

However, the difference in solubility parameter between two polymers of a Bico fiber is only an essential/necessary condition but not a sufficient condition for the fiber splitting. In order to practically achieve fiber splitting, several fiber-splitting inducing treatments including hydroentanglement, heat treatment, water treatment, and chemical treatment were to be used to explore fiber splitting in this research. Degree of fiber splitting and changes in web structure and property were also to be investigated.

2 PRELIMINARY STUDY ON FIBER SPLITTING IN S/S BICO MB NONWOVEN WEBS THROUGH HYDROENTANGLEMENT

2.1 Introduction

Hydroentangling (HE), also referred to as spunlacing, water entangling, hydraulically needling, water needling, jet entangling, etc., was officially introduced by DuPont in 1973 (Sontara®) [90]. It is a process of entangling a web of loose fibers on a porous belt or moving perforated or patterned screen to form a sheet structure by subjecting the fibers to multiple rows of fine high-pressure jets of water [91], as shown in Figure 2.1. In this process, the fiber re-arrangements and entanglements occur within the web by mean of hydrodynamic forces and bring about frictional inter-locking of the fibers.

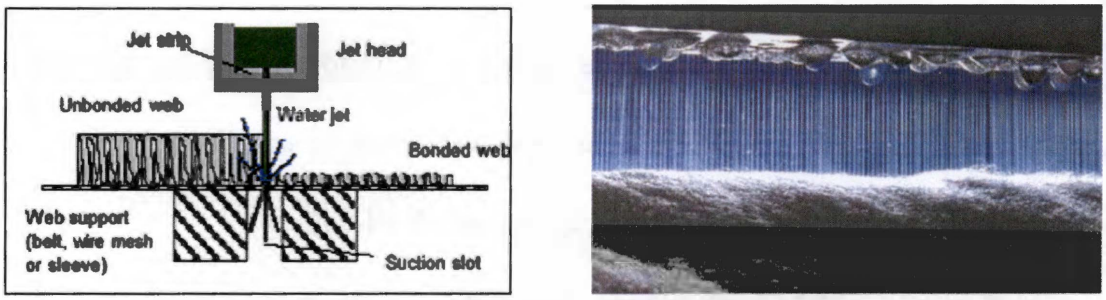

Figure 2.1 Hydroentanglement process
(Taken from Reference [92])

One or both of the web sides can be treated. Lower impact energies often do not generate the desired degree of separation. However, greater separation can be achieved by subjecting both of the sides of the nonwoven webs to the treatment for two or more times, at lower impact energy.

Several parameters [93] may influence the hydroentangling effects. The machine parameters include water jet pressure/impulse force, jet strip hole diameter, number of jet manifolds, number of holes per inch, hole geometry, quality of hole manifolds, structure of supporting members (perforated or not; perforated patterns, etc.), production speed, and so on; the to-be-treated web (nonwovens or composites) parameters include type of polymer, denier per filament, basis weight, and so forth.

Historically hydroentanglement has been used to achieve web bonding (consolidation/integrity), laminating, and/or fabric surface texturing purposes. Hydroentanglement can impart nonwoven webs with better properties, such as softness, bulk, absorbency, wetting, strength, elongation and abrasion resistance, better hand, surface appearance, smoothness, and so on. Nowadays it already became the commercial way to split fibers in bicomponent nonwoven webs such as spunbonded webs and carded/thermally-bonded nonwoven webs, and so on [83, 94-96].

The most widely used splitting fiber method is the hydroentangling process, which utilizes a pressurized stream of water to split multicomponent conjugate fibers. In

general, the process simultaneously splits and entangles the fibers to form a bonded nonwoven web. However, known split fiber production techniques may not be suitable for splitting Bico meltblown fibers. The water-needling process has not been used to produce split meltblown fiber webs since the meltblown webs are composed of fine breakable fibers and almost randomly distributed self-adhesive bonds, which restrict fiber movements, therefore it will be difficult to split meltblown fibers with the mechanical splitting process alone.

Hydroentanglement post treatment was applied to side-by-side bicomponent meltblown fabrics in this research to investigate fiber splitting which may occur during hydroentanglement. In addition, the changes in web property and fiber diameter were also examined.

2.2 Experiments

A total of eight side-by-side bicomponent meltblown nonwoven fabrics with different polymer compositions (PA/PE, PA/PP and pa/pet) were produced on the Reifenhäuser Bico MB line, TANDEC (Textile and Nonwovens Development Center), the University of Tennessee. The sample descriptions and main processing conditions are listed in Table 2.1.

Hydroentanglement experiments at three different treating levels were carried out at Fleissner GmbH & Co., Germany, to each sample of the eight samples; the water

Table 2.1 Meltblown processing conditions and sample description

Sample No.	Sample Composition	Melt Temp. (°F)	Polymer Throughput (g/hole/min)	Air Temp. (°F)	Air Flow Rate (SCFM)	DCD (inch)
1	25PA6/75PE	590/480	0.55	590	550	8
2	50PA6/50PE	590/480	0.55	590	550	8
3	75PA6/25PE	590/480	0.55	590	550	8
4	25PA6/75PP	590/580	0.55	600	350	8
5	50PA6/50PP	590/580	0.55	600	350	8
6	75PA6/25PP	590/580	0.55	600	350	8
7	50PA6/50PET	590/590	0.73	590	520	8
8	75PA6/25PET	590/580	0.73	590	520	8

jet settings for hydroentanglement are listed in Table 2.2. Fiber morphology and web structure were observed under microscope or SEM, including both the treated samples and the untreated samples. Changes in fiber configuration and web structure were obtained by the analysis of the results.

Web characterizations were carried out based on the corresponding test standards, if applicable, including thickness, basis weight, air permeability (ASTM D 737), tensile properties (ASTM D 1117), flexural rigidity (ASTM D 1338-64) and hydrostatic head (IST 80.4-92). In addition, SEM and WebPro [29] were applied to examine web structure.

Table 2.2 Water jet settings for hydro-entanglement

Line speed	Wetting	Pre-entangle	Treatment-1	Treatment-2	Treatment-3
M/min	(Top belt) (bar)	(Top belt) (bar)	Bottom drum (bar)	Bottom drum (bar)	Bottom drum (bar)
10	15	50	80	100	120

2.3 Results and Analysis

2.3.1 Fiber Configuration, Web Structure and Appearance

The typical SEM pictures of Sample 6, before and after three different levels of hydroentanglement treatments are shown in Figures 2.2 through 2.5; SEM photos of Sample 4 before and after three levels of HE treatments are shown in Figure 2.6 — 2.9.

The tiny holes (Figures 2.3 — 2.5) occurred in the treated webs and they became larger with the increase in water pressure while the fibers around the holes became more compacted together compared to the untreated webs; therefore, the thickness might increase due to the compaction of fibers in the non-hole zones. The existence of the tiny holes was responsible for the decrease of mechanical properties of the treated webs.

The fiber configurations changed after treatment (Figures 2.6 — 2.9). Some treated fibers had the configuration of flat-ribbon, and they became finer and weaker due to fiber splitting resulted from the water jets. As fiber split and pin holes occurred, fiber damage and breakage were also observed in the hydroentangled samples, as shown in Figures 2.10 — 2.13.

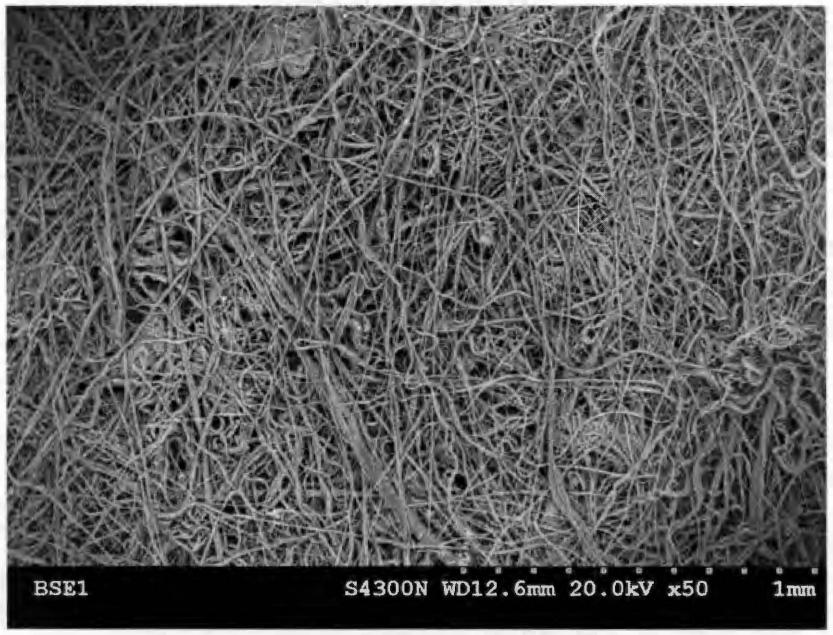

Figure 2.2 Sample 6 (75PA6/25PP) before treatment

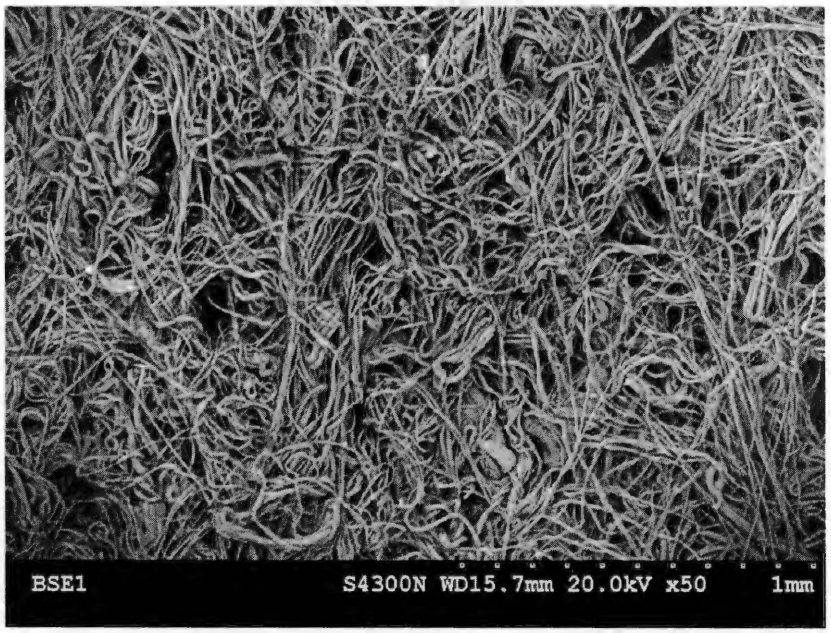

Figure 2.3 Sample 6 (75PA6/25PP) after treatment-1

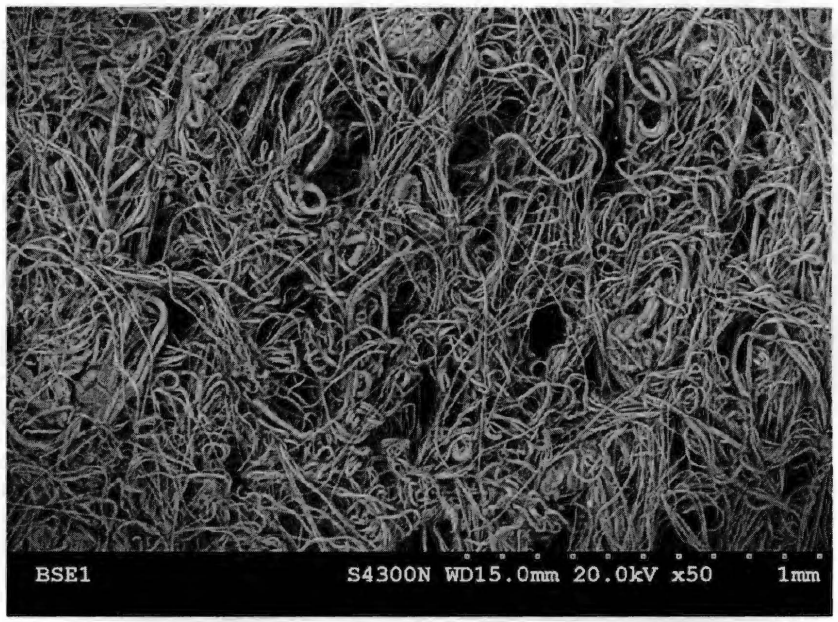

Figure 2.4 Sample 6 (75PA6/25PP) after treatment-2

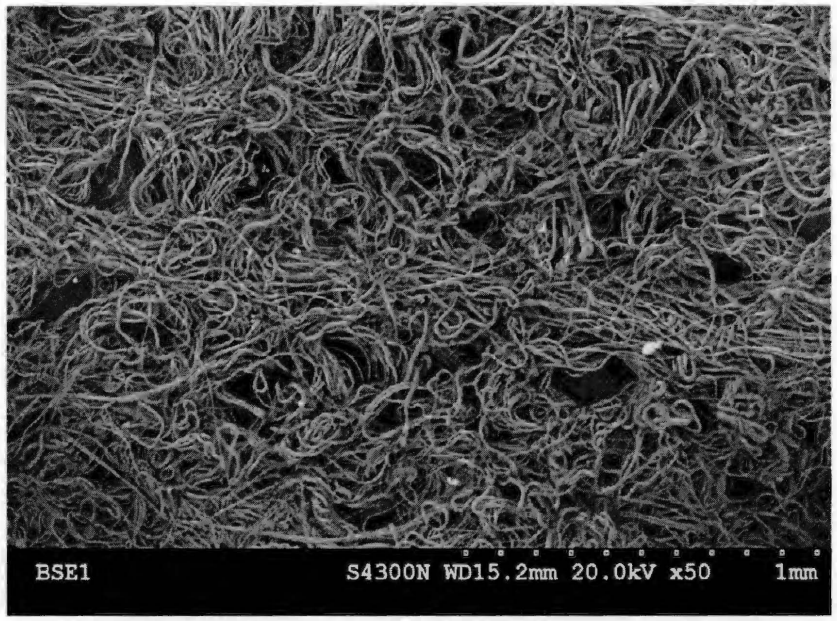

Figure 2.5 Sample 6 (75PA6/25PP) after treatment-3

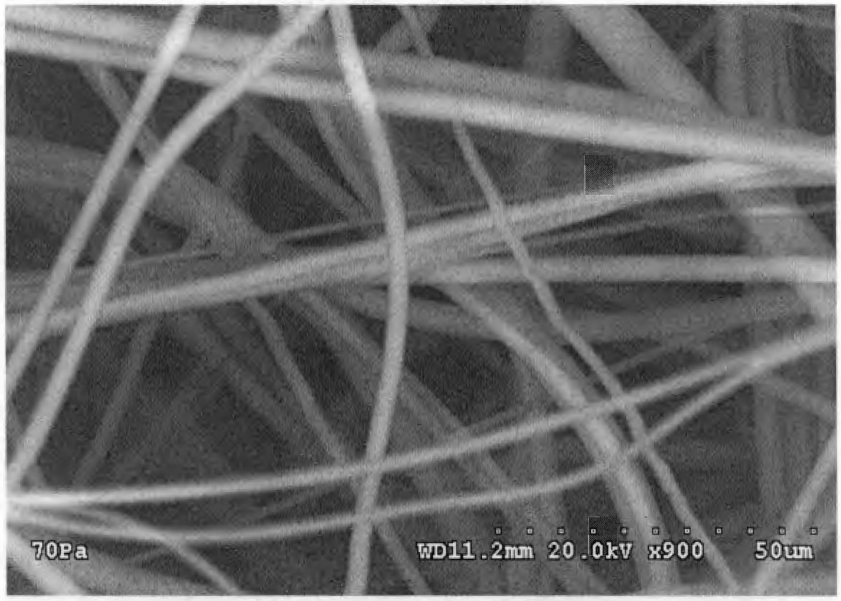

Figure 2.6 Sample 4 (25PA6/75PP) before treatment

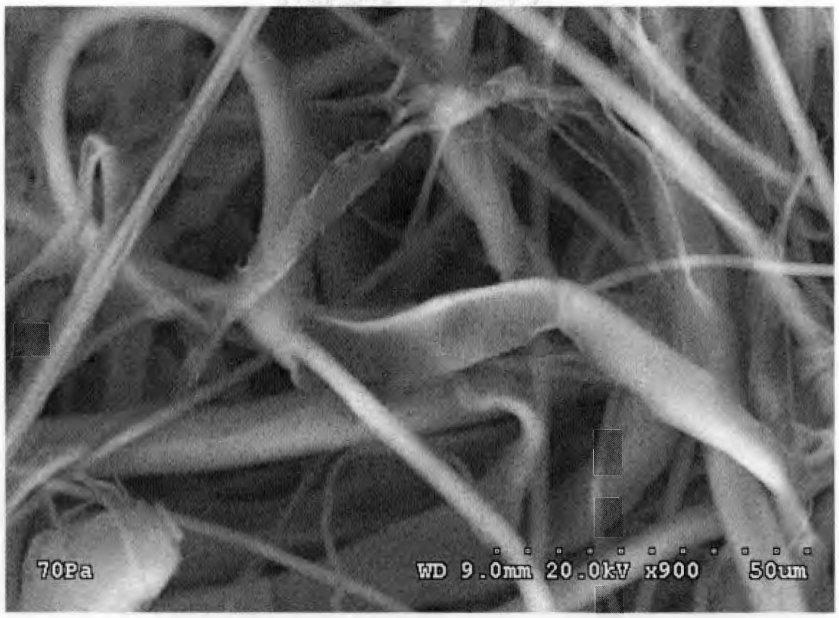

Figure 2.7 Sample 4 (25PA6/75PP) after treatment-1

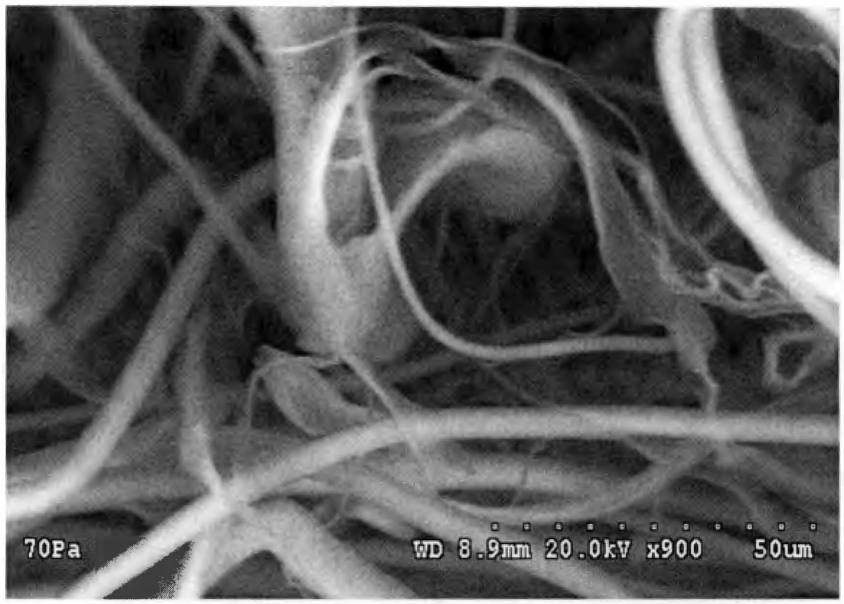

Figure 2.8 Sample 4 (25PA6/75PP) after treatment-2

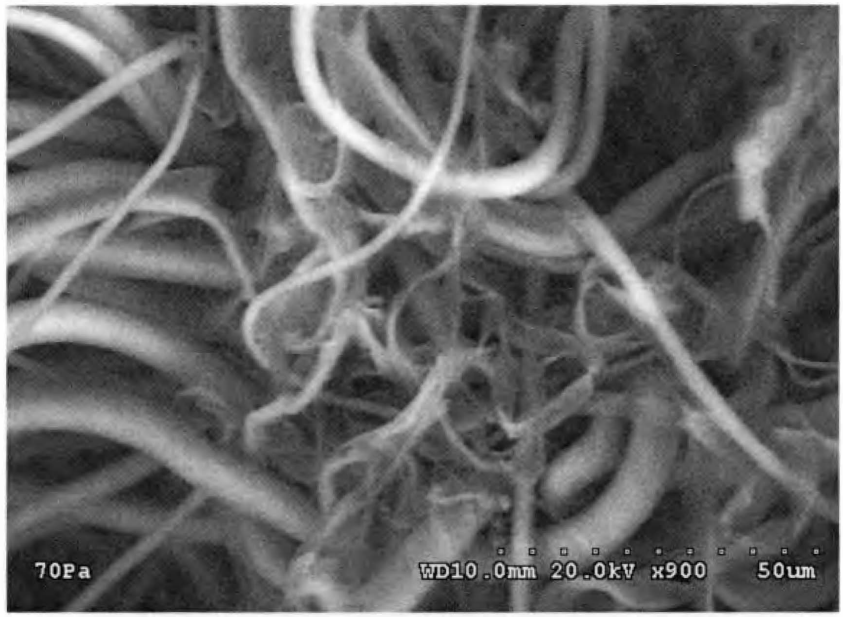

Figure 2.9 Sample 4 (25PA6/75PP) after treatment-3

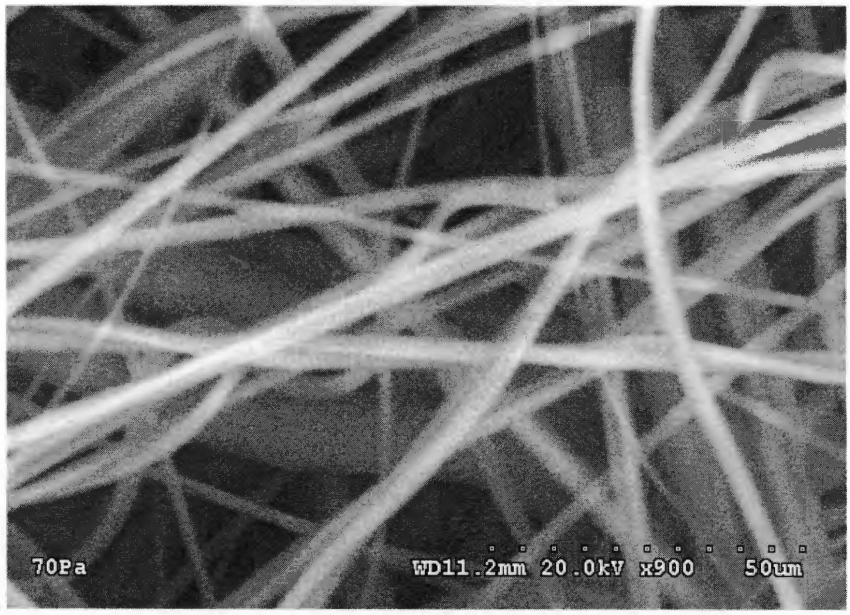

Figure 2.10 Sample 7 (50PA6/50PET) before treatment

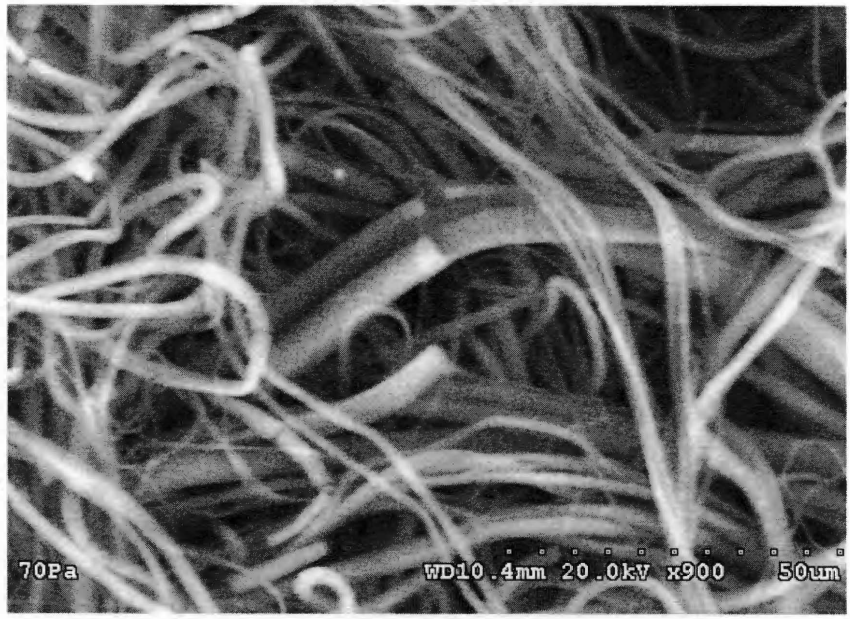

Figure 2.11 Sample 7 (50PA6/50PET) after treatment-1

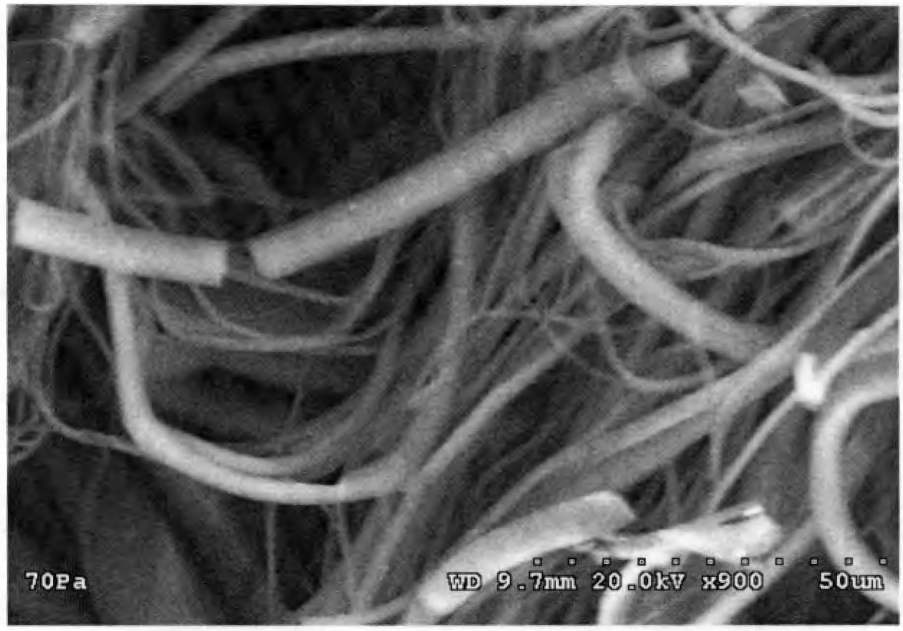

Figure 2.12 Sample 7(50PA6/50PET) after treatment-2

Figure 2.13 Sample 7 (50PA6/50PET) after treatment-3

2.3.2 Fiber Diameter, Basis Weight, Thickness and Flexural Rigidity

Fiber diameter, measured with 35 fibers under a microscope, decreased after HE treatment, as shown in Figure 2.14. Generally speaking, higher water pressure should result in finer fiber diameter, due to more fiber splitting and more fiber damage occurring during the hydroentangling treatment.

Thickness (Figure 2.15) increased after HE treatment, with an exception of PA/PP Bico MB webs; and the total trend of the thickness increased with the increase in water jets pressure from 80 bar to 100 bar and 120 bar, which indicated that, the degree of the fiber entanglement and web shrinkage enhanced with the increase in the water needling degree. Increase in thickness indicated web shrinkage after HE treatment.

The slight increase in basis weight, as shown in Figure 2.16, was due to the web shrinkage after treatment, but an exception for PA/PET webs occurred, which was possibly due to the fiber loss during the hydroentanglement.

Flexural rigidity (Figure 2.17) decreased dramatically after HE due to the impact from water jets. The flexural rigidity of PA/PET webs increased after HE treatment, due to the poor bonding of the original webs and web shrinkage.

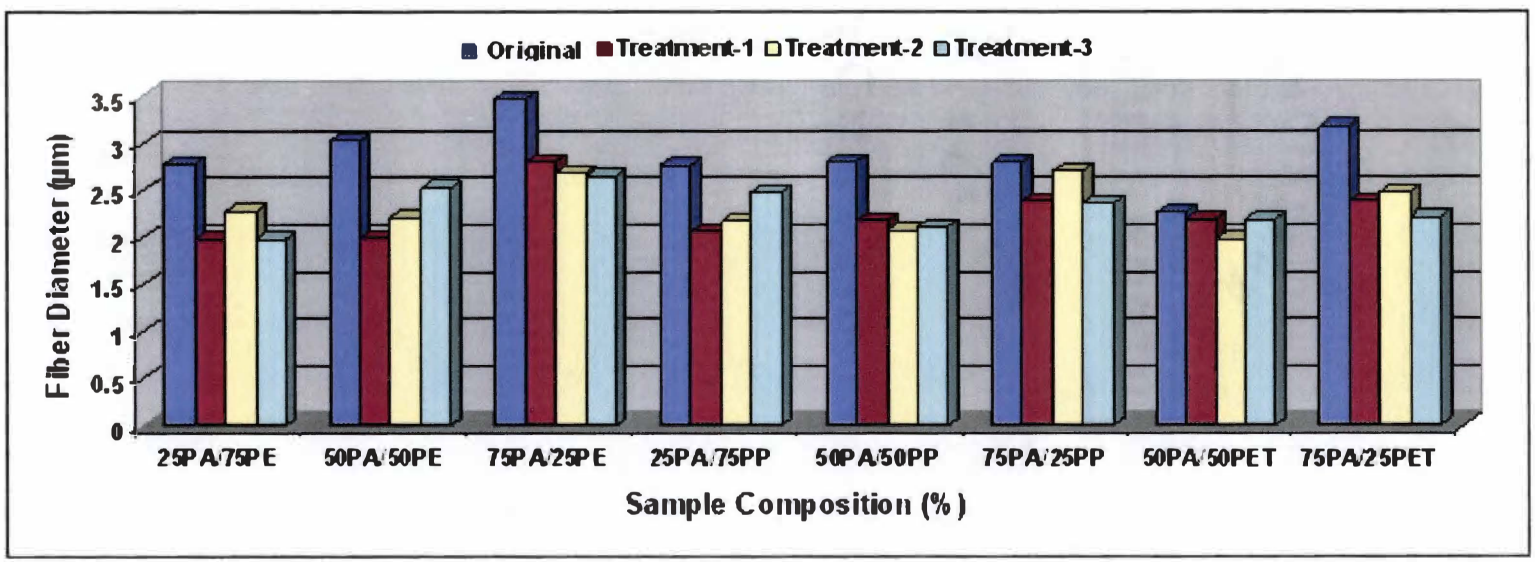

Figure 2.14 Change in fiber diameter after hydroentanglement

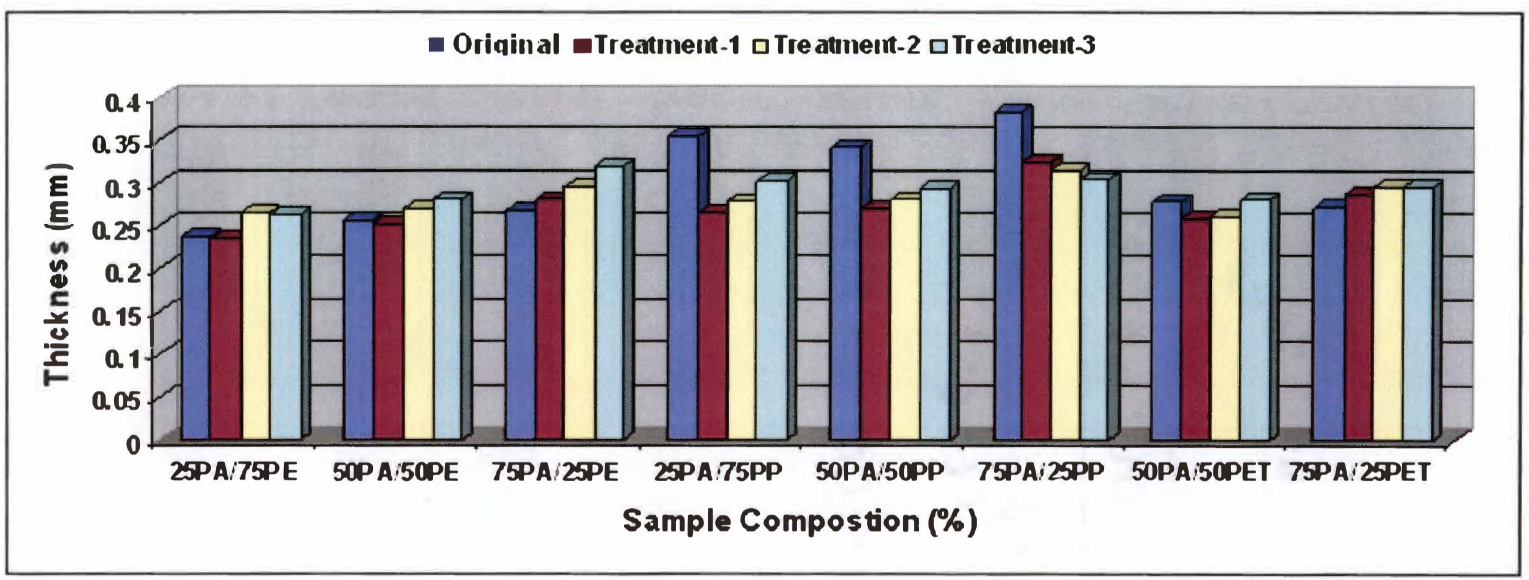

Figure 2.15 Change in web thickness after hydroentanglement

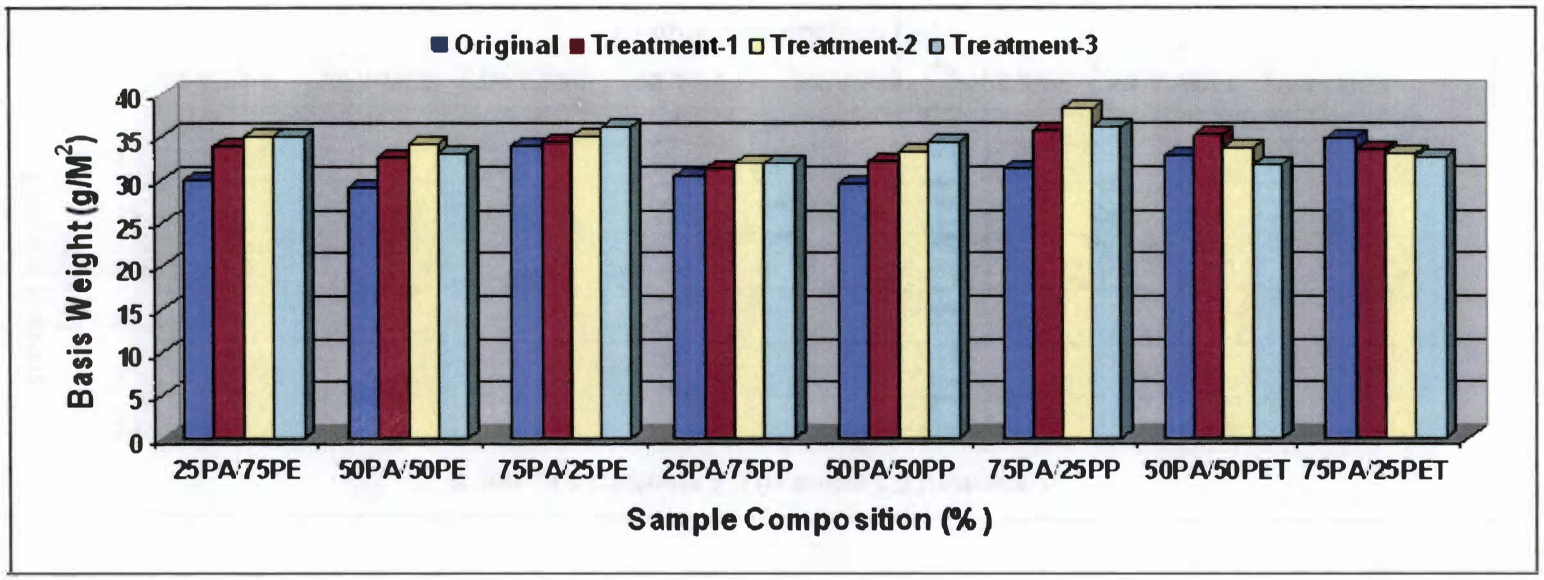

Figure 2.16 Change in basis weight after hydroentanglement

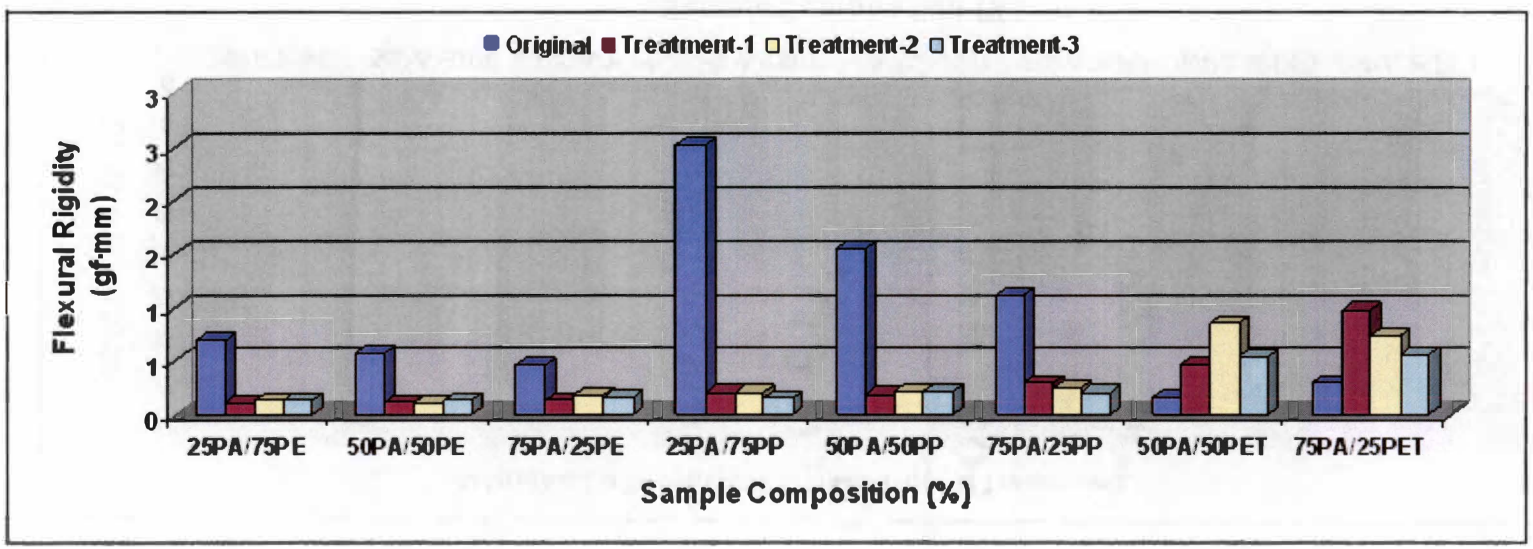

Figure 2.17 Change in flexural rigidity after hydroentanglement

2.3.3 Web Uniformity

Numerous pin holes were observed in the HE treated webs, and the number of the holes increased with HE level (water jets pressure). This might deteriorate web uniformity, and thus have adverse influence on barrier properties and absorption property. Therefore, web uniformity before and after HE was evaluated using WebPro technology.

WebPro is an image analysis system used to evaluate nonwoven web uniformity developed at TANDEC, UTK [29, 30]. This analysis provides results in terms of cell-area-dependant web CV%, i.e., the coefficients of variation for the mean pixel brightness of cells are computed for various cell sizes. The web CV% is calculated as followings: An image is divided into many cells of the same size with each cell consisting of n×n pixels and the coefficient of variation among the cells is calculated for the mean pixel brightness of the cells; this yields one value of the Web CV% (i.e. for cells of size n×n). As the number n is changed, (i.e. cell size is changed), one can obtain a plot of the Web CV% versus cell size. This plot is called the web uniformity spectrum. Three uniformity spectra may be computed: MD, CD, and Total Uniformity Spectra [32].

256 images were selected to evaluate the web uniformity in this test. The web had higher CV after hydroentangling, indicating that web uniformity decreased (Figure 2.18). The pinholes deteriorated the web uniformity which was proved by Webpro measurement, as mentioned earlier in this research.

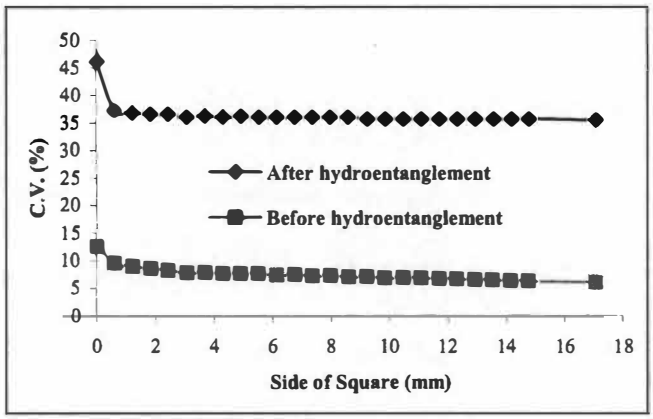

Figure 2.18 Change in total web uniformity of sample 7 after treatment-1

2.3.4 Air Permeability and Hydrostatic Head

The air permeability (Figure 2.19.) increased after hydro-entanglement, which could be attributed to the occurrence of tiny holes in the treated webs, as shown in Figures 2.1 — 2.4. Air permeability of the treated webs increased with the increase of water pressure. The hydro-head (Figure 2.20.) decreased significantly after treatment, which may be due to the same reasons as described about the change in air permeability.

2.3.5 Tensile Properties

The peak load (Figure 2.21.) increased after the hydroentangling treatments, except for three webs (25PA/75PE, 25PA/75PP, and 50PA/50PP); possibly due to the improvement in fiber cohesion in the web caused by the fiber splitting and the enhanced fiber entanglement resulted from hydrodynamic force.

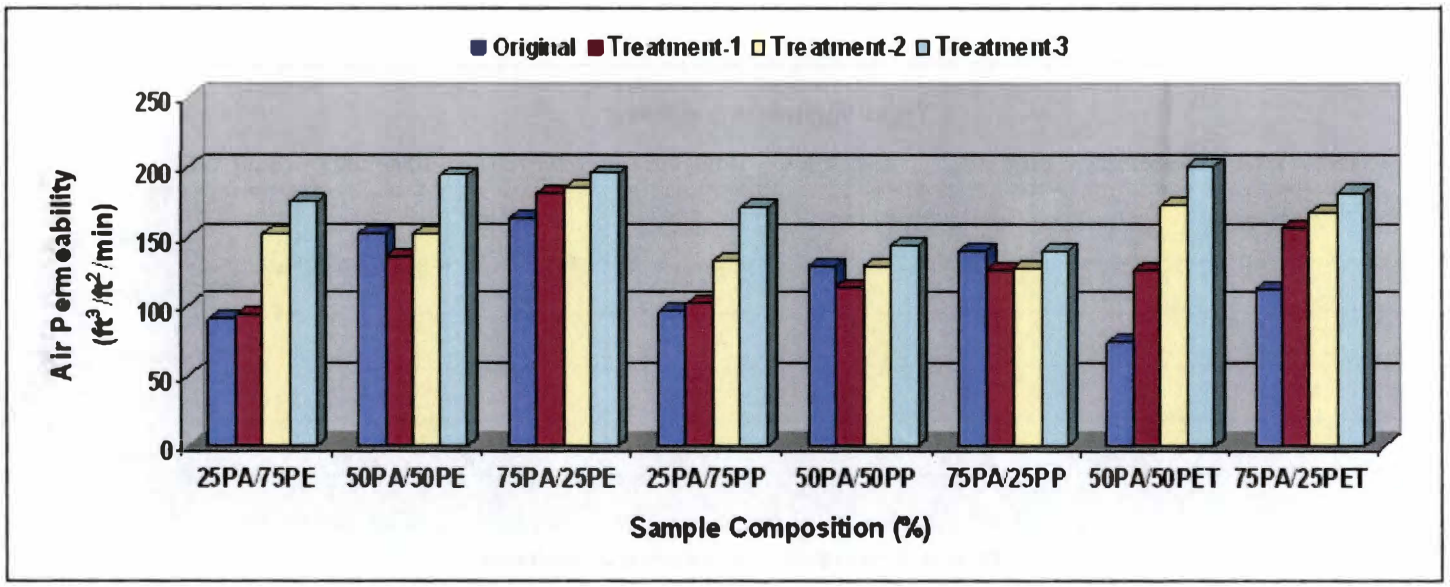

Figure 2.19 Change in air permeability after hydroentanglement

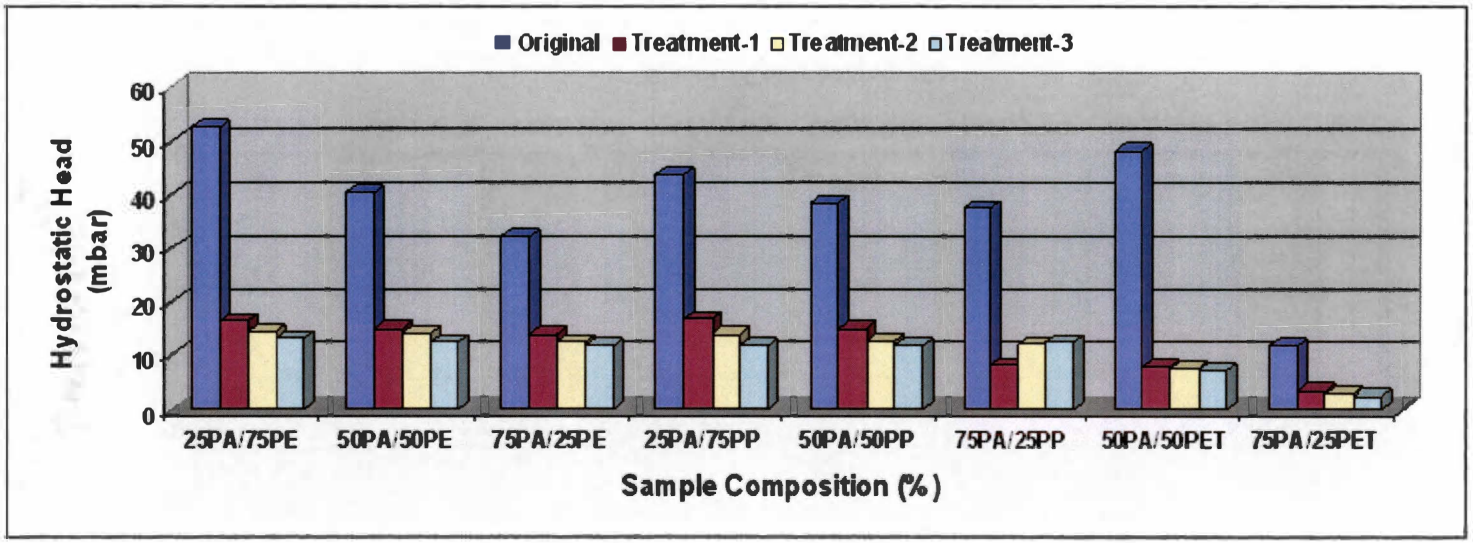

Figure 2.20 Change in hydrohead after hydroentanglement

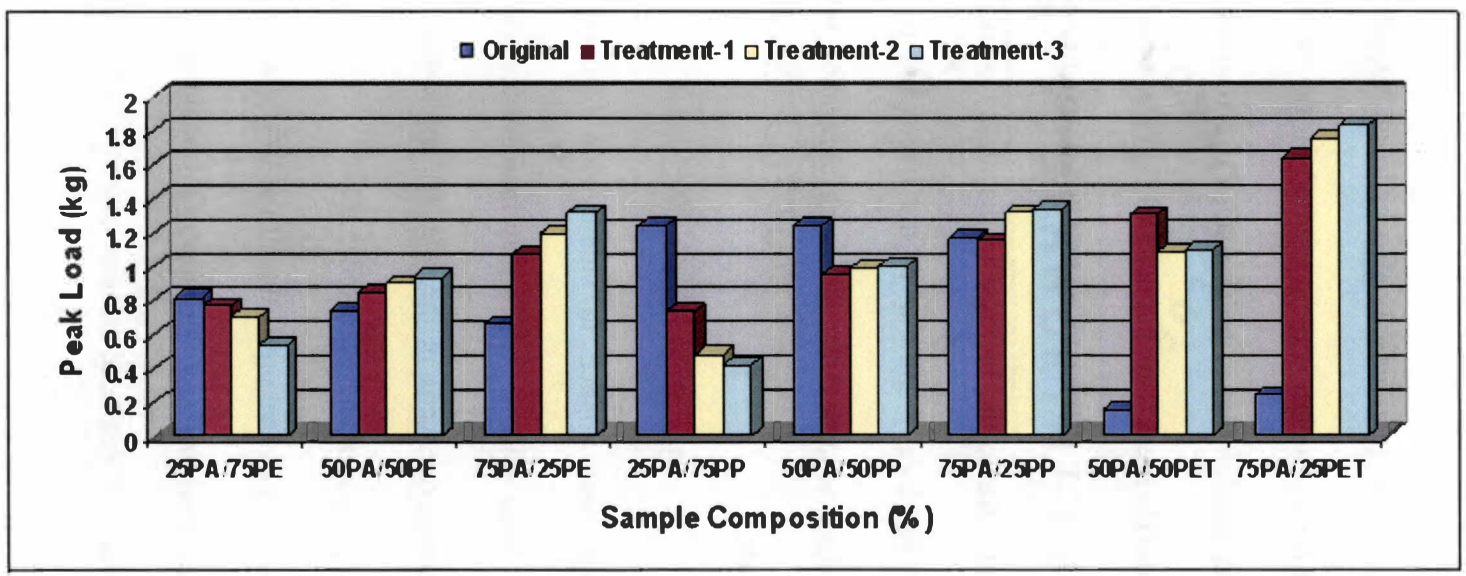

Figure 2.21 Change in peak load after hydroentanglement

Figure 2.22 shows the change in tenacity after hydroentanglement. Among the 8 samples, tenacity increased for 4 samples, while decreased for the other 4 samples. The change trend of tenacity depends on that of break load and that of basis weight, since tenacity is directly proportional to break load, but inversely proportional to basis weight.

As shown in Figure 2.23, the total trend of break extension increased after treatment, which was mainly due to the increase in the ability of deformation of the whole web, as a result of the locally splitting of the fibers and more intense fiber entanglement. There is a slight tendency that the break elongation increases with the increase of water jets pressure.

2.4 Summary

Hydroentanglement has been applied to side-by-side bicomponent meltblown nonwoven webs to achieve fiber splitting, which may increase the application value of bicomponent meltblown nonwoven webs in the relevant application fields, such like filtration, wipers, absorbency, hospital and many other areas.

The configurations and physical properties of the fiber and web changed during hydroentanglement. The thickness increased for most of the samples except PA/PP webs. Air permeability increased while hydro-head pressure decreased after treatment.

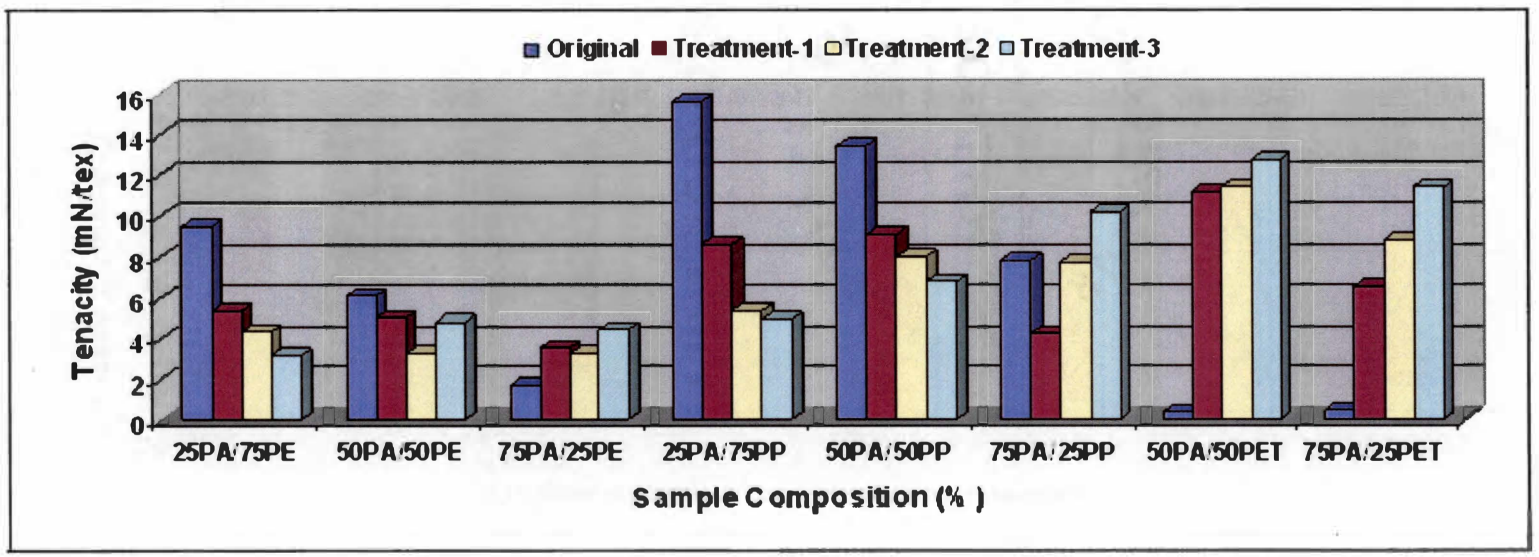

Figure 2.22 Change in tenacity after hydroentanglement

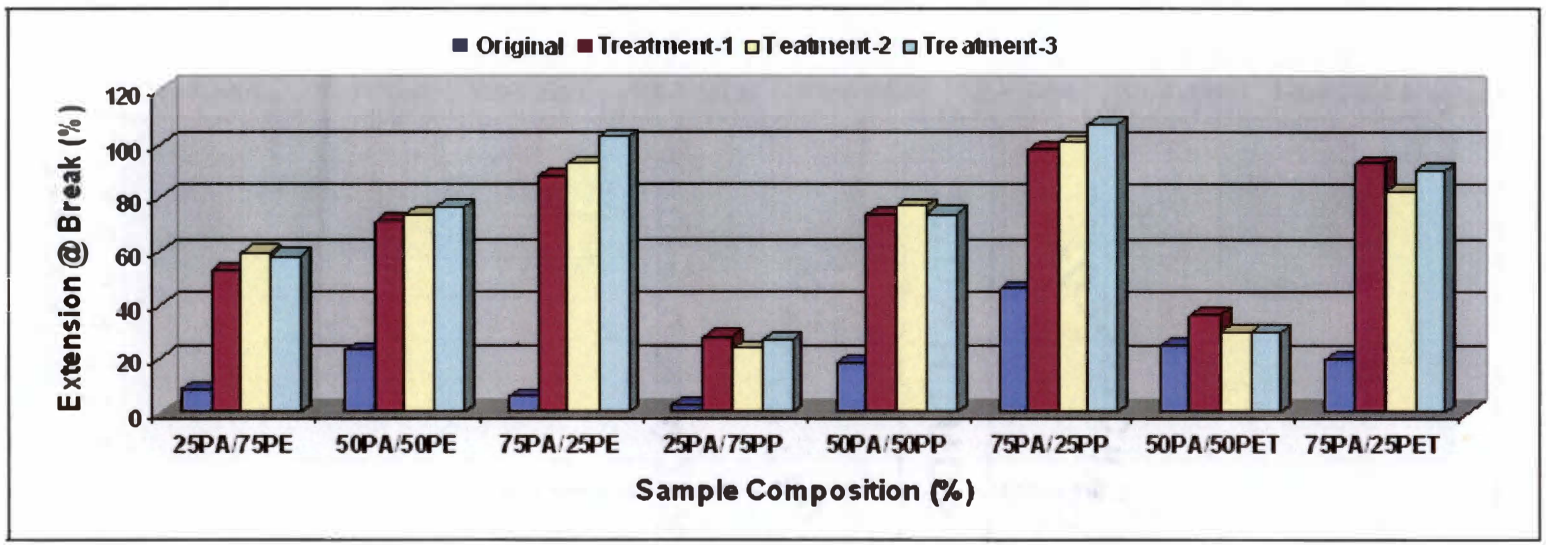

Figure 2.23 Change in extension @ break after hydroentanglement

The peak load overall increased and so did the break extension after treatment. The post-hydroentanglement improved the web softness of PA/PE bicomponent webs and stiffness of the PA/PET webs.

The fiber size decreased due to fiber splitting (Figures 2.8, 2.9 and 2.13) to some extent, after the hydroentangling treatment, especially at higher water pressure. The split fibers after hydroentangling exhibited flat-ribbon like cross-sectional configuration.

Both the fibers and webs treated by hydroentanglement were found damaged from high speed water jets to different degrees. Some fibers exhibited "bitten" configuration along fiber axis; some fibers were broken along the weakest parts of their bulk polymers, instead of splitting at the interface between the two polymers. Bitten-like damage to the fibers could be found in both the non-split fibers and split fibers.

Numerous pin holes could be observed under a microscope and the number of the holes increased with the water jet pressure of the hydroentangling, i.e., the pressure of the water jets. This might deteriorate web structure and hence caused the decrease in filtration and absorbency property as a result, indicating that hydroentangling, which has been successful for splitting spunbonded nonwoven fibers though, might not be suitable for fiber splitting in S/S Bico MB nonwoven webs.

Generally speaking, autogenously bonded meltblown fiber webs are quite weak due to very low molecular orientation. There are numerous interfibrous bonds in MB webs, which are formed when the filaments are still tacky as they are collected. The bonds restrict fiber movements. Therefore, these webs are difficult to split with a mechanical splitting process, such as hydroentanglement.

Although the results of fiber spitting has been partially achieved in S/S Bico/ MB nonwoven webs through hydroentanglement technology, and the web strength, hand and softness could be enhanced, the fibers in the treated webs and the structure of the treated webs exhibited more damage compared to fiber splitting. Therefore, other treating methods were considered to split S/S Bico MB fibers in this research.

3 PRELIMINARY STUDY ON FIBER SPLITTING IN S/S BICO MB NW WEBS THROUGH HEAT-STRETCHING TREATMENT

3.1 Introduction

Heat-stretching (HST) treatment may result in stretchable MB webs, which are desirable in the application fields such as facemasks, diapers and other items designed to seal, since the elastic property impart the webs with softness and comfortability. Heat stretched meltblown webs have the enhanced potential as filters since the heat stretching process can reduce pore size distributions to improve the filtration efficiency [5, 6].

Fiber splitting, which can result in finer microfibers, may occur to S/S Bico MB nonwoven webs during heat-stretching treatment if there is a distinctive difference in stretchability between the two polymer components, based on the previous analysis on fiber-splitting possibility. Meltblown nonwoven fabrics with finer fibers are desirable mainly for the applications in filtration industry (air and liquid), absorbents, wipers, hygiene and hospital protective garments, etc.

Heat treatment has been applied to Bico fiber splitting in melt-spun fibers, carded nonwoven staple fibers and spunbonded nonwoven fibers [42, 47, 85, 88, 97, 98], during which stretching or drawing was incorporated along with heat treatment to induce fiber splitting. However, the fiber composition should be designed to facilitate the fiber

splitting in bicomponent nonwoven fibers. The two components of the bicomponent fibers must be incompatible chemically or physically, such as in chemical structure or heat shrinkage/stretchability/elasticity, etc.

3.2 Experiments

Side-by-side bicomponent meltblown nonwoven webs, produced on Reifenhaüser Bico MB line at TANDEC, UTK, were used to investigate fiber splitting by heat-stretching treatment in this research. The production conditions for the samples used for HST treatment were listed in Table 3.1.

Heat stretching treatments were made at 250 °F and 270 °F respectively on the Stretch Consolidation Pilot Line at the Demonstration Laboratory of TANDEC, UTK. The increasing heat stretching ratios were used until the stretched webs broke, to investigate the possible fiber splitting. A schematic of HST for the equipment used in this research is shown in Figure 3.1.

Table 3.1 Production conditions of the samples used for heat stretching treatments

Sample No.	Sample Composition	Melt Temp. (°F)	Polymer Throughput (g/hole/min)	Air Temp. (°F)	Air Flow Rate (SCFM)	DCD (inch)
1	25PA/75PE	590/480	0.6	580	500	8
2	75PA/25PP	590/580	0.6	600	500	8
3	25PA/75PP	590/580	0.6	600	500	8

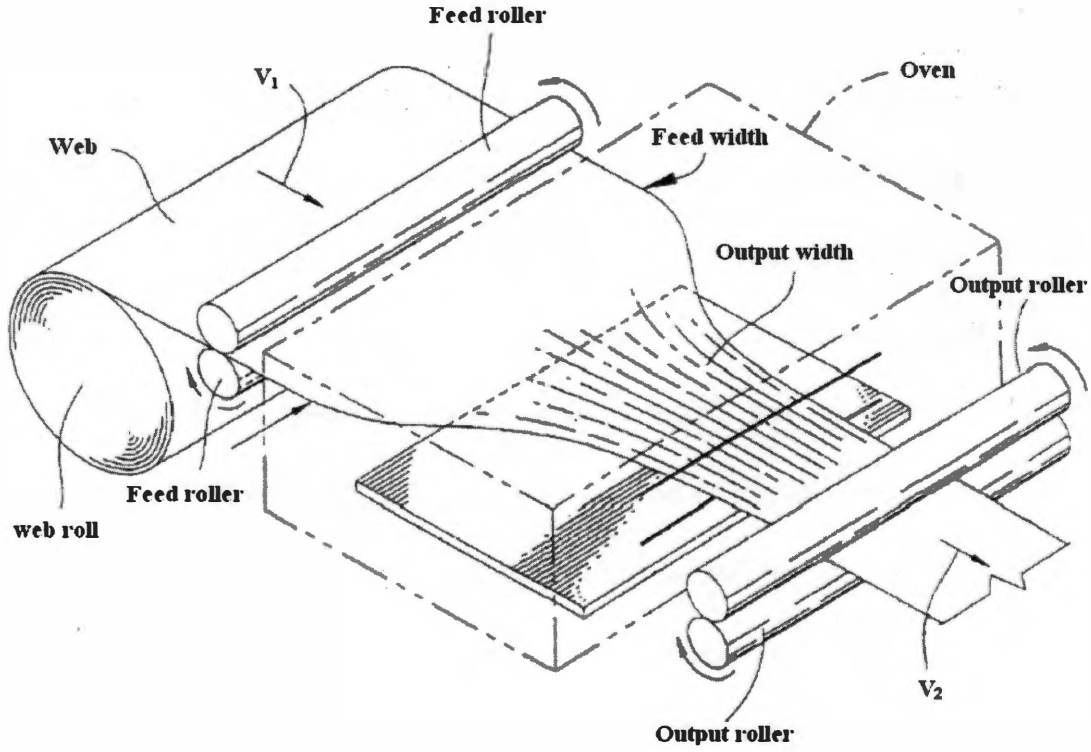

Figure 3.1 Schematic of heat-stretching apparatus

(Revised after Reference[2])

The nonwoven web was passed through a heated zone [2-4, 7] to increase the temperature of the web to its softening temperature while drawing the web in MD thereby greatly plastically bending the CD fibers in the web which consolidates the web in the CD reducing the maximum pore size of the NW web by at least 20%.

Initially the sample web is unwound from roll and fed through the nip of feed rollers, through oven, and finally through the nip of output rollers. The oven is maintained at a temperature to heat the precursor web to a temperature between its softening point and the melting point of the polymers in the web. The rotating rollers are driven at a speed in excess of the rotating feed rollers so that the output velocity V_2 of the web is in the excess of the feed velocity V_1 of the web for the draw ratio which is a function of the velocity ratio V_2/V_1. The initial drawing of the web under thermal conditions causes web to contract within the oven from its feed width to output width.

The changes in fiber diameter, basis weight, web thickness, air permeability, water permeability, tensile property and bending property of the side-by-side bicomponent meltblown webs were examined before and after the heat stretching treatment, according to the corresponding test standards, respectively. In addition, the SEM photos were taken to compare the change in web structure and to examine the phenomenon of fiber splitting.

3.3 Results and analysis

The experimental results for property change of the heat stretched samples are discussed in this section, based on the corresponding ASTM standards. Fiber diameter was measured under a microscope, and totally 35 fibers were measured. (Note: the data at Heat stretching ratio = 1.0, having an orange color line through all of which, indicate the data before the heat stretching treatment, and it is not related to the temperature of the heat stretching treatment).

3.3.1 Changes in Fiber Diameter after Heat Stretching Treatment

As shown in Figure 3.2, fiber diameter decreased for most HST treated samples, but the opposite change in fiber diameter were observed for Sample 1 (25PA/75PE) at 1.4X (i.e., the HST ratio is 1.4), 250 °F, and Sample 2 (75PA/25PP) at 2.0X, 270 °F. In order to evaluate the change of fiber size after different HST treatments, significance tests were performed for the fiber diameter data.

The data set of fiber diameter before and after different HST treatments were listed in Table 3.2. The hypothesis test for two independent samples with different known variances was used to test the significance of fiber diameter change after HST treatment. Now that more than 30 fibers were measured for fiber diameter of each sample, the fiber diameter distribution in each sample could be considered as a normal distribution, namely:

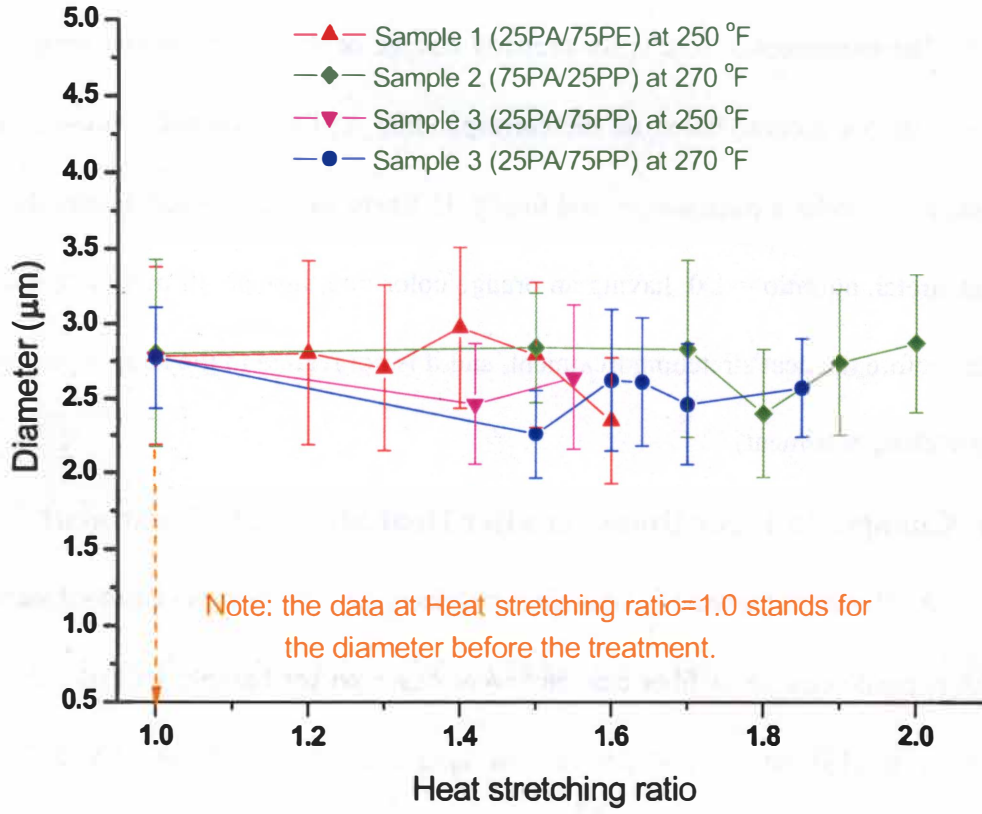

Figure 3.2 Change in fiber diameter after heat stretching treatment

Table 3.2 Fiber diameter before and after HST treatment

Sample 1 (25PA/75PE) HST at 250 °F	HST ratio	1.00	1.2	1.3	**1.4**	1.5	**1.6**
	Mean (μm)	2.78	2.80	2.70	**2.97**	2.79	**2.35**
	STDV (μm)	1.19	1.23	1.11	**1.07**	0.97	**0.84**
Sample 2 (75PA/25PP) HST at 270 °F	HST ratio	1.00	1.50	1.70	**1.80**	1.90	**2.00**
	Mean (μm)	2.80	2.84	2.83	**2.40**	2.74	**2.87**
	STDV (μm)	1.25	0.73	1.18	**0.86**	0.98	**0.92**
Sample 3 (25PA/75PP) HST at 250 °F	HST ratio	1.00	**1.42**	**1.55**			
	Mean (μm)	2.77	**2.46**	**2.64**			
	STDV (μm)	0.67	**0.81**	**0.97**			
Sample 3 (25PA/75PP) HST at 270 °F	HST ratio	1.00	**1.50**	1.60	1.64	**1.70**	**1.85**
	Mean (μm)	2.77	**2.26**	2.62	2.61	**2.46**	**2.57**
	STDV (μm)	0.67	**0.59**	0.95	0.86	**0.81**	**0.66**

Note: Sample size for the original sample was $n_1 = 35$; Sample size for HST samples was $n_2 = 35$. Data at HST ratio = 1.00 stands for the original fiber diameter; STDV stands for standard deviation of fiber diameter.

Original fiber diameter: $X_1, \ldots\ldots, X_{n1} \sim N(\mu_1, \sigma_1^2)$;

HST fiber diameter: $X_2, \ldots\ldots, X_{n2} \sim N(\mu_2, \sigma_2^2)$;

$(\mu_1 - \mu_2)$ yields to z-distribution;

where, Xi is fiber diameter of each sample;

μ_1 and μ_2 are fiber diameters of the original web population and HST treated web population, respectively;

σ_1^2 and σ_2^2 are variances of fiber diameters of the original web population and the HST treated web population, respectively; they are simply the squares of standard deviations (STDVs) of fiber diameters when sample size $n > 30$ (i.e., $s^2 = \sigma^2$);

The following statistic strategy can be used for significance test for fiber diameter change after HST treatment:

Hypothesis test for diameter decrease after HST treatment

H_0: $\mu_1 - \mu_2 \leq 0$ vs. H_1: $\mu_1 - \mu_2 > 0$

If the test statistic $z > z_\alpha$, then reject H_0 and accept H_1 and we can say that fiber diameter decreased significantly at α significance level after HST treatment; if $z < z_\alpha$, then H_0 cannot be rejected, and we cannot say that fiber diameter decreased significantly after HST treatment, at α significance level.

Hypothesis test for diameter increase after HST treatment

H_0: $\mu_1 - \mu_2 \geq 0$ vs. H_1: $\mu_1 - \mu_2 < 0$

If the test statistic $z < -z_\alpha$, then reject H_0 and accept H_1 and we can say that fiber diameter increased significantly at α level after HST treatment; if $z > -z_\alpha$, then H_0 cannot be rejected and we cannot say that fiber diameter increased significantly at α level after HST treatment.

Descriptions of symbols used in statistical test strategy

$$z = \frac{\bar{x}_1 - \bar{x}_2}{\sqrt{\frac{\sigma_1^2}{n_1} + \frac{\sigma_2^2}{n_2}}};$$

$\bar{x}_1$ and $\bar{x}_2$ are fiber diameter means of the original sample and HST treated sample, respectively;

n_1 and n_2 are sample sizes (measured numbers of fibers) of the original sample and HST treated sample, respectively;

α is significance level, (1– α) is confidence level; $z_\alpha = 1.645$ at $\alpha = 0.05$.

The typical results of 9 significance tests for the diameter data in bold (see Table 3.2) were listed in Table 3.3.

Fiber diameter did not significantly decrease for other HST samples that were not listed in Table 3.3.

Table 3.3 Significance tests results for change in fiber diameter after HST treatment

Sample	Test for diameter change	Z value	Comparison of z and z_α	Significance
Sample 1, 1.6X, 250 °F	Decreased	1. 746	$z > z_\alpha$	Yes
Sample 1, 1.4X, 250 °F	Increased	– 0.702	$z > -z_\alpha$	No
Sample 2, 1.8X, 270 °F	Decreased	1.560	$z < z_\alpha$	No
Sample 2, 2.0X, 270 °F	Increased	– 0.267	$z > -z_\alpha$	No
Sample 3, 1.42X, 250 °F	Decreased	1.745	$z > z_\alpha$	Yes
Sample 3, 1.55X, 250 °F	Decreased	0.652	$z < z_\alpha$	No
Sample 3, 1.5X, 270 °F	Decreased	3.380	$z > z_\alpha$	Yes
Sample 3, 1.7X, 270 °F	Decreased	1.745	$z > z_\alpha$	Yes
Sample 3, 1.85X, 270 °F	Decreased	1.258	$z < z_\alpha$	No

Based on the significance tests above, the increase in fiber diameter after HST treatment was not statistically significant; it was possibly caused due to the difficulties in measurement. As known in the art, the webs shrank greatly in CD after HST in MD; it became rather hard to measure fiber diameter of MB microfibers under a microscope. Therefore, it could not be concluded that fiber diameter increased after HST treatment.

In fact, fiber diameter decreased after HST treatment for most of the HST treated samples, though the decrease in diameter was not significant for some samples. Although we may conclude that fiber diameter decreased after HST treatment, no fiber splitting was observed in the SEM photos of the HST treated samples, as discussed later in this chapter. The decrease in fiber diameter possibly resulted from fiber elongation

during the HST treatment at temperatures between softening points and melting points of the polymer components. Fibers possibly already broke before they could be stretched to split, due to the poor strength of MB fibers.

However, most of web properties changed after heat stretching treatment as analyzed in the followings.

3.3.2 Changes in Web Thickness after Heat Stretching Treatment

During the heat stretching of the webs, fibers align along the machine direction of the web, therefore two controversial changing trends in the web structure will have an influence on the change in thickness with the increase in heat stretching ratio: the webs will be stretched along MD meanwhile shrink along CD. If the MD elongation dominates the CD shrinkage, the web thickness will decrease as a result; if the CD shrinkage dominates the MD elongation, the web thickness will increase finally. The results of change in web thickness were shown in Figure 3.3.

For sample 1(25PA/75PE), the thickness increased after heat stretching and kept increasing with the increase in heat stretching ratio, which indicates that the web was stretched all the way until breakage. The web could achieve a greater thickness at 250 °F compared to the thickness achieved at 270 °F, which indicates, that the web shrinkage dominated when stretched at 250 °F, however, the web elongation dominated when

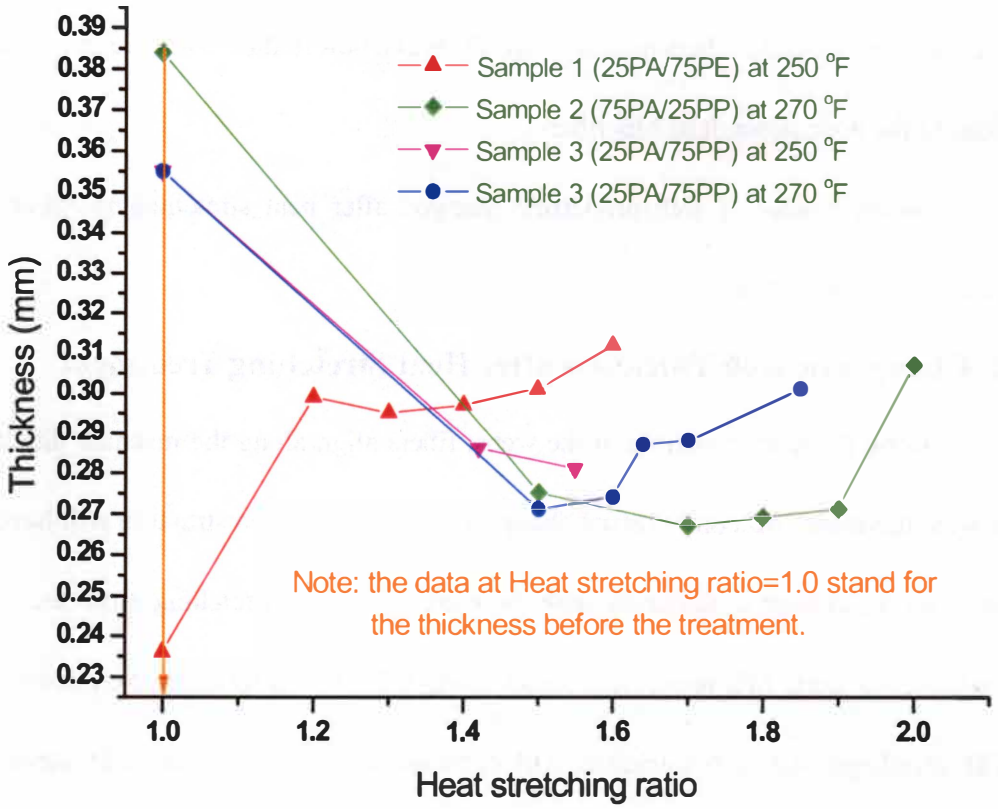

Figure 3.3 Change in thickness after heat stretching treatment

stretched at 270 °F. In addition, the thickness decreased after stretching at 270 °F, but increased after stretching at 250 °F.

Sample 3 (75 PP/25PA) were stretched at the temperature of 250 °F and 270 °F respectively. The sample thickness changed in the similar tendency, except that the thickness of the sample stretched at 250 °F was a little bit greater than that at 270 °F. The thickness of the web decreased after HST treatment.

When stretching Sample 3 at 250 °F, thickness decreased with the increase of stretching ratio; but the thickness increased with the increase in stretching ratio, when stretching at 270 °F, indicating that the web elongation dominated in the former process, but the web shrinkage dominated in the latter process. The web thickness decreased after stretching treatment at both the temperatures.

3.3.3 Changes in Basis Weight after Heat Stretching Treatment

Web structure, including web thickness, web uniformity, fiber orientation, etc, has important influence on the basis weight of nonwoven web. Sample 1 had the greatest basis weight after HST among the four treated samples due to the greatest CD shrinkage. The changes in web basis weight after HST treatment were shown in Figure 3.4.

For sample 1, basis weight increased first then decreased before web breaking, indicating that web turned thicker first but became thinner right before breaking when stretched at 250 °F.

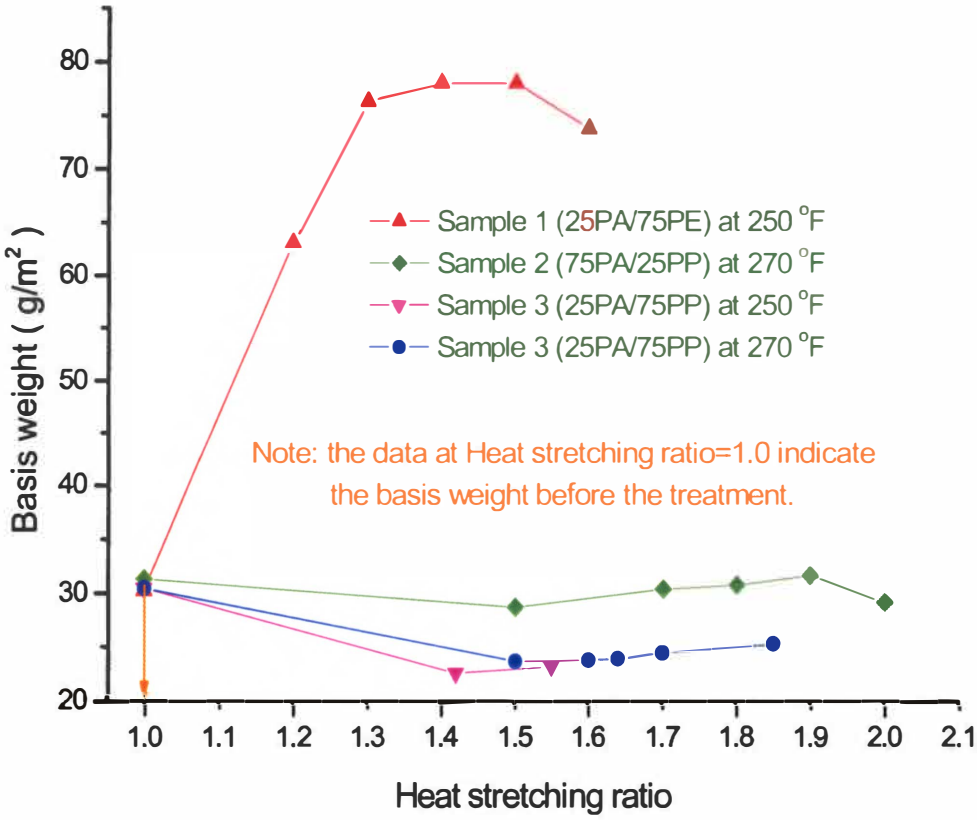

Figure 3.4 Change in basis weight after heat stretching treatment

For samples 2 and 3, the thickness decreased after stretching treatment and then increased with the increase in stretching ratio, except of sample 2 (at 270 °F) decreased slightly right before web breakage. Sample 3 only could bear a smaller stretching ratio when stretched at 250 °F, but it could bear a higher ratio when stretched at 270 °F.

3.3.4 Changes in Air Permeability after Heat Stretching Treatment

The air permeability of all the samples, as shown in Figure 3.5, decreased after heat stretching treatment, and decreased with the increase in heat stretching ratio, except sample 3 (at 270 °F), which indicated a thicker web before web breakage, and the web broke with greater strength and less elongation. No matter web thickness increased or not after stretching, air permeability decreased with the increase in HST ratio, due to the porosity decrease caused by the alignment of fibers along machine direction.

3.3.5 Changes in Bending Stiffness after Heat Stretching Treatment

The bending stiffness is directly proportional to basis weight and bending length, which are related to the web structure and fiber structure. The MD bending stiffness (Figure 3.6) of all the samples exhibited exactly the same trend or similar trend as it appeared to basis weight versus heat-stretching ratio.

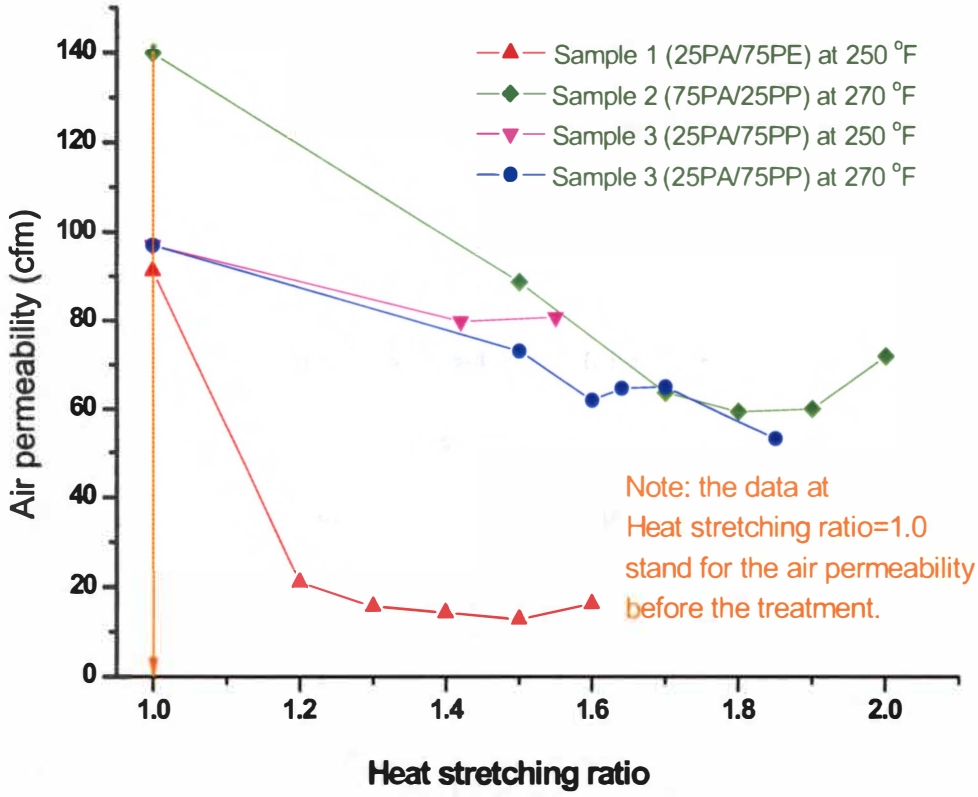

Figure 3.5 Change in air permeability after heat stretching treatment.

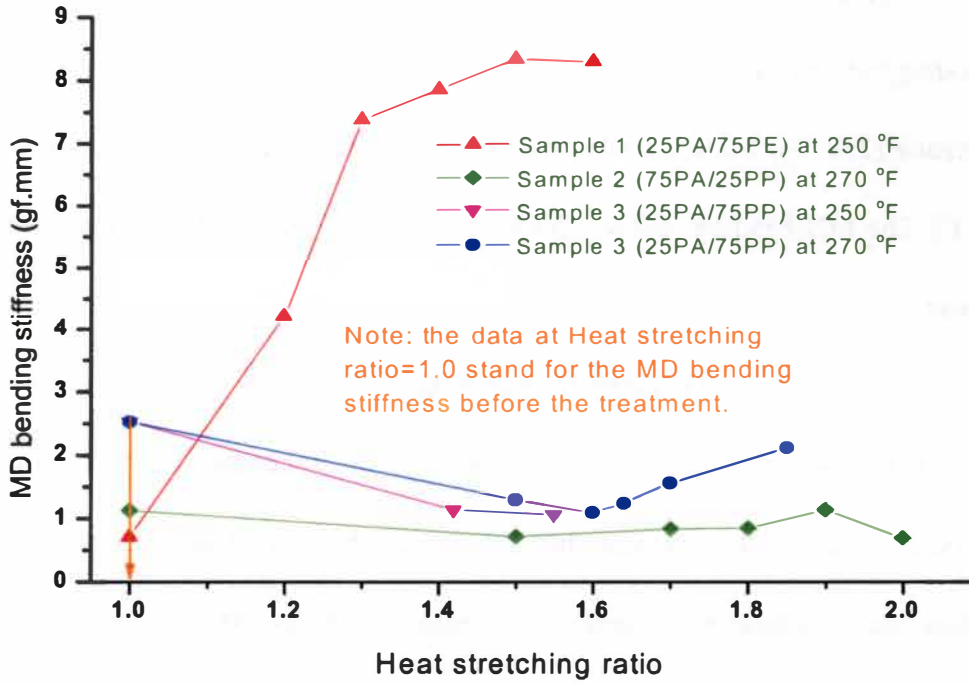

Figure 3.6 Change in bending stiffness (MD) after heat stretching treatment

Sample 3 was stretched at 250 °F and 270 °F respectively, and it was found from the bending test results, , that sample 3 only could stand smaller stretching ratios at lower temperature (250 °F), while it could bear greater stretching ratios at higher temperature (270 °F). The MD bending stiffness for all the samples increased after heat stretching treatment.

The results of CD bending stiffness (Figure 3.7) of all the samples showed the similar trend after heat stretching treatment. The CD bending stiffness decreased dramatically after HST treatment, but the values did not change greatly with the stretching ratio. Before the treatment, the meltblown webs exhibited nearly isotropic structure; while after HST treatment, the fibers in the treated web aligned dominantly along machine direction, therefore web properties exhibited anisotropic after HST treatment.

3.3.6 Changes in Peak Load after Heat Stretching Treatment

Generally, the more the fibers align along a certain direction of the web, the more strength of the web along this direction, because more fibers can bear the foreign force at the same time; meanwhile, the strength in the other direction will decrease. However, the increase in strength usually results in the adverse change in breaking elongation of the web. The elongational ability of the web will be influenced by the temperature at which the web is heat-treated, and to what extent it is stretched.

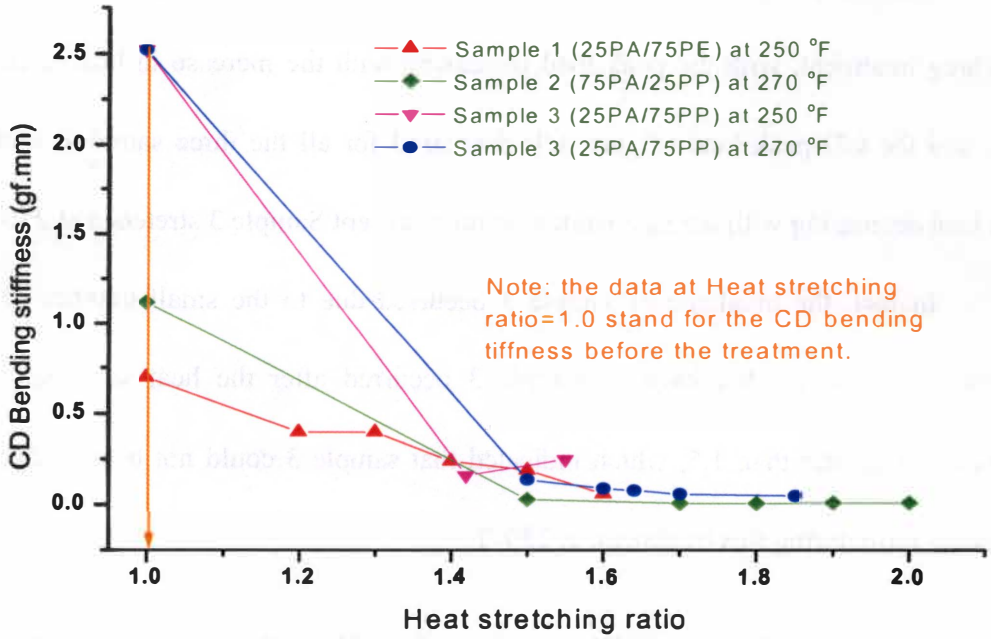

Figure 3.7 Change in bending stiffness (CD) after heat stretching treatment

The MD peak load (Figure 3.8) increased for all the three samples after the heat stretching treatment, with the peak load increasing with the increase in heat stretching ratio; and the CD peak load (Figure 3.9) decreased for all the three samples, with the peak load decreasing with the heat stretching ratio, except Sample 3 stretched at 250 °F.

In fact, the breakage of sample 3 occurred due to the small number of data obtained. In fact, the breakage of sample 3 occurred after the heat stretching ratio increased to greater than 1.5, which indicated that sample 3 could not bear higher heat stretching ratio during this treatment, at 250 °F.

3.3.7 Changes in Breaking Elongation after Heat Stretching Treatment

The MD elongation (Figure 3.10) of sample 1 and sample 2 decreased after heat stretching treatment, with the elongation decreasing with the increase in heat stretching ratio. This was because the fibers dominantly aligned along the machine direction after the heat-stretching treatment, therefore the ability of the fiber slipping among each other decreased, and hence the elongation at break decreased as a result. But, the adverse trend occurred to sample 3, stretched at both the temperatures of 250 °F and 270 °F. The MD elongation at break of sample 3 increased by a small amount after heat stretching treatment, but the trend of the increase in MD elongation at break with the increase in stretching ratio is not significant, based on the observation to the curves in Figure 3.9.

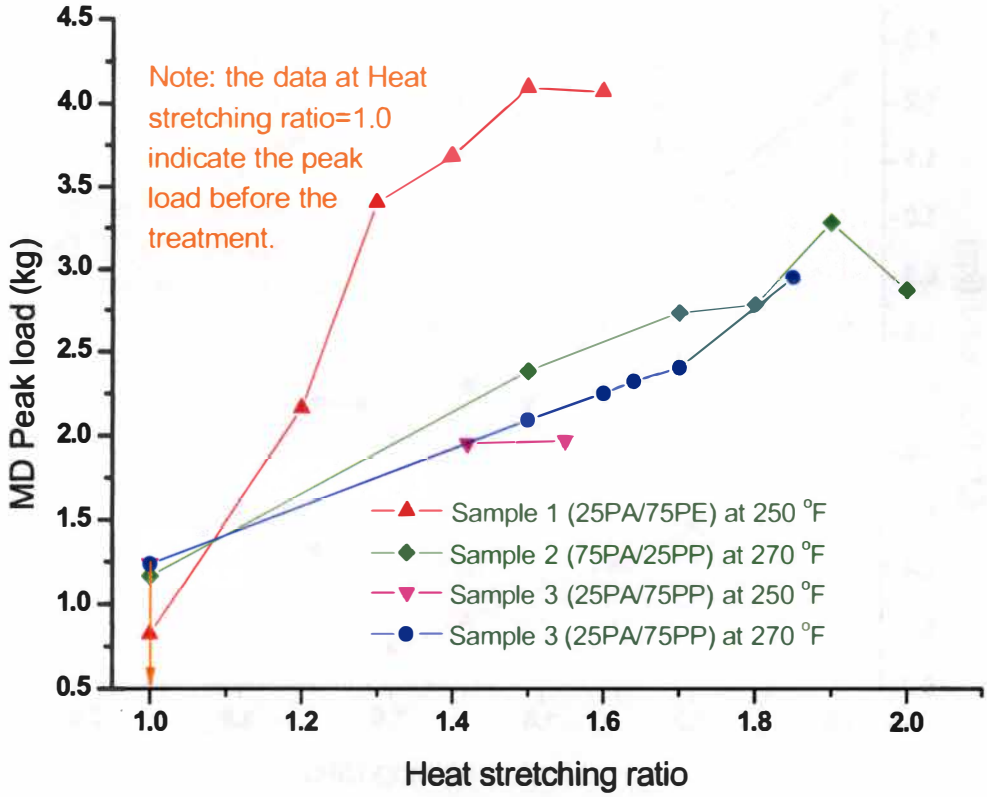

Figure 3.8 Change in MD peak load after heat stretching treatment

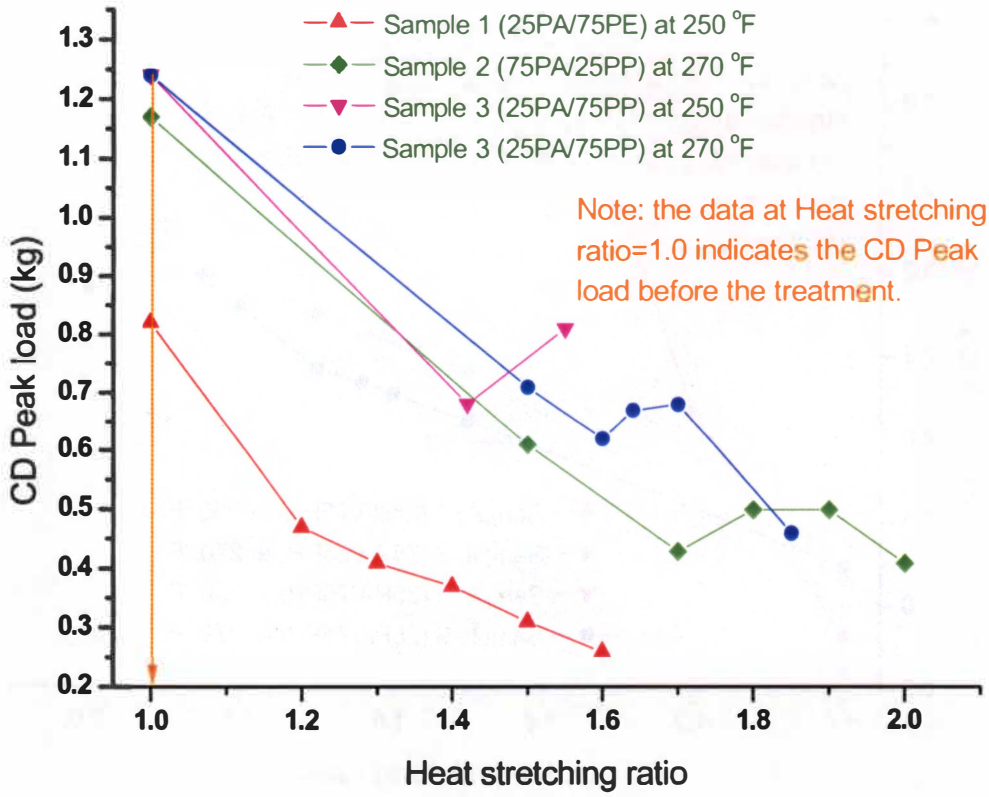

Figure 3.9 Change in CD peak load after heat stretching treatment

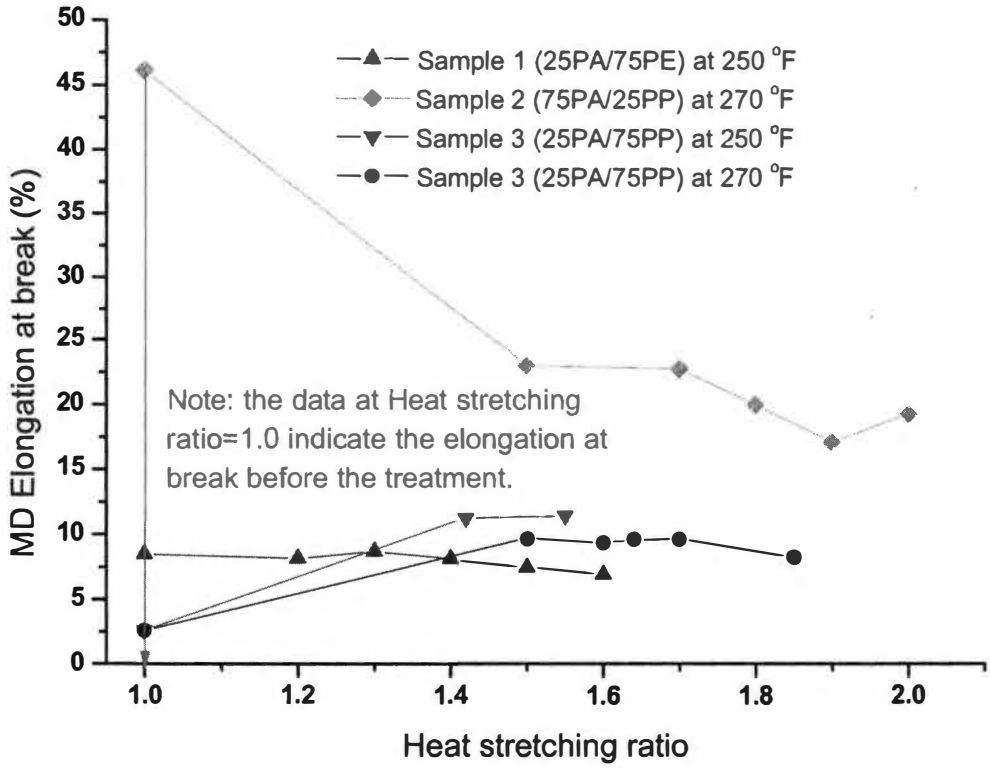

Figure 3.10 Change in MD Elongation at break after heat stretching treatment

The CD elongation (Figure 3.11) of all the samples increased after heat stretching treatments, and increased with the increase in stretching ratio.

3.3.8 Changes in Tenacity after Heat Stretching Treatment

As shown in Figures 3.12 and 3.13, after heat stretching treatment, the tenacity in both MD and CD directions increased. The MD tenacity increased with the increase in heat stretching ratio because more fibers aligned along MD with the increase in stretching ratio; while the CD tenacity decreased with the increase in heat stretching ratio as a general trend, except for sample 3 treated at the temperature of 270 °F. The increase in CD tenacity after treatment was mainly due to the increase in elongation ability, so that the web could bear greater stretching, after the heat stretching treatment. As we know, the web may have a greater breaking strength if the web is stronger, or it can deform greatly when subjected to the action of a foreign force.

3.3.9 Changes in Elasticity after Heat Stretching Treatment

Since no standard method is available for the measurement of elastic recovery ability of the nonwoven fabrics, the recovery measurement from the stain of 50% elongation at break of the web was designed based on the following steps: (1) calculate each elongation needed for the strain of 50% elongation at break for each sample at different stretching ratio; (2) set the gage length of the specimen at 3 in., and the tensile speed at 12 mm/min; (3) stop the crosshead and let it go back to the original gage length

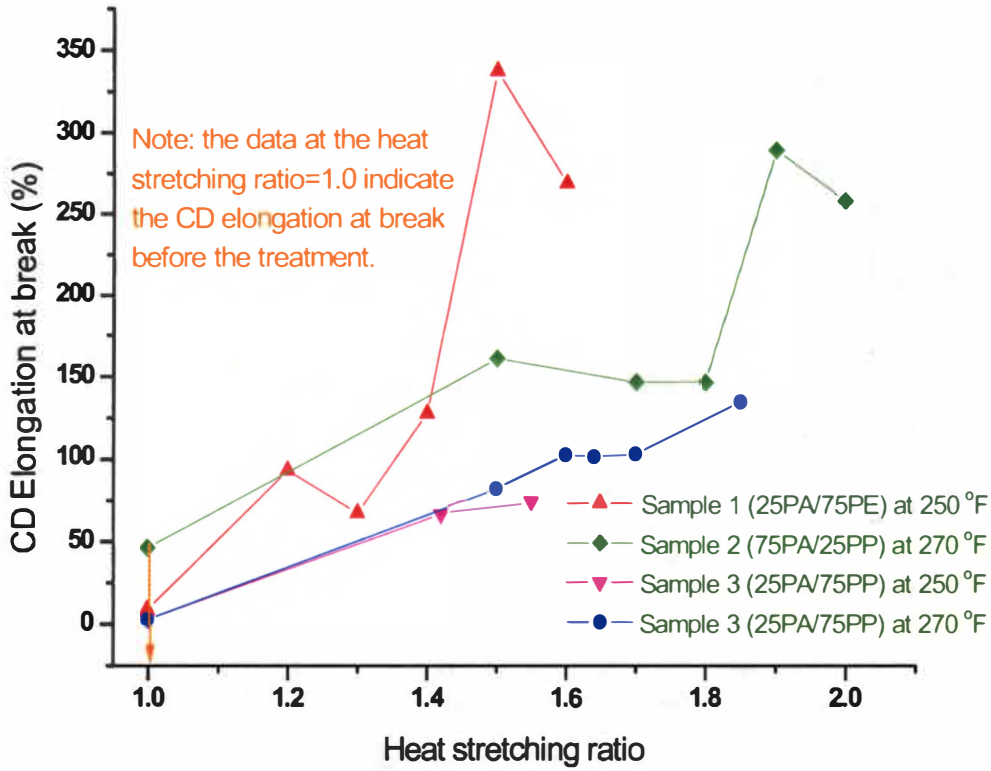

Figure 3.11 Change in CD elongation at break after heat stretching treatment

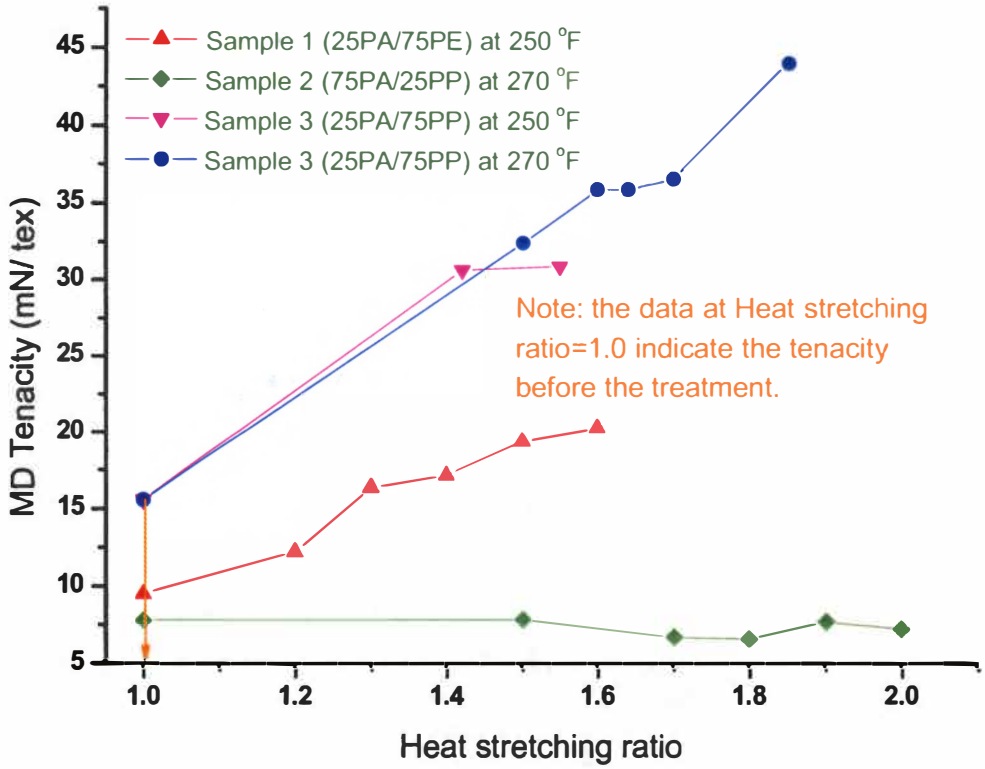

Figure 3.12 Change in MD tenacity after heat stretching treatment

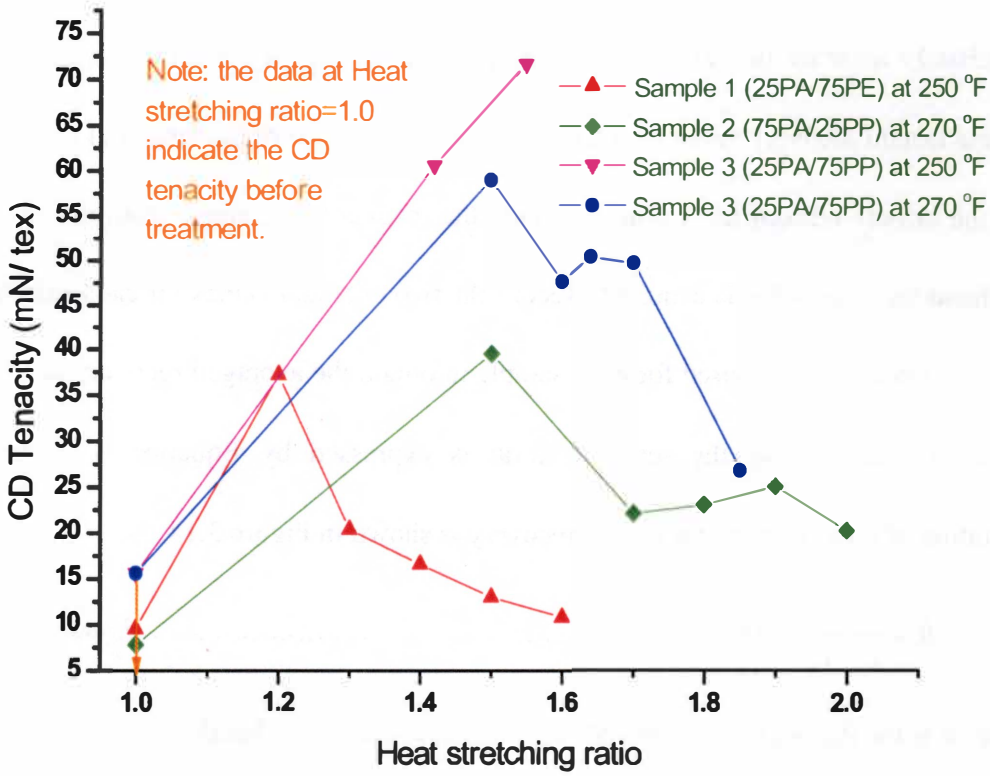

Figure 3.13 Change in CD tenacity after heat stretching treatment

position when the desired elongation position determined in step (1) is reached; (4) immediately measure the length of the sample after getting it off the testing machine, then the instant recovery value is obtained this way. Re-measure the length of the sample after the sample relaxed for 3 min., and then the recovery percentage from the strain of 50% breaking elongation is acquired. Record the two obtained values for each sample; (5) three specimens are measured for each sample to obtain the averaged recovery ratio. The formula for calculating the recovery ratio is expressed by Equation 3.1, and the illustration of measurement for elastic recovery is shown in Figure 3.14.

$$R = \frac{L - L'}{L - L_0} \times 100\% \quad \text{.....} \textit{Equation 3.1}$$

where, R is the Recovery (%) from 50% strain of elongation @ break;

L_0 is the original gage length (3 inch) between the two mark lines before drawing;

L is the set length, L = L_0 + 50% strain of elongation @ break;

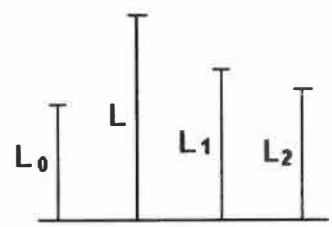

Figure 3.14 Illustration for elastic recovery test for HST treated sample

L' is the sample length between the two marking lines on the sample measured immediately after the sample was released from the tensile tester (L_1) or measured after the sample was removed from the tester and relaxed for 3 min (L_2).

Only sample 3 (25PA/75PP) stretched at 270 °F was selected for the investigation of the elastic recovery ability of the webs treated with HST and was compared to the recovery data before the heat stretching treatment (Figure 3.15). Since the breaking elongation of this sample before heat stretching treatment was only 2.56%, therefore its recovery (%) from the 50% strain of its breaking elongation was as high as 90.6%, due to the elongation of 1.28% was still in the region of its elastic deformation limit. Therefore, for this sample, the recovery (%) from its 50% strain of breaking elongation before the heat stretching treatment was greater than those after the treatment. But this did not mean that the sample was stretchable before the treatment, because it only could be stretched to 2.56% before breakage; but after the treatment, it could be stretched to around 150% before breakage at 270 °F. After the treatment, both the curves of instant recovery, and the recovery at 3 min., from the strain of 50% breaking elongation were observed to exhibit a "W" shape, with the increase in heat stretching ratio, with the recovery at 3 min being greater than the instant recovery. The recovery percentages for both the instant recovery and the recovery at 3 min range from about

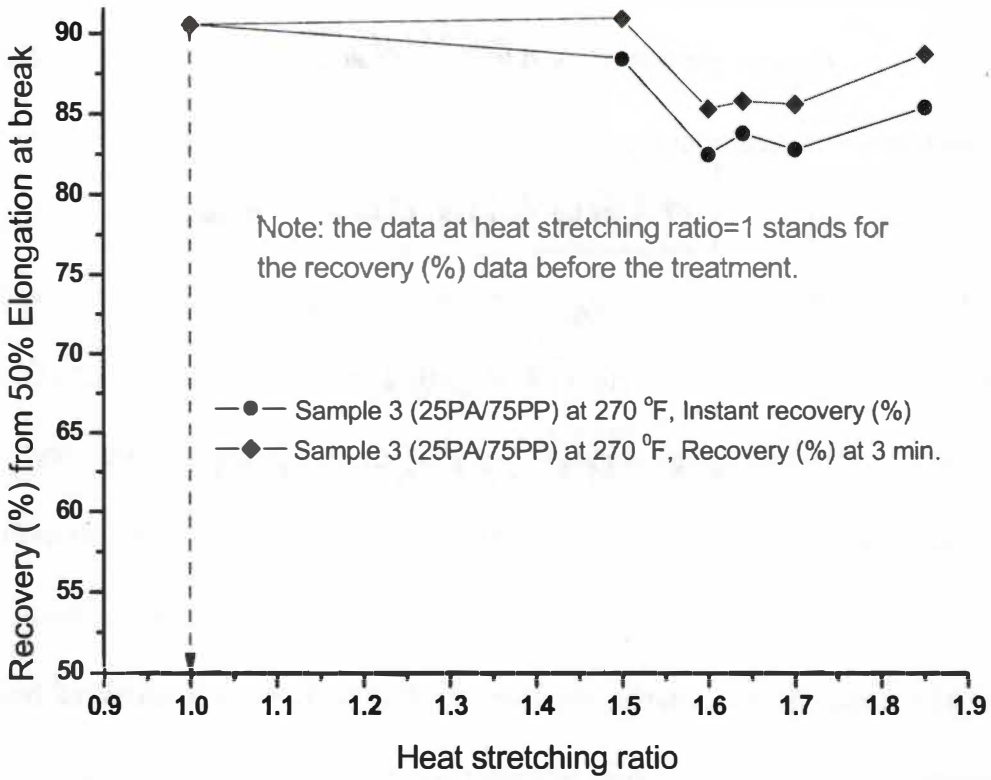

Figure 3.15 Elastic Recovery (%) from the strain of 50% elongation at break

82.5% to about 91%, indicating that the elastic recovery ability of the heat stretched sample 3 (at 270 °F) is high enough, and the meltblown nonwoven webs after heat stretching treatment may be considered as elastic material for the associated applications, such as the diapers and other applications. However, before the treatment, both the instant recovery and the recovery at 3 min were the same, due to this sample was too brittle before the treatment, and 3min time period could not help much in the recovery.

3.3.10 Changes in Web Structure after Heat Stretching Treatment

The SEM photos of the samples taken before and after the heat stretching (Figures 3.16-3.19) showed that the fibers dominantly arranged along the machine direction after the heat stretching treatment; no fiber splitting was observed after the treatment.

3.4 Summary

The general trends of changes in web structure and properties after heat stretching treatments, excluding few exceptions were summarized below; all the changes resulted from the permanent thermoplastic deformation during heat stretching treatment with the fiber being rearranged in the stretched webs.

Web thickness increased, as the result of web shrinkage after heat-stretching; but it might decrease before web breaking as the HST ratio increased highly enough. Fibers aligned preferentially along machine direction after HST treatment. No fiber

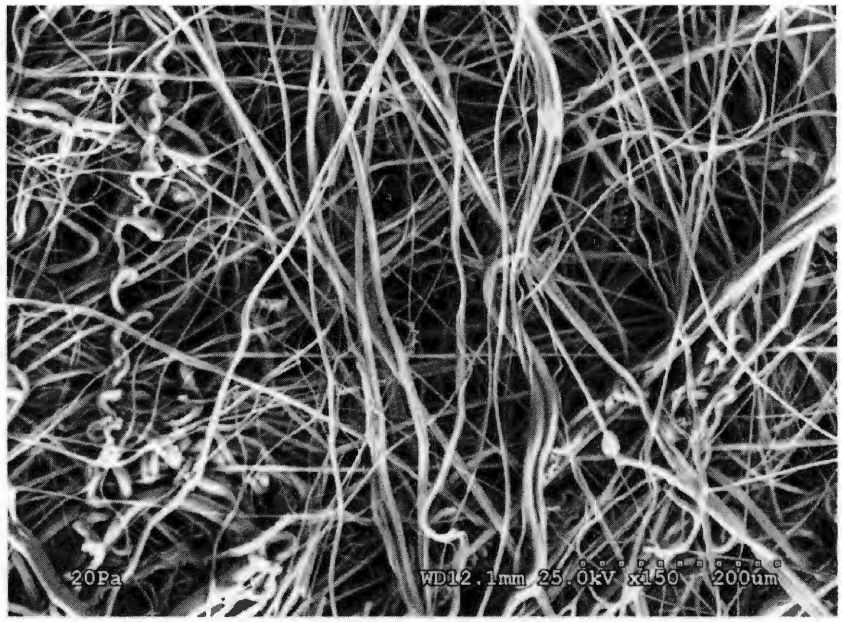

Figure 3.16 Fibers are randomly distributed in the web of sample 3 (75PP/25PA) before heat stretching treatment

Figure 3.17 Fibers aligned along machine direction in the web of sample 3 (75PP/25PA) after HST at 250 °F, with HST ratio 1.55

Figure 3.18 SEM photo of sample 1 (75PE/25PA) before heat stretching treatment

Figure 3.19 SEM photo of sample 1 (75PE/25PA) after heat stretching treatment

splitting was observed after heat stretching treatment for all the samples in this research; therefore the heat-stretching treatment alone could not result in fiber splitting in bicomponent meltblown nonwoven fabrics used in this research.

Basis weight increased, due to the dominant fiber orientation along MD direction and web shrinkage. MD flexibility increased while CD flexibility decreased after heat stretching treatment, due to the fiber orientation along MD direction. Air permeability decreased, as the result of web shrinkage after heat-stretching treatment; but it might increased before web broke if the HST ratio increased highly enough.

It appeared that fiber diameter decreased slightly after the heat stretching treatment, and the decrease in fiber diameter was significant for some HST treated samples. However, the meltblown webs gained more elasticity after heat-stretching treatment; the recovery (%) from the strain of 50% breaking elongation ranged from about 82.5% to around 91%.

Tensile properties of the meltblown web samples changed greatly after heat stretching treatment. Generally, the tensile properties along the machine direction were improved in terms of MD peak load and tenacity, but the elongation at break decreased; while the tensile properties in the cross machine direction increased in terms of CD elongation at break and tenacity, with the strength being decreased. The CD tenacity decreased with the increase in heat stretching ratio.

4 PRELIMINARY STUDY OF FIBER SPLITTING IN S/S BICO MB NONWOVEN WEBS USING NaOH TREATMENT

4.1 Introduction

NaOH has been used as an agent in weight-reduction post-treatment to achieve finer PET fibers in traditional melt-spinning industry and textile industry [85-89], through the hydrolytic reaction between PET structure and NaOH. After the dissolving of the outside part of PET fibers, the PET fibers become finer but lose some weight and strength, and the resultant PET fabric has a hand feeling and appearance of suede. NaOH may cause fiber splitting in nonwoven webs as a swelling agent if treating bicomponent nonwoven web composed of PET or PBT component in NaOH solution at appropriate conditions. The concentration of the solution, temperature, bath ratio and time are important parameters influencing on the results of NaOH treatment.

NaOH was used as a fiber-splitting inducing agent in the post treatment to investigate fiber splitting in PE/PET and PP/PBT S/S MB NW webs in this research. The conditions for NaOH treatments were investigated based on the corresponding SEM photos. Fiber diameter and web properties were tested for the change before and after NaOH treatment.

4.2 Fiber Splitting in 25PE/75PET S/S Bico MB Web

The S/S MB nonwoven web samples with the composition of 25PE/75PET (sample ID 7-27-99-1.19) were treated in NaOH (Fish ChemAlert® Guide NaOH pellet, Fisher Scientific, NF/FCC) solutions under different conditions, to investigate the optimal condition for fiber splitting.

4.2.1 Experiments of NaOH Treatment

The fiber splitting possibility was examined by treating the 25PE/75PET S/S MB sample in the NaOH solution with the concentration of 50g/l ($NaOH/H_2O$) (5% NaOH/solution) at 100 °C for 150 min. The bath ratio (web/water by weight) was 1:20. After that, the sample was treated in the NaOH solution with increased concentration, i.e., 200g/l (16.7%) and 300g/l (23.1%) respectively, for different time periods.

The treated webs and the residue alkaline solutions were neutralized with the HCl solution of the equivalent concentration to safely dispose the alkaline remained in the solution.

4.2.2 Results and Analysis

The results of diameter change after NaOH treatment with the Bath ratio of 1/20 and temperature of 100 °C is listed in Table 4.1.

Table 4.1 Diameter change after NaOH treatment of 25PE/75PET MB web

Concentration (weight ratio)	50 g/l (5 % NaOH/solution)	200 g/l (16.7 % NaOH/solution)					300 g/l (23.1 % NaOH/solution)			
Time (min)	150	1	3	8	15	30	1	3	8	15
Diameter(μm)	1.82	2.17	2.12	1.51	1.55	1.80	2.22	1.74	1.37	1.45

Note: The fiber diameter before treatment is 2.40 μm.

The decreased fiber diameter was observed for all the treated conditions, compared to the original fiber diameter of 2.4 μm.

When treating the sample in the NaOH solution with both the concentrations of 200g/l (16.7%) and 300 g/l (23.1%), the fiber diameter decreased with the increase in treating time before 15 min; but, after that time, the fiber diameter increased, possibly because the fibers became too weak after strong treatment with NaOH solution, and the split, finer fibers might break and then were washed off after rinsing with water.

The sample lost its strength after treating with 300 g/l (23.1%) NaOH solution for 30 min, therefore its diameter was not listed in the table above.

The decrease in fiber diameter encouraged the further investigation of the fiber splitting possibility using the NaOH solution treatment to the bicomponent meltblown samples.

4.3 Fiber Splitting in 50PBT/50PP S/S Bico MB Web

Based on the preliminary study on fiber splitting in 25 PE/75PET S/S MB web, the concentration of 200 g/l (16.7%) might be selected as the appropriate NaOH treating condition, since the treated web lost most of strength after treating with 300 g/l NaOH solution. Both 8 min and 15 min could be proper treating time for later NaOH treatments.

Although fiber diameter was decreased from 2.40 μm to 1.51 μm (200 g/l, 8 min) and 1.37 μm (300 g/l, 8 min), no obvious fiber splitting was observed with the corresponding SEM photos. In the later research, 50PBT/50PP S/S MB web was selected for the investigation of Bico fiber splitting, because PBT also belongs to polyester polymer family; the reaction could occur between NaOH and PET may happen to NaOH and PBT. In addition, the 50/50 Bico ratio may result in greater increase in fiber surface area, if the Bico fiber could be split.

4.3.1 Experiments and Results

The S/S Bico MB nonwoven web composed of 50PBT/50PP (sample ID: 7/28/99-2.14), was treated in the NaOH solution with the concentration of 200 g/l (16.7%), bath ratio of 1/20, at the temperature of 100 °C, for 1, 3, 8, 15, 30 and 45 min, respectively.

Before putting into NaOH solutions, the samples were pre-treated with surfactant solution to improve the wettability, which could facilitate the treatment of 50PBT/50PP MB web in NaOH solution. After soaking in surfactant solution for 15 min or so, gentle patting the samples to help wetting them until they got wet thoroughly; then took out the samples and washed them sufficiently with water, treated them using the NaOH solution at the foresaid conditions.

The treated 50PBT/50PP MB samples were measured the fiber diameter and weight loss, and the results were listed in Table 4.2.

The weight loss was resulted from the superficial hydrolysis of the PBT component in the Bico MB fibers. The reaction possibly happened during the NaOH solution treatment might be expressed as Equation 4.1:

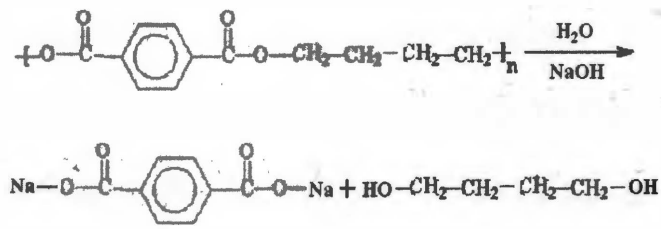

.....*Equation 4.1*

Table 4.2 Results of NaOH treatment of 50PBT/50PP MB web at different time

Treating time (min)	0	1	3	8	15	30	45
Fiber diameter (μm)	2.35	2.33	2.21	2.01	1.87	1.83	1.82
Weight loss ratio (%)	0	1.00	2.33	11.3	24.7	40.2	48.3

The hydrolysis reaction occurred to the surface of PBT part in 50PBT/50PP MB web during the NaOH solution treatment, it was easy for the hydrolysis to the PBT part when alkaline existed in the solution as the catalyst, at the temperature around 100 °C. The hydrolysis of PBT component in the 50PBT/50PP Bico MB fibers made the alkaline treated samples lose weight; therefore basis weight and tensile properties might change after the NaOH solution treatment.

SEM photos were taken to examine the possible fiber splitting before and after the foresaid treatments, as shown in Figures 4.1 to 4.4 respectively (blue circles – split fibers; green circles – damaged fibers).

Based on the SEM pictures above, the hand and appearance of the treated webs, the following results were observed: (1) Fiber splitting began when the treating time achieved 3 min; (2) Fiber splitting was only achieved to a limit degree, but treated fibers were damaged by NaOH; (3) Some fibers began to partially dissolve with the increase in NaOH concentration, and the webs lost strength and weight when the treating time was longer than 15 minutes at higher NaOH concentration; (4) The optimal NaOH treating conditions could be taken to be the condition with bath ratio 1/20, temperature 100 °C, concentration 16.7% and time 15 min, since fiber splitting was observed most obviously in the SEM photos of the sample treated at this condition, and the properties of the

Figure 4.1 50PBT/50PP MB web after treating with 16.7% NaOH for 3 min

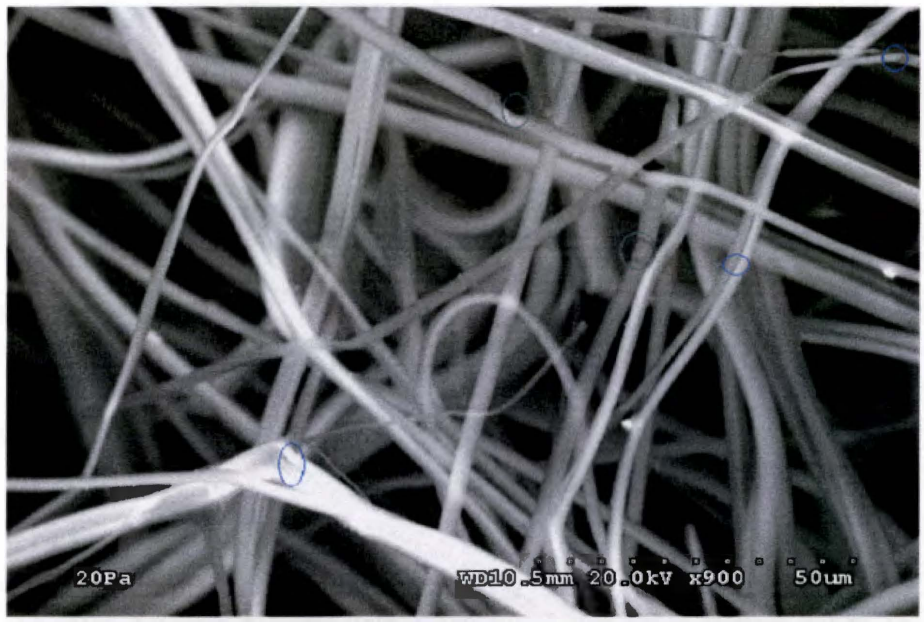

Figure 4.2 50PBT/50PP MB web after treating with 16.7% NaOH for 15 min

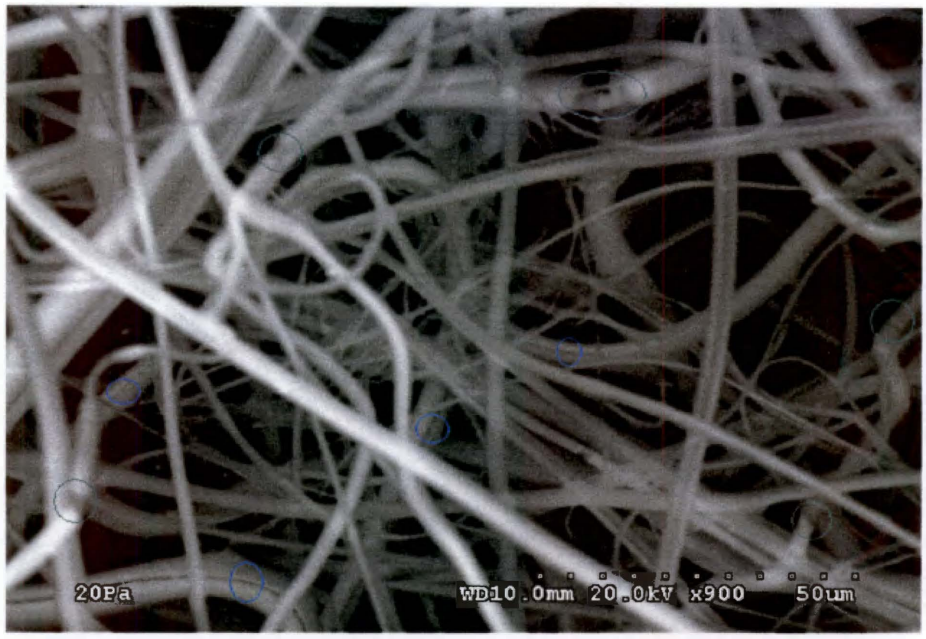

Figure 4.3 50PBT/50PP MB web after treating with 16.7% NaOH for 30 min

Figure 4.4 50PBT/50PP MB web after treating with 16.7% NaOH for 45 min

treated web did not deteriorate too much; namely, the treated web did not lose much of its strength, as found in the subsequent property analysis.

4.3.2 Changes in Web Structure and Property after NaOH Treatment

Fiber splitting was observed in the SEM picture of the 50PBT/50PP S/S MB web treated with NaOH solution under the condition of bath ratio 1/20, temperature 100 °C, and concentration 16.7 % at different treating time. The changes in web structure and web property of the 50PBT/50PP MB web, before and after NaOH treatment, were investigated, including the control sample, which was treated in water.

The 50PBT/50PP S/S MB web was cut into two types of samples: (1) 10 in ×10 in size, 8 pieces for the measurements of web shrinkage, basis weight, thickness, air permeability and hydrostatic head tests; (2) 10 in × 1 in size, 8 pieces in MD for tensile properties and bending property test. For better wetting, the samples were soaked in surfactant solution (e. g., the liquid soap) for 10 to 15 min, until all the samples were wet thoroughly, and then the pre-treated samples were pressed to remove the water from them. For comparison, the control experiment was done under the same conditions except water was used for treating the samples. The treating conditions were listed in Table 4.3.

The NaOH treated sample and the control sample as well as the original sample were tested for the web structure and property. Changes in fiber size, general web properties including web shrinkage ratio, basis weight, web thickness, fiber diameter, air

Table 4.3 NaOH treating conditions for 50PBT/50PP MB sample

	Bath ratio	Concentration (%) (200 g/l)	Temperature (° C)	Time (min.)
Treatment	1:20	16.7	100	15
Control	1:20	0	100	15

permeability, hydro head, tensile properties and flexural rigidity were measured based on the corresponding test standards. The results were illustrated in Figures 4.5 and 4.6. The tensile property and bending property shown in Figures 4.5 and 4.6 were measured along machine direction (MD).

Figures 4.5 showed that the fiber diameter decreased after treating the 50PBT/50PP S/S MB NW samples with water and NaOH solution, with the fiber diameter decreasing from 3.14 μm to 2.57 μm (water treated) and then to 1.73 μm (NaOH treated). The following significance tests show that the decrease in fiber diameter was statistically significant at significance level 0.05. The parameters used for the significance tests and the test results were shown in Table 4.4.

Although fiber diameter of water-treated sample decreased significantly from 3.14 μm to 2.57 μm, there was no proof showing fiber spitting after the control treatment; the reason for the fiber diameter change was possibly due to the systematic error occurred during the measurements and wide fiber distribution in the original MB web.

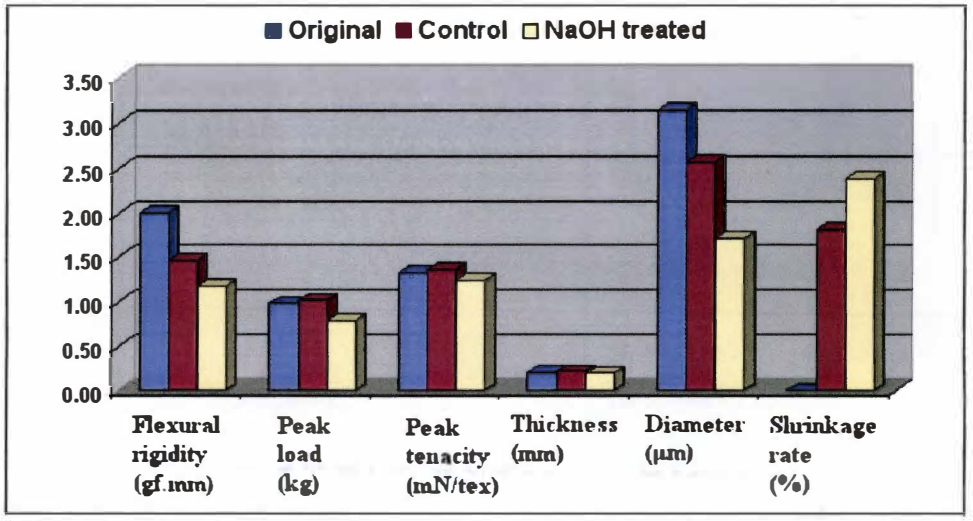

Figure 4.5 Changes in web stiffness, peak load, tenacity, thickness and fiber diameter among the original, control and treated samples

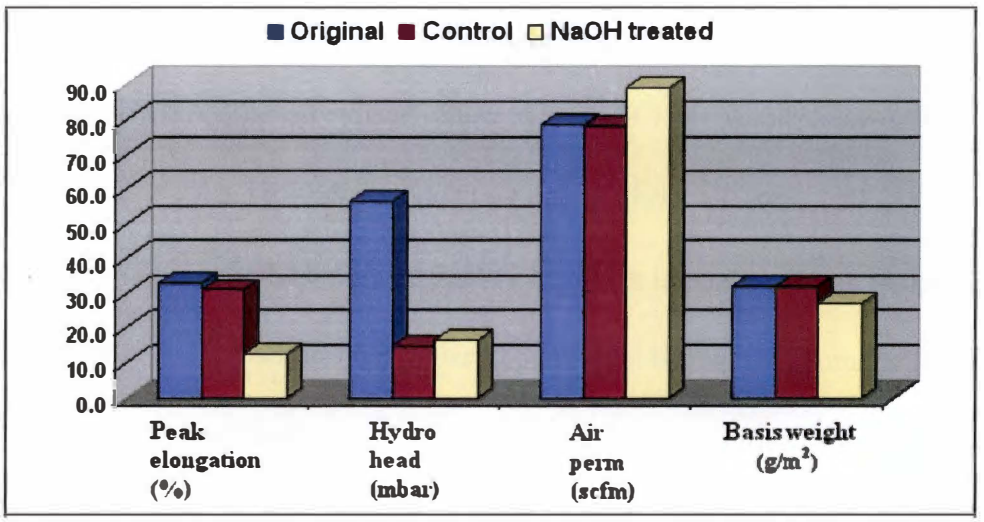

Figure 4.6 Changes in web elongation @ peak, hydrohead, air perm and basis weight among the original, control and treated samples

Table 4.4 Parameters and results of significant test for diameter change

Sample	Test parameters	Test for	z value	Comparison of z and z_α	Significance
Control	$\bar{x}_1 = 3.14, s_1 = 1.01, n_1 = 38$ $\bar{x}_2 = 2.57, s_2 = 0.62, n_2 = 38$	Diameter decreased	2.965	$z > z_\alpha$	Yes
NaOH	$\bar{x}_1 = 3.14, s_1 = 1.01, n_1 = 38$ $\bar{x}_2 = 1.73, s_2 = 0.57, n_2 = 38$	Diameter decreased	7.495	$z > z_\alpha$	Yes

Note: Significance level $\alpha = 0.05$; $z_\alpha = 1.645$.

However, things are different for the fiber diameter of NaOH treated samples. Fiber diameter of 50PBT/50PP S/S MB NW web significantly changed after treating with NaOH solution at the foresaid conditions (1:20 bath ratio, 200 g/l concentration, 100 °C, and 15 min time), due to the possible hydrolysis on PBT surface.

The Web shrank by 1.83% after water treatment and by 2.39% after NaOH treatment resulted from the swelling and shrinkage of the PBT part in the Bico fibers. Web thickness and basis weight exhibited a consistent trend after treating with pure water and NaOH solution. The web thickness and basis weight of the control sample increased slightly due to web shrinkage during the treatment in pure water but no significant fiber splitting occurred during the water treatment. In addition, the once-in-a-while agitation during the water treatment might cause fiber entanglement on the web surface, and thus

the web thickness might increase slightly after water treatment. But the web thickness and basis weight of NaOH treated sample decreased slightly due to the web shrinkage and slightly fiber splitting, and/or web weight reduction. The web weight reduction possibly resulted from the hydrolysis of the surface of PBT component of the Bico MB fibers, as explained before.

Air permeability decreased slightly after treating the sample with water and increased after treating with NaOH solution. The increase in air permeability of the NaOH treated sample could be attributed to the weight reduction of the web, which could be proved by the notable decrease in web basis weight, and the slight fiber splitting after the NaOH treatment. Hydrohead decreased dramatically after treating the 50PBT/50PP sample in water and NaOH solution. However, this did not mean that the split fibers contributed to the increase in water permeability; the application of surfactant as a pre-wetting agent might cause the water molecules to easily transport from one side of the web to the other side. The similar results could be observed in the later experiment in which the samples were pre-treated in surfactant solution to improve wettability before treating with water and other chemical agent (benzoic acid).

Peak load and peak tenacity increased slightly after water treatment and then decreased after NaOH treatment. Elongation at peak load decreased due to web shrinkage

and fiber/web damage from weight reduction, which resulted from the hydrolysis of the PBT part in the Bico MB fibers.

Flexural rigidity decreased after water treatment and alkaline treatment respectively, due to the fiber size decrease and weight loss. The smaller fibers resulted in the softer treated webs.

Although fiber splitting was observed in the SEM photos of NaOH treated samples, we could not conclude that NaOH might cause fibers to split, because the degree of fiber splitting was very low, and the corresponding control experiments were not performed. It was hard to say if water caused fiber to split during NaOH treatment. However, the results showed that NaOH treatment was not an appropriate way for fiber splitting in S/S polyolefin/polyester MB webs.

4.4 Summary

NaOH treatment was used to investigate fiber splitting in 25PE/75PET and 50PBT/50PP S/S Bico MB NW webs respectively. After NaOH treatment, fiber diameter of the two webs decreased with treating time and concentration of NaOH solution. 25PE/75PET web lost much of its original strength after NaOH treatment for longer time or with higher concentration. 50PBT/50PP web lost weight due to hydrolysis of PBT component. After treating for 45 min with 16.7% NaOH at 100 °C, fibers in 50PBT/50PP web started to dissolve.

Fiber splitting was observed in 50PBT/50PP web, but meanwhile more damaged fibers were observed. Web properties of 50PBT/50PP MB web were evaluated after treated with NaOH solution under the condition of 1:20, 16.7%, 100 °C and 15 min. Fiber diameter decreased significantly after NaOH treatment due to hydrolysis of PBT component. Web lost weight and basis weight decreased. Thickness increased slightly due to web shrank after NaOH treatment. Web strength decreased due to web damage from NaOH treatment, but the treated web gained softness. Air permeability increased due to web shrinkage and hydrohead decreased due to pre-treating web with surfactant.

NaOH treatment was not a good way to split fibers in 25PE/75PET and 50PBT/50PP S/S Bico MB webs, due to the lower degree of fiber splitting and the deteriorated web properties after treatment.

5 FUNDAMENTAL STUDY OF FIBER SPLITTING IN S/S BICO MB NONWOVEN WEBS THROUGH BENZOIC ACID TREATMENT

Based on the diffusion theory addressed in Chapter 1, greater difference in solubility parameter between the two polymers in the Bico fiber may result in less compatibility between the two components, and hence the higher tendency of fiber splitting during the subsequent treatments. Therefore, the selection of the Bico polymer pair and the post treating agent (solvent), which can help to induce fiber splitting, is a very important issue.

5.1 Selection of S/S MB Samples and Post-treating Agent Suitable for Fiber Splitting

It has been shown in the previous preliminary studies (Chapter 2 through Chapter 4), that splitting S/S Bico MB fibers was rather difficult compared with splitting spunbonded and carded nonwoven fibers. Therefore, the selection of Bico polymer pairs and post-treating methods appeared to be very important in the research of Bico MB fiber splitting. The Bico polymer pairs and appropriate chemical agent would be selected based on the fiber splitting mechanism discussed in Chapter 1.

5.1.1 Selection of 50PA6/50PET Bico MB Webs for the Investigation of Fiber Splitting

The polymer pairs with the difference in solubility parameter greater than 2 $(cal/cm^3)^{1/2}$ were considered to be used for fiber splitting in this research, since they are theoretically immiscible/incompatible and they would tend to separate later on in the fiber-splitting inducing post-treatment. The solution parameters of PET, PA6 and PP are 10.7 $(cal/cm^3)^{1/2}$, 13.0 $(cal/cm^3)^{1/2}$ and 8.3 $(cal/cm^3)^{1/2}$, respectively [76, 78, 99]. Since the difference in solubility parameter between PET and PA6 is 2.3 $(cal/cm^3)^{1/2}$, and that between PA6 and PP is 4.7 $(cal/cm^3)^{1/2}$, there existed the potential possibility for fiber splitting in S/S Bico MB webs with the composition of PA6/PET and PA6/PP. The 50/50 Bico weight ratio was selected for the fiber splitting investigation, since there would be largest increased surface area if fiber splitting occurred in the subsequent BA treatment. Therefore, the S/S Bico MB NW webs with the Bico ratios of 50PET/50PA6 and 50PA6/50PP were selected for the investigation of fiber spitting.

5.1.2 Selection of Benzoic Acid as the Fiber-splitting Inducing Agent

The solubility parameter of benzoic acid was calculated based on the Small Theory [100], as shown in Equation 5.1:

$$\delta_3 = \rho \Sigma F_i / M_0 \quad \text{Equation 5.1}$$

where ρ is the density, F_i is the molar attraction constant, and M_0 is the molecular weight.

The solubility parameter of benzoic acid is calculated to be 12.1 $(cal/cm^3)^{1/2}$, based on the equation above, using the parameters given below:

ρ = 1.2659 g/cm^3, M_0 = 122; F(carboxyl) = 1000.1 $(J\ cm^3)^{1/2}$ and F(phenyl) = 1398.4 $(J\ cm^3)^{1/2}$ [100] , knowing that 1 J = 0.23884 cal.

When the 50PET/50PA6 S/S MB meltblown web was treated in BA solution, the benzoic acid was expected to enter and swell both of the two components, although more benzoic acid would be expected to react with PA6, since the difference in solution parameter between BA and PA6 is 0.9 $(J/cm^3)^{1/2}$, less than that between BA and PET, which is 1.4 $(J/cm^3)^{1/2}$.

Since the difference in solution parameters between PP and PA6 is 4.7, therefore the 50PP/50PA6 S/S Bico MB web could be suitable for fiber splitting through benzoic acid treatments. However, the difference in solution parameters between PP and benzoic acid is 3.8, and that between PA6 and benzoic acid is only 0.9, therefore the benzoic acid was expected to enter PA6 polymer and swell the PA6 part, at lower concentration, to form internal stress at the interface between PA6 and PP, and decrease the adhesion strength at the interface, and finally result in the separation of the two components of the fiber.

The benzoic acid possibly does not have the effect of swelling the PP part of the bicomponent fiber, based on the analysis on the difference in solution parameters

between PP and benzoic acid.

5.2 Selection of Methods for Evaluating the Degree of Fiber Splitting

Split fibers in Bico MB NW webs may result in increased specific surface area of the fibers in the web, and thus increase the adsorption efficiency of the nonwoven web; more split fibers would bring about greater adsorption of the Bico nonwoven webs. The aim of splitting Bico fibers was to increase the specific surface area of the fibers in the web, and hence improve the adsorption ability of the nonwoven web. Therefore, it was necessary to develop proper methods to describe the increasing degree of (specific) surface area of the fibers after fiber splitting.

Two characterization terminologies could be employed to describe the change in (specific) surface area of the fibers in the treated Bico S/S MB webs, i.e., **fiber splitting ratio** and **initial dye adsorption ratio/initial dyeing ratio**.

5.2.1 Fiber Splitting Ratio

Fiber splitting ratio, as an indicator of the change in fiber surface area, could be related to the specific surface area of the fiber. Traditionally, the degree of fiber splitting was represented by **fiber splitting ratio (%)**, which may be the ratio of the number of split fibers divided by the total number of visible fibers in a SEM photo or a microscopic photo; or the ratio of the cross-sectional area of the split fibers vs. the total

cross-sectional area of the total fibers in an image. There would be no difference between these two methods if all the fibers in the sample have exactly the same diameter, and assume that the cross-sectional area of the fibers do not change after the treatment and cutting for SEM/microscopic photos. However, the deviation in MB fiber diameter is very great; therefore there would be great difference in fiber splitting ratio obtained from the two different calculating methods. In this research, the former method (counting number of fibers) was used to characterize the degree of fiber splitting.

Assume that a fiber split from one end all the way to the other end (completely split) with the averaged fiber length of l, and the fiber has a perfect round cross-sectional configuration with the averaged diameter D. Then a splittable 50/50 bicomponent fiber could become two equal parts after fiber splitting with the splitting ratio R (%), as shown in Figure 5.1.

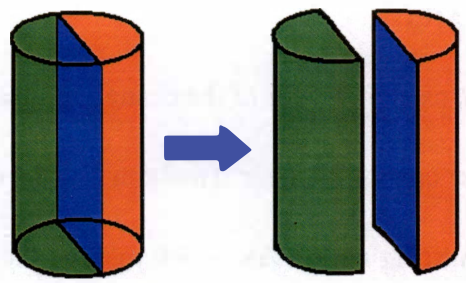

Bicomponent fiber = Component A + Component B

Figure 5.1 Illustration of Bico fiber splitting

Assume that the total number of fibers in a Bico nonwoven sample is n, then the increased ratio of (specific) surface area ΔS (in fact, the increased ratio of specific surface area is equal to the increased ratio of surface area, since the volume of a Bico fiber does not change after the Bico fiber splits into two parts) could be expressed as:

$$\Delta S = \frac{(n \times R) \times 2 \times (D \times l)}{n \times (\pi \times D \times l)} \times 100\% = \frac{2 \times R}{\pi} \times 100\% \quad \text{.....Equation 5.2}$$

where, $(n \times R)$ is the number of split fibers;

$2 \times (D \times l)$ is the total area of the two interfaces of the two components;

$(\pi \times D \times l)$ is the surface area of the total fibers in the sample, ignoring the small area of the cross-sectional area of the two ends of the fiber, since MB fiber is only 2-4 μm fine, and MB fiber is typically long and continuous fiber.

The fiber splitting ratio can be calculated as in Equation 5.3:

$$\textit{Fiber splitting ratio } R\ (\%) = \frac{N_S}{N_V} \times 100\% \quad \text{.....Equation 5.3}$$

where N_S and N_V are the total number of split fibers and the total number of visible fibers, respectively; if $R = 100\%$, $\Delta S = 2/\pi \approx 64\%$.

5.2.2 Initial Dye Adsorption Ratio

The process of adsorption involves separation of a substance from one phase accompanied by its accumulation or concentration at the surface of another. The adsorbing phase is the adsorbent, and the material concentrated or adsorbed at the surface

of that phase is the adsorbate. Physical adsorption is caused mainly by van der Waals forces and electrostatic forces between adsorbate molecules and the atoms which compose the adsorbent surface [101]. Thus adsorbents are characterized first by surface properties such as surface area and polarity. A large specific surface area is preferable for providing large adsorption capacity. The difference between adsorption and absorption is that adsorption is the attraction between the outer surface of a solid particle and a contaminant, whereas absorption is the uptake of the contaminant into the physical structure of the solid [102].

The fiber diameters in the meltblown web are normally distributed in a large range. The finest diameter can be less than 1 μm, but the largest fiber diameter may be greater than 10μm. It was found that more fiber splitting occurred in large fibers and less happened to small fibers. Splitting in large fibers might increase the uniformity of the meltblown webs, and decrease the average fiber size, and then the specific surface area of the fibers could be increased; as a result, the adsorption ability of the nonwoven web would increase. Therefore, adsorption ability could be an indicator of surface area change and fiber splitting ratio.

Many technologies could be used to test the adsorption ability of a material. The adsorption ability of a material is usually specified by the amount of a certain test chemical it can adsorb per unit weight of this material. For the filter used for filtering air

and gases, the test chemical used could be Carbon Tetrachloride (CCl_4). For the filter used in filtering water and liquids, the test chemical used is usually Iodine mixed with water [103]. Nitrogen [103] and hydrogen [104] also can be used to measure adsorption and surface area of a material. However, for nonwoven webs containing PET and/or PA components or fibers, the most convenient way should be dyeing method. Therefore the dyeing experiments were carried out to measure the change in initial dye adsorption ratio/initial dyeing ratio to describe the change in fiber surface area after fiber splitting, combined with the employment of spectrophotometer or spectrometer.

Split fibers have increased specific surface area, and the absorbing ability is expected to increase. The concentration of dye solution is expected to decrease after dyeing a nonwoven web in this solution, and the concentration should decrease more if the dyed web has increased surface area; therefore, less concentration of the residue dye solution means that the dyed web has a greater surface area, indicating more split fibers in the treated web.

The concentration of dye solution can be measured either with spectrophotometer or spectrometer using visible light. Assume that the initial dye solution has a concentration C_0, and the concentration of the residue dye solution has a concentration C, then the dye adsorption ratio (dyeing ratio) D (%) can be expressed as:

$$D = \frac{C_0 - C}{C_0} \times 100\% \quad \text{Equation 5.4}$$

The measurement of the concentration of dye solution is based on the well-known Beer's Law [105], which is expressed as Equation 5.5:

$$A = \log\frac{P_0}{P} = \varepsilon bc \quad \text{Equation 5.5}$$

where, A is Absorbance/Optical density/Extinction;

P_0 and P are Radiant power, the incident beam power and the emergent beam power, respectively.

c is the concentration of the solution (g/L, or mol/L);

b is the Path length of radiation (1 cm);

ε is Absorptivity/Extinction coefficient(L g^{-1} cm^{-1}), or Molar Absorptivity/Molar extinction coefficient (L mol^{-1} cm^{-1}). It is a measure of how strongly the species absorbs light at a given wavelength and it is an intrinsic property of the species.

The change in concentration of dye solution D can be expressed as Equation 5.6 by combining Equations 5.4 and 5.5:

$$D = \frac{A_0 - A}{A_0} \times 100\% \quad \text{Equation 5.6}$$

where, A_0 is the Absorbance of the initial dye solution, without dyeing any samples; A is the Absorbance of the residue dye solution after dyeing a certain sample.

Although we found the relation between fiber splitting ratio and increasing ratio of fiber surface area, we could not construct the relation between dye adsorption ratio and increasing ratio of fiber surface area, because the dye adsorption on fiber surface is

variable; the adsorption layers could be one or two, or maybe more, depending on the fiber type and dye type.

5.3 Investigation of Fiber Splitting in 50PET/50PA6 S/S MB Web with Benzoic Acid Solution

50PET/50PA6 (sample ID: 4-11-01-2) Bico MB NW web samples were treated in BA solution and water (control experiment), to investigate the possibility of fiber splitting. Both of the evaluation methods for the degree of fiber splitting were employed to compare the two methods. The experiments were carried out under the designed experimental conditions. The conclusion was drawn about fiber splitting in 50PET/50PA6 Bico MB NW web based on the analysis on the experimental results.

5.3.1 Experimental Design

In order to obtain the optimal treating conditions for fiber splitting in 50PET/50PA6 meltblown web, a 4-factor-3-level experimental plan was adopted, as shown in Table 5.1.

Table 5.1 Experimental factors and levels

	Temperature (° C)	Bath ratio	Concentration (g/l)	Time (min.)
Level 1	70	1:60	4	60
Level 2	90	1:70	6	90
Level 3	110	1:80	8	120

5.3.2 Experiments for Fiber Splitting

The experiments were carried out, according to the orthogonal experimental design table (Table 5.2), respectively, with agitation once a while. The web samples were placed in the beakers, which were put on the heaters with light stirring. Since the water in benzoic acid solution could evaporate during the treatments, water was refilled every 10 min period.

The experimental samples in the beakers were used to wipe the benzoic acid on the upper inside of the beakers every 5 minutes, to keep the constant concentration during the experiment. It is better to do these experiments in a closed system. The benzoic acid treating experiments at 110°C were performed in a sealed high-pressure vessel.

Table 5.2 Orthogonal experimental table of BA treatment

	Temperature (°C)	Bath ratio	Concentration (g/l)	Time (min)
1	70	1:60	8	120
2	70	1:70	4	90
3	70	1:80	6	60
4	90	1:60	6	90
5	90	1:70	8	60
6	90	1:80	4	120
7	110	1:60	4	60
8	110	1:70	6	120
9	110	1:80	8	90

The treated samples were taken out from the beakers, when the time was up. After that, the residue benzoic solution was neutralized with the NaOH solution with the equivalent concentration, and then the samples were pressed and then placed on the screen to dry out naturally at standard temperature and humidity (20 °C, 65% RH). The BA treated samples were subject to the measurements of fiber splitting ratio, based on SEM and/or microscopic techniques, and dye adsorption ratio, to examine the degree of fiber splitting. The optimal treating technology could be obtained based on the statistical analysis of the fiber spitting ratios and dye adsorption ratios at different treating conditions. Web structure and web properties, including fiber diameter were examined before and after treating with optimal BA treating conditions. In addition, control experiment was carried out to investigate the influence on fiber splitting from water.

5.3.2.1 Fiber Splitting Ratio Based on the SEM Photos

Take a small piece of treated sample and coil it up into a tight, regular column shape, then fix the shape using adhesive tape. Put this sample coil into liquid nitrogen. Take the sample coil out of the liquid nitrogen after 5 min and cut it cross-sectionally immediately, to prevent the deformation of the sample. Put the cross-sectional part of the sample into SEM machine; count the numbers of split fibers and visible fibers, respectively and then took down the numbers.

5.3.2.2 Initial Dye Adsorption Ratio

Total web weight: 0.4g (containing 5 pieces of 10 mg weight webs); dyestuff concentration: 0.5 g/l; bath ratio: 1:100. The web samples were dyed at 40°C. Extract 1 ml of the dyeing residue at the dyeing time 0.5 min., 1 min., 2 min., 3 min., 5min., and 10 min. respectively and put the residue into a container of 10 ml volume, then dilute the residue to the scale; meanwhile, take out a piece of sample with 10 mg weight, to keep the constant bath ratio of the dyeing bath. The curves of initial dyeing ratio against time were then obtained this way. The applied dyestuff was Polar Yellow, a weak acidic anion dyestuff.

The dyeing residue extracted at different time was tested using the visible light spectrophotometer (SF600 Plus-CT, from Datacolor® International), for Absorbance A, and the Absorbance A_0 of the original dye solution. Then the Dye adsorption ratio/dyeing ratio can be calculated based on Equation 5.6:

Dye adsorption ratio (%) $= \frac{A_0 - A}{A_0} \times 100\%$, where A_0 and A are the Absorbance (peak value) of the initial dye solution and the residue dye solution after dyeing samples, respectively.

The calculated dye adsorption ratio is the initial dye adsorption ratio, if the dyeing time is limited within a short time, such as 3 min, to limit the dye only to be adsorbed on the surface of the fibers, not into the inside of the fibers. It is the function of

specific surface area of the fibers and hence can indirectly represent the degree of fiber splitting. More split fibers would cause greater dye adsorption ratio of the treated webs and less optical Absorbance of the residue dye solution, but a linear relationship between initial dyeing ratio and the increasing ratio of fiber surface area could not be constructed without knowing the adsorption layers on the surface of the fibers.

5.3.3 Results and Analysis

5.3.3.1 Observation of Fiber Splitting with SEM/Microscopic Technique

5.3.3.1.1 Longitudinal View of Split Fibers in SEM Photo

The SEM photos of 50ET/50PA6 meltblown samples before and after benzoic acid treatments are selectively shown in Figures 5.2 and 5.3 respectively.

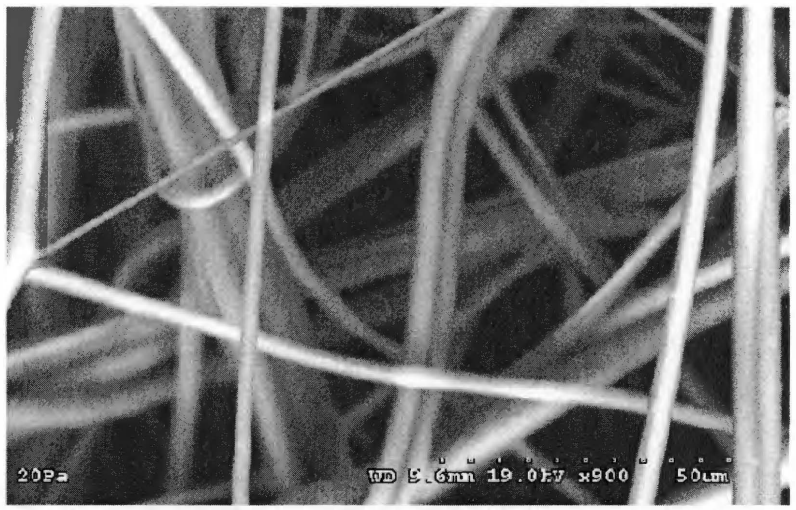

Figure 5.2 Before treatment

Figure 5.3 After Experiment 9

The SEM pictures in Figure 5.2 and 5.3 were obtained on SEM machine (model: Hitachi S-3500 N) without coating gold. It was difficult to obtain a clear SEM photo of fiber splitting due to static charge on the samples during testing period.

It was obviously shown in the Figures 5.3, that the PET/PA6 meltblown fibers were split partially after the treatments using benzoic acid solution, and no obvious damage to the fibers were observed. This indicates that benzoic acid treatment is possible for fiber splitting in side-by-side bicomponent meltblown web. In fact more split fibers should be observed in the SEM photos of the BA treated web; however, the charging problem disturbed the clear observation of the split fibers. The static charge tended to close the two split parts when taking the SEM photos. So the photos should be taken as

quickly as possible.

Benzoic acid is a relatively strong organic acid, and its PH value is 2.6 at 40 °C with the concentration of 6g/l. It can break the H-bonds and intermolecular forces between PET and PA6, and hence enter inside of the molecules. A great amount of water will be brought into the molecules due to the entrance of polar part of BA, and eventually the fiber will begin to swell. However, benzoic acid only swells the fiber to a limited degree; the two components, i.e., PET and PA6 will both shrink during the process of benzoic acid treatment. Since there is difference in shrinkage between PET and PA6, the adhesion at the interface between PET and PA6 will decrease gradually; finally, the interface contracts until the two components separate from each other. But, it is difficult for benzoic acid to enter the inside of the fibers, due to its large size, compared to the inorganic acid like HCl (hydrochloric acid), therefore, the swelling process of the fiber needs more time and heat energy.

5.3.3.1.2 Cross-sectional View of Split Fibers in SEM / Microscopic Photos

The typical SEM (model: Hitachi S-4300SE/N) picture and laser microscopy (Model: Leica® TCS SP2) of the cross-sections of the 50PET/50PA Bico MB web were shown in Figures 5.4 and 5.5, respectively, and the calculated fiber splitting ratios based on the SEM pictures of the cross-sections of the treated MB fibers are listed in Table 5.3. The samples for SEM tests were frozen in liquid nitrogen for 2-3 min then cut immediately

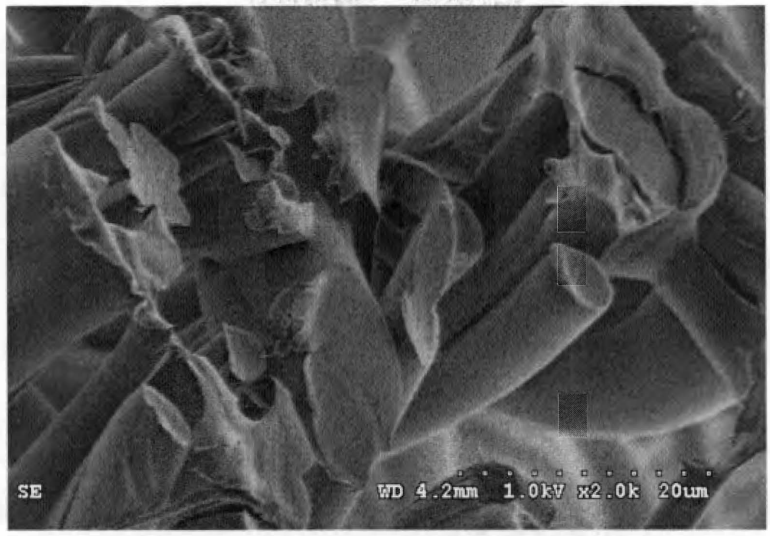

Figure 5.4 SEM photo of the fiber cross-sections of benzoic acid treated web (50PET/50PA6)

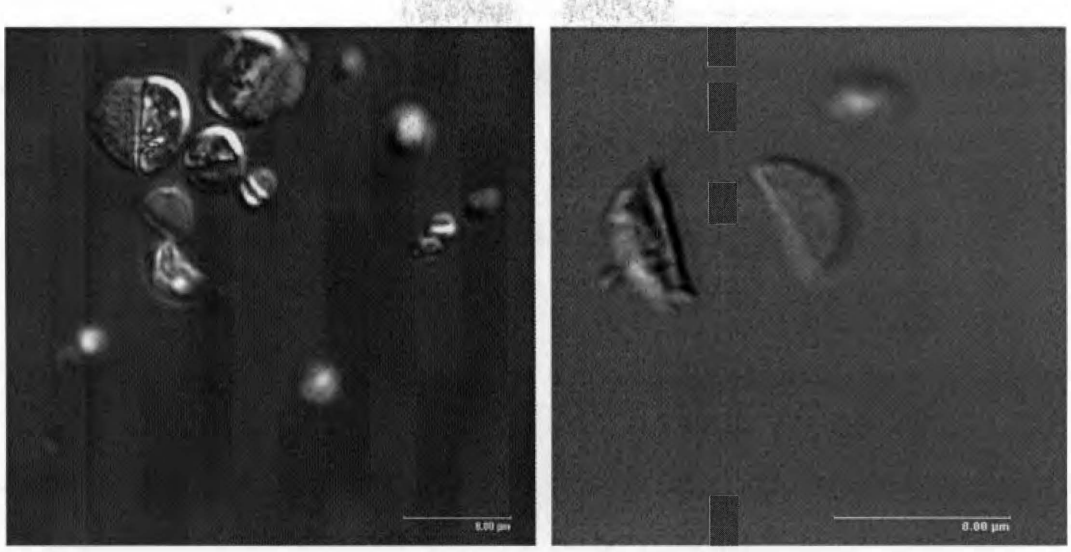

Figure 5.5 Microscopic picture of the same sample in Figure 5.4.

Table 5.3 Orthogonal analysis table of fiber splitting ratio

	Temp. (°C)	Bath ratio	Conc. (g/l)	Time (min)	Splitting ratio (%)	Increased ratio of surface area (%)
1	70	1:60	8	120	35.3	22.48
2	70	1:70	4	90	32.0	20.38
3	70	1:80	6	60	28.0	17.83
4	90	1:60	6	90	45.5	28.98
5	90	1:70	8	60	47.5	30.25
6	90	1:80	4	120	32.0	20.38
7	110	1:60	4	60	38.0	24.20
8	110	1:70	6	120	41.5	26.43
9	110	1:80	8	90	37.5	23.88
I_J	95.0	118.8	102.0	113.5		
II_J	125.0	121.0	115.0	115.0		
III_J	117.0	97.5	120.3	108.8		
R_J	30.0	23.5	18.3	6.2		

Note: (1) I – Level 1, II – Level 2, III – Level 3, R – Range;

(2) Increased ratio of (specific) surface area $= \frac{2 \times R}{\pi} \times 100\%$.

using a safety razor. The samples for microscope samples were cured for 14 hrs at 68°C embedded in the epoxy resin (Spurr) and then cut into 1 micron thickness using microtome (model: Reichert OMU 3); the microscopic images were obtained under a high-level laser microscope, using the technology of differential interference contrast. However, it is impossible that the counting of the number of split fibers in a SEM picture of the MB web cross-section is as accurate as that in a SEM picture of the cross-section of the bundled melt-spun fibers, due to the isotropic feature of the fiber distribution in the MB web relative to spunbonded web and carded web. Only a few fibers were observed to exhibit their cross-sections if they were perpendicular to the SEM screen; other fibers were paralleled to the SEM screen or skewed to the screen. In addition, the morphology of the web cross-section depended on the cutting technology used and the cutting skill of the operator.

For the SEM photos, the well-known liquid nitrogen freezing method was used to make the cross-sectional sample.

5.3.3.2 Determination of Fiber Splitting Ratio and the Change in (Specific) Surface Area

The SEM tests of the 50PET/50PA6 MB web samples treated at different conditions, including the control sample and the original sample, were performed at the same magnification to count the numbers of split fibers and the total visible fibers for the

calculation of fiber splitting ratio; and 10 SEM pictures of each sample were examined for the averaged fiber splitting ratio. The numbers of split fibers and total visible fibers in a photo were recorded quickly and respectively, to avoid the severe charging problem. The fiber splitting ratio for each sample was calculated according to Equation 5.3, and the results were shown in Table 5.3 and Figure 5.6, respectively.

It should be realized that the morphology of the cross-section of a MB web in a SEM photo might exhibit irregularity due to the random distribution of MB fibers in the web, and the MB web was too soft to get a sharp cut. Therefore, it was difficult to identify the split fibers in cross-sections, and the resulting fiber splitting ratios might not be all accurate. The corresponding microscopic photo of the same sample was illustrated in Figure 5.5, where the fibers exhibited good-looking cross-sections.

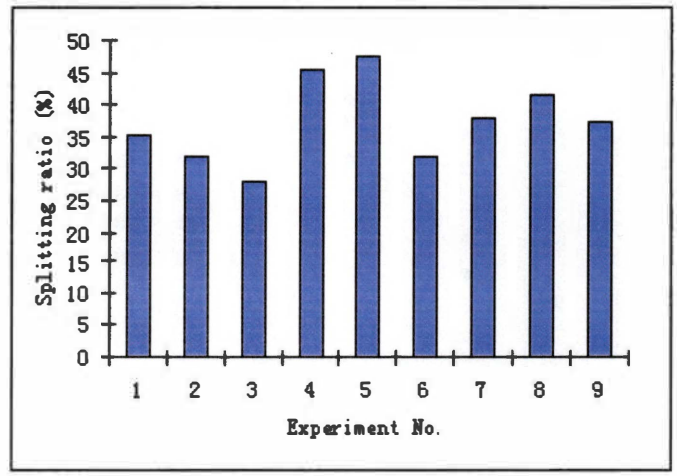

Figure 5.6 Splitting ratio vs. experiment No.

The primary and secondary factors influencing the fiber splitting ratio were temperature, bath ratio, concentration and time respectively, based on the range analysis in Table 5.3 above. The optimal treating condition based on Figure 5.7 was preliminarily selected to be: 90 °C, 1:70, 8 g/l, and 90 min. This condition is similar to that in Experiment 5 (90 °C, 1:70, 8 g/l and 60 min.), except for the time parameter.

But, *time* is the secondary factor according to Table 5.3; therefore Experiment 5 may be considered to be the optimal treating technology. The result of Experiment 5 was also the best among the 9 experimental results based on Figure 5.6, indicating the reasonability of the orthogonal experimental method.

The fiber splitting ratio based on the SEM photos could be as high as 47.5%, and the corresponding increasing ratio in fiber surface area could achieve 30.25%, after

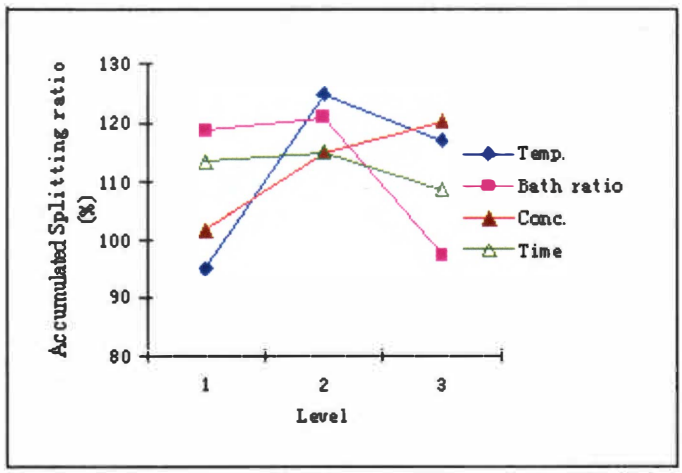

Figure 5.7 Visual analysis diagram of orthogonal experiment data

treating the 50PET/50PA6 Bico MB NW web using BA solution at the treating conditions of 90 °C, 1:70, 8 g/l and 60 min.

However, there is limitation in determining the degree of fiber splitting based on the calculation about fiber splitting ratio from SEM pictures, since the sampling size in SEM tests is too small, also only one or two layers of fibers can be examined due to the problem of the depth of field. If the interface of the split fibers is parallel to the SEM screen, or the spit fibers are closed when we try to take photos due to the electrostatic accumulation, we will count less number of split fibers than actually. When the two parts of a split fiber became closed, we even cannot see the splitting line clearly, due to the bright color of the charging region. In addition, we cannot get the SEM picture about the opposite side of the SEM specimen, because it will be damaged when we examine the other side. So the fiber splitting ratio determined based on the numbers of split fibers and visible fibers in one SEM photo is not always accurate, and we need other better methods to determine the degree of fiber splitting.

In addition, charging was seriously problematic when taking SEM photos. Although charging could be limited by coating the powder of good conductor, such as gold, etc., but coating might cause unclear image of the MB microfiber, especially it would be hard to tell the difference between the fiber twins in the MB web and the split two components in the single MB fibers. One had to count the split fibers and the total

visible fibers as quickly as one can, because charging occurred before saving the images, and the fast charging might make the two split components close very quickly. The actual fiber splitting ratio might be greater than what we saw in the SEM photos, due to the charging-closing problem. Therefore, fiber splitting ratio might not be the best way to evaluate the degree of fiber splitting in 50PET/50PA6 S/S Bico MB web.

5.3.3.3 Initial Dye Adsorption Ratio

Since with the increase in temperature and time, the dyestuff will enter the deep of the fibers, in this case the dyeing ratio cannot reflect the change in specific surface area before and after fiber splitting; therefore the temperature and time should be limited to a certain degree. The initial adsorption ratios of the sample 50PET/50PA6 were measured at 40 °C, 0.5 min, 1 min, 2 min, 3 min, 5 min and 10 min, respectively, including the untreated samples. The results are shown in Figure 5.8. Increasing ratio of initial dyeing ratio was shown in Table 5.4 ("0" stands for original samples).

Since it was easy for the initial dyeing ratio at 0.5 min to be affected by the ambient conditions, the subsequent statistical analysis would exclude the experimental values at 0.5 min. The corresponding primary and secondary factor analysis results were listed in Table 5.5, based on the similar statistical analysis as done in the part of fiber splitting ratio. It was found that the order of the primary and secondary factors is:

Temperature > Concentration > Bath ratio > Time.

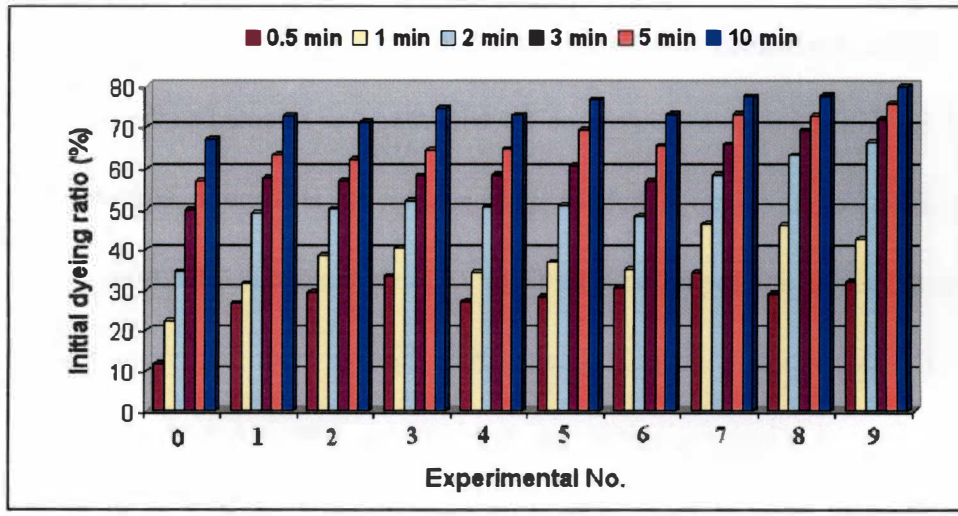

Figure 5.8 Initial dyeing ratios at different time (40°C)

Table 5.4 Increasing ratio of initial dyeing ratio for 50PA6/50PET webs

Experiment No.	Initial dyeing rate (%) at 3 min	Increasing ratio (%) of initial dyeing ratio
0	49.9	
1	57.6	15.43
2	57.0	14.23
3	58.2	16.63
4	58.4	17.03
5	60.7	21.64
6	56.8	13.83
7	65.8	31.86
8	69.1	38.48
9	72.0	44.29

Table 5.5 Increasing ratio of initial dyeing ratio for 50PA6/50PET webs

1 min	Temperature > time > concentration > bath ratio
2 min	Temperature > concentration > bath ratio > time
3 min	Temperature > concentration > bath ratio > time
5 min	Temperature > concentration > time > bath ratio
10 min	Temperature > concentration > time > bath ratio

It was undoubted that temperature and concentration should be the first two items of the primary factors. The reason for why *time* was selected as the last factor was that the initial dyeing ratio had been approaching the adsorption equilibrium of the dyeing bath system, and the influencing factors already changed at that time.

Considering the overall influence from the four main factors, it was better to select the optimal treating condition as: 110 °C, 8g/l, 1:80 and 120 min, for the fiber splitting in 50PET/50PA S/S MB nonwoven web, instead of the condition of 90 °C, 1:70, 8 g/l and 60 min.

5.3.3.4 Comparison of the two Evaluation Methods for the Degree of Fiber Splitting

It could not be expected that a single fiber would split into two parts from one end to the other end, or all the fibers in the web will split into two separate components. Therefore, the fiber splitting ratio based on the SEM photos could not reflect the true splitting ratio. But, the initial dyeing ratio method could reflect the increasing ratio of adsorption more objectively, compared to SEM method. The reasonability of the latter lies in the fact, that there would be no difference in fiber splitting ratio based on the SEM method, no matter whether the fibers split completely or partially; but there would be a difference in the initial dyeing ratio between the two cases. (When calculating the fiber splitting ratio based on SEM photos, both the partially split fibers and completely split

fibers are counted as split fibers.)

Based on the analysis on the two evaluation methods, dye adsorption ratio was considered as the better method, due to the reason of accuracy, simplicity, speed advantage. In the later research, only dye adsorption ratio was selected to examine the degree of fiber splitting. However, the dye adsorption ratio only could reflect the relative change in dye adsorption ratio; it could not give the absolute value of fiber splitting ratio, though it can reflect the relative change in specific surface area of fibers.

5.3.3.5 Change in Structure and Property of 50PA6/50PET S/S MB NW Webs after BA Treatment

Many changes occurred to the BA treated webs in both web structure and web properties. The 50PA6/50PET S/S MB webs were treated with BA solution using the selected optimal treating condition, i.e., 110 °C, 8g/l, 1:80 and 120 min; for comparison, the same web was treated with the same condition in pure water to obtain the control sample. The main changes were summarized in Figure 5.9 and Figure 5.10 separately. The tensile properties and web stiffness were only measured in the machine direction (MD).

After water and BA treatment, as shown in Figures 5.9, the fiber diameter decreased as a result of fiber splitting. Although we could observe more split fibers in the SEM photos of BA treated samples than water treated (control) samples, fiber diameter

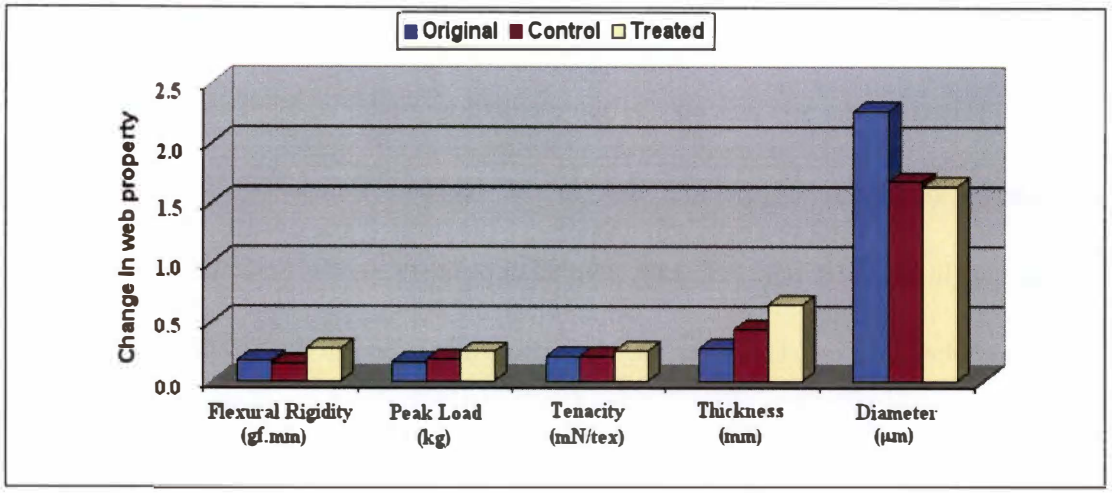

Figure 5.9 Changes in fiber diameter, web thickness, tenacity, peak load and flexural rigidity

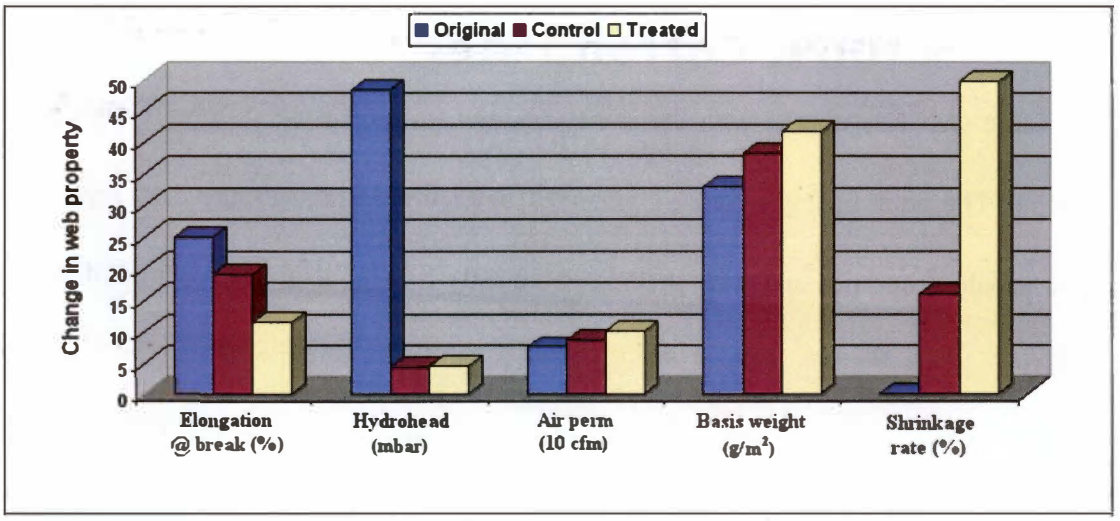

Figure 5.10 Change in shrinkage, basis weight, air perm, hydro head and breaking elongation

did not reflect this phenomenon in Figure 5.9. This indicated that the terminology of fiber splitting ratio possibly did not reflect the actual degree of fiber splitting in the treated webs, due to the presence state of split fibers in the treated webs.

If the two components of a split fiber lies in a SEM photo in the way that their interface is paralleled to the screen plane but overlapped with each other, then the split fiber can not be taken as a split fiber, and its diameter is the same as before splitting; only when the interface of a split fiber is almost vertical to the screen plane, then the split fiber can be seen and thus its diameter can be taken as half of the original diameter, the average diameter may decrease as the result of fiber splitting in the treated web. Therefore, the fiber diameter should decreased more due to the possible underestimation of the number of split fibers shown in the SEM photos.

Web thickness, basis weight increased as the result of web shrinkage and fiber splitting. Web tenacity, peak load increased, while the breaking extension decreased. The web flexural rigidity increased as the web became thicker and shrunk.

Hydrohead decreased dramatically after treated with water and BA respectively, which was an unexpected result. Possibly the surfactant on the surface of the treated web had some influence on the hydro head measurements. The surfactant may absorb a great amount of water onto one side of the web, and transfer the water molecules rapidly from this side to the other side through the capillary channels in the web, which did not need

too much water pressure to do so.

The air perm increased after water treatment and BA treatment, which was not surprising either. Of course the filtration efficiency was expected to increase due to fiber splitting and web shrinkage, but the air permeability might increase due to the creation of more capillary channels as the result of fiber splitting in the web.

5.4 Investigation of Fiber Splitting in 50PP/50PA6 S/S MB Web with Benzoic Acid Solution

Meltblown web samples having the composition of 50PP/50PA6 were treated with benzoic acid at different conditions, to investigate the optimal condition for fiber splitting. The changes in structure before and after the treatments were examined using microscopy (for fiber diameter), SEM (for fiber splitting), and DSC (for T_g, T_m and crystallinity); tensile tests, bending stiffness (flexural rigidity), water permeability, air permeability, thickness, and basis weight were examined according to the corresponding ASTM standards, respectively. In addition, shrinkage ratio of the treated webs was measured as well, to examine influence from shrinkage on the changes in other properties. Also, the control experiments were conducted in water with the same bath ratio, temperature, and time.

35 fibers were measured for averaged fiber diameter in each sample.

5.4.1 Preliminary Experiments for Optimal Fiber Splitting Conditions

The preliminary experiments were performed to obtain the most obvious fiber splitting by the observation of SEM photos. The experiment conditions are shown in Table 5.6 below. The obvious phenomena of fiber splitting in 50PP/50PA6 meltblown web through different treatments of benzoic acid were selectively shown in Figure 5.11.

Based on the SEM photos of the 50PP/50PA6 samples treated with benzoic acid at different conditions, the fiber splitting phenomena were observed most obviously in those of Experiment-1 and Experiment-10, respectively, but the treated web samples kept most of their original hand and appearance.

Table 5.6 Conditions for the preliminary experiments using benzoic treatment

50PP/50PA6 Experiment#	Bath ratio	Concentration (g/l)	Temperature (°C)	Time (min)	Fiber splitting (Through SEM)
1	1:80	8	90-100	90	Obvious
2	1:200	15	90-100	30	Not obvious
3	1:200	15	90-100	60	Not obvious
4	1:200	15	90-100	90	Not obvious
5	1:200	15	90-100	120	Obvious
6	1:200	20	90-100	30	Not obvious
7	1:200	20	90-100	60	Not obvious
8	1:200	20	90-100	90	Not obvious
9	1:200	20	90-100	120	Obvious
10	1:200	30	90-100	30	Obvious
11	1:200	30	90-100	60	Not obvious
12	1:200	30	90-100	90	Not obvious
13	1:200	30	90-100	120	Not obvious

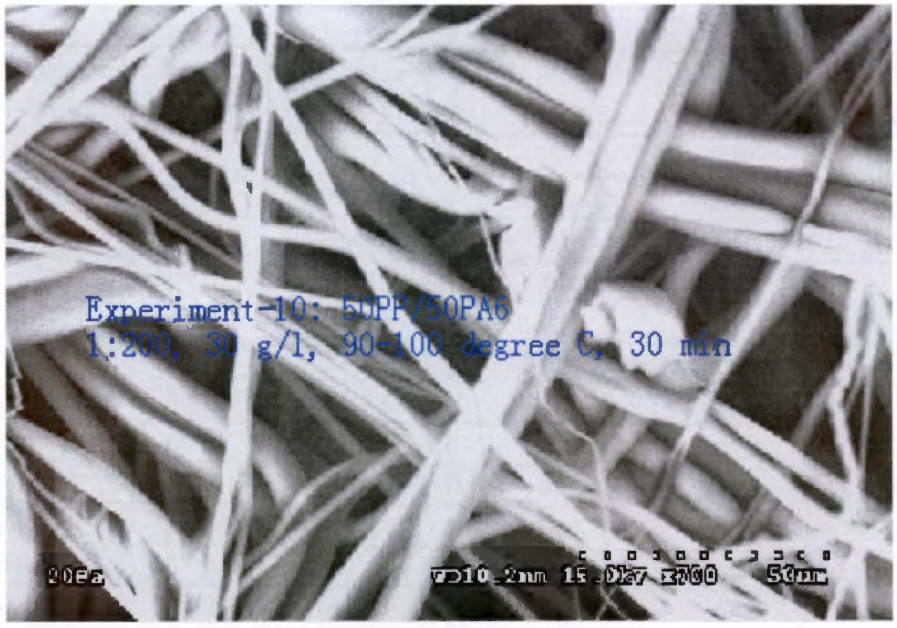

Figure 5.11 Fiber splitting in the preliminary Experiments 1 and 10.

Therefore, further experiments were conducted to examine the changes occurred after post-treatment for fiber splitting; also, the control experiments were carried out meanwhile to find out if water plays a part in the post-treatment when using benzoic acid solution as the splitting agent. Therefore, two groups of contrast experiments were carried out under the following conditions, as shown in Table 5.7.

5.4.2 Experimental Results

The experimental results were illustrated below. Split fibers were found in the control samples, although they were not as many as in the benzoic acid-treated samples; fiber splitting phenomenon was not observed in the untreated 50PP/50PA6 meltblown web, as shown in Figure 5.12.

Table 5.7 The experimental design table for 50PP/50PA6 sample

50PP/50PA6 Experiment No.	Bath ratio	Concentration (g/l)	Temperature (°C)	Time (min)
Experiment-1 (Exp-1)	1:80	8	90-100	90
Control-1 (Exp-1-0)	1:80	0	90-100	90
Experiment-2 (Exp-2)	1:200	30	90-100	30
Control-2 (Exp-2-0)	1:200	0	90-100	30

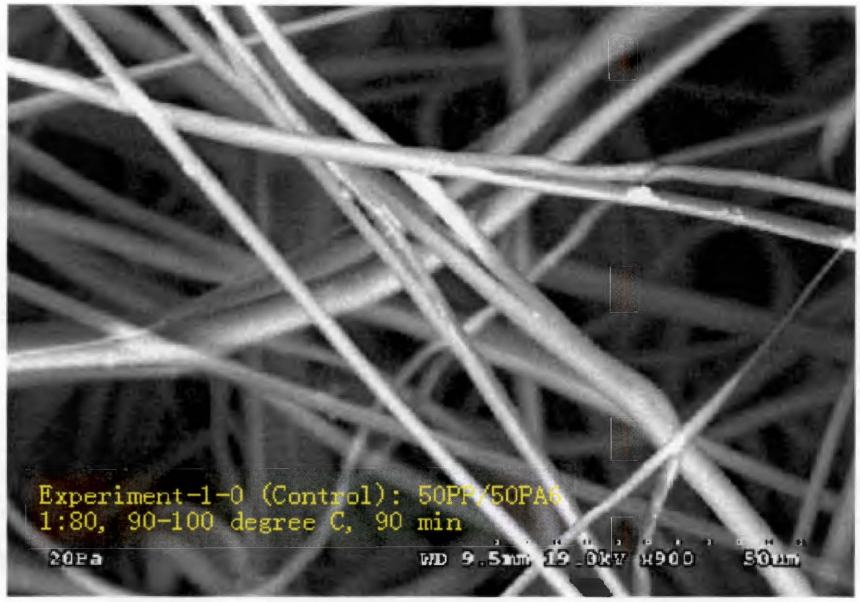

(a)

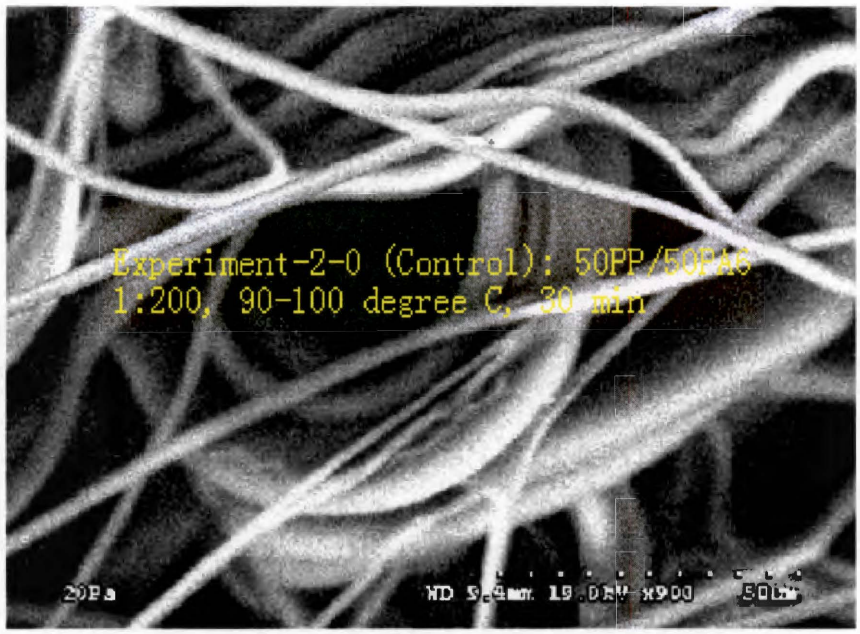

(b)

Figure 5.12 SEM photos of the control samples

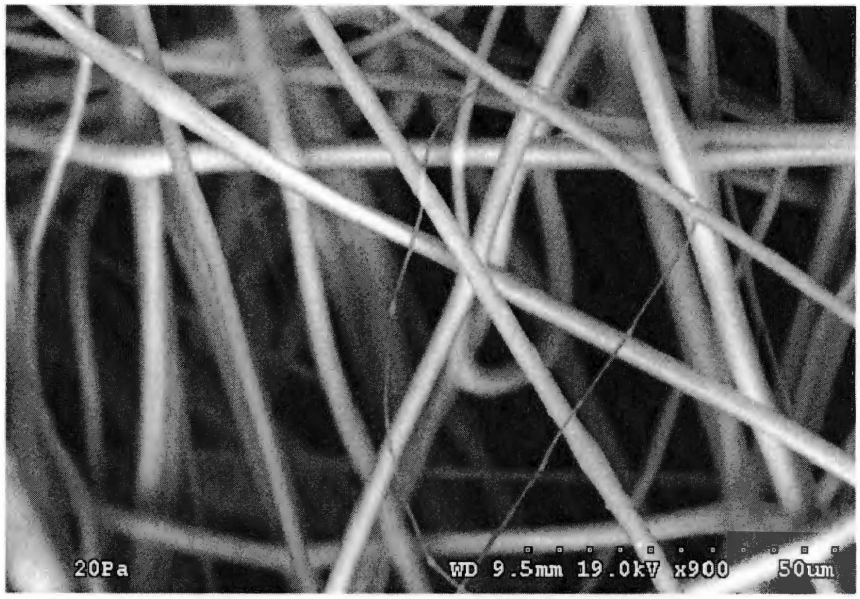

(c)

Figure 5.12 (Continued) SEM photo of the original sample

5.4.2.1 SEM Photos Showing Fiber Splitting after Control Treatments

It was not surprising that split fibers were found in control samples; because the water molecules may enter into the amorphous region of the PA part of the Control samples, especially at high temperature, as time goes on. The water molecules that entered the PA part of the fiber might weaken the interaction force among the PA molecules; especially it could break up the H-bonds among the PA molecules on the interface between PP and PA, where is naturally weak in adhesive bonding, due to the incompatibility between PP and PA. Then the interface of PA will contract until the internal stress on the interface is large enough to overcome the adhesion strength on the

interface, the fiber will split into two parts eventually. The bicomponent meltblown fibers are not expected to split completely from one end of the fiber till the other end, due to the characteristics of continuity, entanglement, and self-adhesion of meltblown fibers. The polar part in benzoic acid may bring more water molecules into the spaces in the amorphous region of PA component. Therefore benzoic acid treatment may cause more fibers to split in the PP/PA6 fibers. This is consistent with the splitting mechanism analysis part in this paper.

5.4.2.2 Initial Dye Adsorption Ratio

The dyestuff Lanaset® Red 2B from Ciba Inc., with the composition of 1:2 metal complex acid dye/reactive dye, was used to analyze the dye adsorption ratio of the benzoic treated samples, and the untreated sample. Totally 1 liter of dye solution was prepared for the absorbance tests; with the concentration being 0.1g/L. The dyeing conditions are: bath ratio = 1:100; dye/web = 1% w/w; temperature = 60 °C; dyeing time = 3 min. For each test, 100 ml dye solution was used and the web weight was 1g.

The 50PP/50PA6 webs were measured with a spectrometer (BioMate 5, UV-VIS spectrometer, from Thermo Spectronic Inc.) for the initial dyeing ratio. The pure water was taken as the reference sample, and the initial dye solution prior to dyeing any webs was tested with the UV-VIS spectrometer first for the initial Absorbance of dye solution, A_0, with the wave length of the incident beam ranging from 350 to 800 nm (usually the

visible light has the wave length range of 380 to 780 nm). Then the untreated web, Control-1 web, Experiment-1 web, Control-2 web and Experiment-2 web (see table 5.6) were tested for the Absorbance value using the UV-VIS spectrometer respectively. The typical Absorbance curve from the UV-VIS spectrometer was shown in Figure 5.13, and the maximum Absorbance values of the 6 measurements, corresponding to the wave length 507 nm were shown in Table 5.8.

Figure 5.13 showed the Absorbance of the residue dye solution after dyeing the Experiment-1 sample achieved its peak value 0.344 at the wave length of 507 nm, and this peak Absorbance is right the feature absorbency value of the Lanaset® Red 2B at 507 nm wave length.

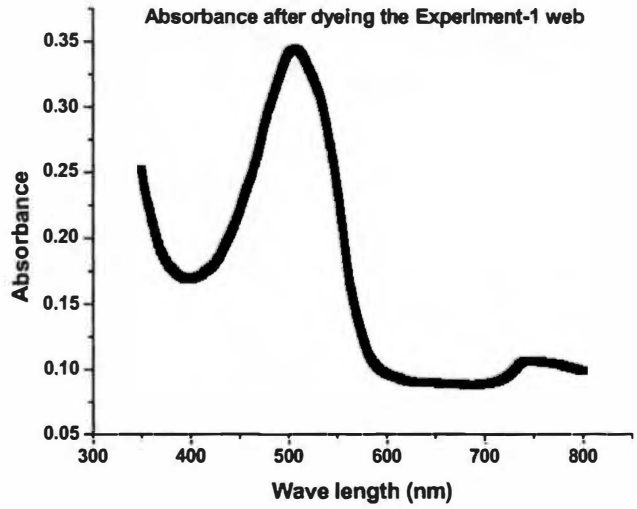

Figure 5.13 Typical curve of the Absorbance vs. wave length

Table 5.8 The peak value of absorbance of dye solution

λ (nm)	A_0	A_{UN}	A_{C1}	A_{E1}	A_{C2}	A_{E2}
507	1.225	0.540	0.530	0.344	0.480	0.238

Note: λ—the wave length at which the peak Absorbance was detected;

A_0—the Absorbance of the original dye solution;

A_{UN}—the Absorbance of the residue dye solution after dyeing the untreated web;

A_{C1}—the Absorbance of the residue dye solution after dyeing the Control-1 web;

A_{E1}—the Absorbance of the residue dye solution after dyeing the Experitment-1 web;

A_{C2}—the Absorbance of the residue dye solution after dyeing the Control-2 web;

A_{E2}—the Absorbance of the residue dye solution after dyeing the Experiment-2 web.

Table 5.8 showed that significant change occurred to the Absorbance of the dye solution among the untreated and treated MB web samples; the dye adsorption ratio/dyeing ratio was calculated based on Equation 5.7 and Table 5.8, listed in Table 5.9.

The increasing ratio in dye adsorption ratio/dyeing ratio between the treated and untreated samples was listed in Table 5.10.

The results in Table 5.10 indicated, that both benzoic acid and water could split 50/PP/50PA6 S/S MB nonwoven fibers at the appropriate conditions to increase the specific surface area of the Bico MB fibers; however, benzoic acid could split more fibers and increased more surface area than water did to the same sample, at the same treating conditions.

Table 5.9 Dye adsorption ratio/dyeing ratio (%) of 50/PP/50PA6 S/S MB webs

Wave length	Untreated	Control-1	Experiment-1	Control-2	Experiment-2
507 nm	55.92	56.73	71.92	60.82	80.57

Table 5.10 Increasing ratio (%) of dye adsorption ratio (after benzoic acid treatment and water treatment)

Wave length	Control-1	Experiment-1	Control-2	Experiment-2
507 nm	1.45	28.61	8.76	44.08

Changes in web properties after treating 50PA6/50PP MB webs with benzoic acid solution, including fiber diameter, were illustrated in Figures 5.14 and 5.15.

5.4.2.3 Fiber Diameter

As shown in Figure 5.14, the fiber diameter did not change significantly among the four treatments, i.e., Control-1, Experiment-1, Control-2 and Experiment-2; the fiber diameter was approximately 2.70 μm, although there was slight difference existing in the four diameters. However, the diameters after treatments with both benzoic acid solution and pure water decreased compared to the original diameter 3.01 μm, indicating, both the benzoic acid and water have an effect on fiber splitting in PP/PA6 meltblown web, and the former is supposed to have more effect than the latter, as observed from the corresponding SEM photos; but it is hard to tell this based on the diameter values, because the split fibers almost have the same diameter, as they were not split, if the two split parts are parallel to the photo plane, with the interface between the two split components being paralleled to the screen. Therefore the change in fiber diameter may not correctly reflect the change in real fiber size. For more accurate fiber size, the apparent fiber diameter may be used, which requires the accurate measurement of fiber cross-sectional area, including both the split fibers and the non-split fibers, then calculate the apparent fiber diameters of the split fibers and the non-split fibers. The fiber diameter obtained this way may correctly reflect the change in fiber diameter after fiber splitting.

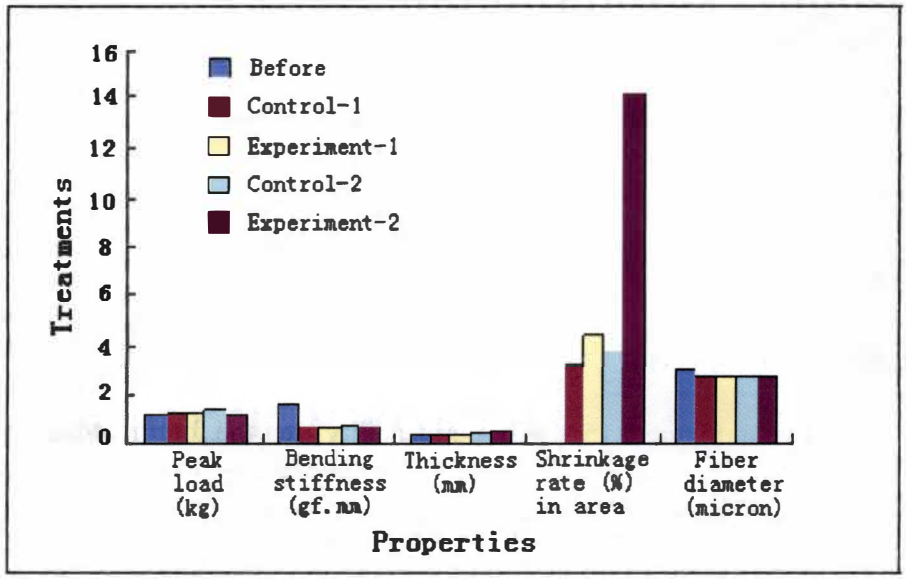

Figure 5.14 The results of peak load, bending stiffness, thickness, shrinkage ratio and fiber diameter before and after different treatments.

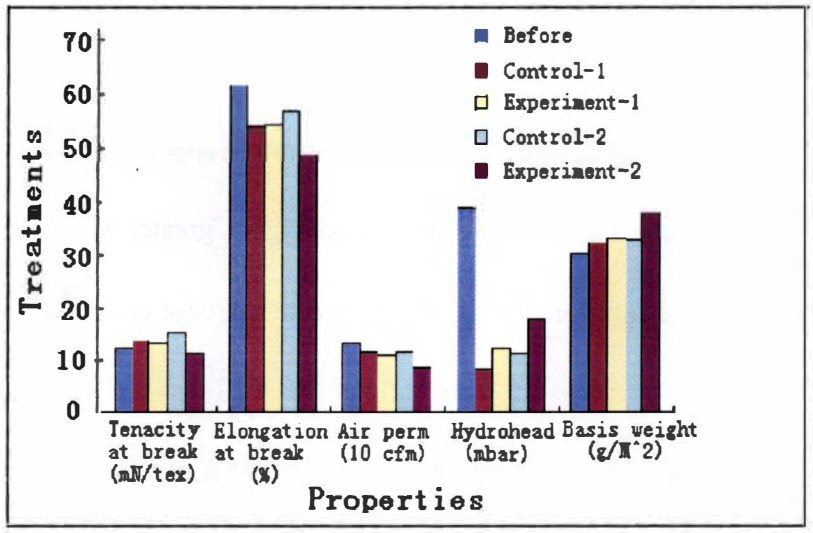

Figure 5.15 The results of breaking tenacity, breaking elongation, air permeability, hydrohead and basis weight, before and after different treatments

Since fibers having larger diameter tended to split during the treatments, therefore, the fiber size would be expected to be more uniform after the treatments, and web structure would tend to become tight with smaller pore size, which is benefit for filtration application.

5.4.2.4 Barrier Property

As shown in Figure 5.15, the air permeability after the four treatments decreased compared with the original sample, and the air permeability decreased the most for the sample subjected to Experiment-2 treatment (bath ratio=1:200, benzoic acid concentration = 30 g/l, temperature = 90 ~ 100 °C, time = 90 min.), which was the most severe treating condition for the samples. The decrease in air perm after treatments were attributed to fiber splitting, improved web structure and web shrinkage after benzoic acid treatments.

All of these changes would facilitate the filtration application of the treated web. After fiber splitting, the fibers in the treated web gain greater specific surface area, therefore the surface absorption ability is expected to increase compared with untreated sample.

However, the treated web tended to absorb more water and allow more water to pass through the web, which was unexpected for these four treatments. The hydrohead values decreased significantly after the four treatments; this was attributed to the

existence of disperse agent in the treated webs; but after the treatments, the hydrohead increased with the increase in severity of the treating conditions. The disperse additive has been used before the treatments to distribute the benzoic acid uniformly through the web; and the same disperse agent was employed also in the two control experiments to keep the same systematic difference between the treating experiments and control experiments. Therefore, the hydrohead values obtained this way might not reflect the true water passing ability correctly; hot water should be used to wash off the waste disperse additive for a longer time in the future experiments. However, this does not have passive influence on water travel ability through the treated web; the water still can pass through the treated web, even in an easier way, due to the existence of the disperse agent residue; but the impurity particles are not be allowed to go through the treated web due to the smaller pore size in the web, and the greater adsorption ability of the treated web.

5.4.2.5 Web Structure

Basis weight, web thickness increased and web shrinkage occurred after the four treatments, compared to the original sample; and the values of these three indexes increased with the increase in the severity of the treating conditions, as shown in Figures 5.14 and 5.15.

Web shrinkage was due to relaxation of the internal stress, resulted from the web production process, in the boiling water or benzoic acid solution. In addition, the

water molecules which were brought by the polar part of benzoic acid, or the water molecules themselves, might break down the original H-bonds among the PA molecules in PA part of the fibers, and constructed more, new H-bonds among the PA molecules, therefore the PA part would swell to cause the web shrinkage.

For the shrinkage ratio in web area, the treated sample using the condition of Experiment-2, has the largest shrinkage ratio, i.e., 14%, which was due to the greatest concentration of benzoic acid (30 g/l), although the shortest time, 30 min, was used in this treatment. This treated web is supposed to have the greatest fiber splitting ratio, the tightest and most uniform web structure, compared to the other three treated samples and the original sample; therefore, Experiment-2 should be considered to be the optimal condition for fiber splitting in 50PP/50PA6 meltblown web.

5.4.2.6 Mechanical Properties

The first three treatments, i.e., Control-1, Experiment-1 and Control-2 resulted in a slight increase in breaking tenacity and peak load; however, the Experiment-2, the treatment with the most severe condition, lead to a slight decrease in breaking tenacity and the peak load did not change. This was because that the tenacity, the relative strength, is inversely proportional to basis weight, the Experiment-2 treated sample has the greatest basis weight, due to the highest shrinkage ratio (14 %) of web area among all the treated samples; it was supposed to have the lowest breaking tenacity, although it perhaps

have the highest breaking load. On the other hand, the breaking load will increase with the increase in basis weight, thickness and web shrinkage ratio. For the first three treatments, the increase in basis weight, thickness and shrinkage ratio was not too great, therefore, the increase in breaking load was dominant in the three cases; but for the last one, Experiment-2, the increase in basis weight was too great and hence it was dominant in this case, therefore, the breaking tenacity exhibited a decreasing trend.

The reason for that the peak load for the Experiment-2 treated sample did not change, as shown in Figure 5.14, was possibly due to the reason that the increasing peak load resulted from the increasing basis weight, shrinkage ratio and thickness was counteracted by the decreasing peak load caused by the damage to the web from benzoic acid solution with higher concentration. As we know, benzoic acid with higher concentration may dissolve or etch the surface of the fibers; this may consequently lead to the deterioration of the treated web strength.

The elongation at break decreased after the four treatments, compared to the original sample. For the last one, i.e., the Experiment-2 treated sample, the elongation decreased greatly with the increase in treating severity, owing to the fiber splitting in the web and web shrinkage. However, the decrease in elongation was not too great to be acceptable.

Bending stiffness decreased after the four treatments, compared to the original sample, due to the fiber splitting in the treated webs. After fiber splitting, fibers became finer and softer; the interaction among the fibers became weak, although web structure became more compact than before the treatments.

However, for the first three treated samples, the bending stiffness increased slightly with the increase in treating condition, this might be attributed to the increase in basis weight, thickness caused by the web shrinkage; the last one is still an exception—its stiffness decreased due to the too severe treating condition.

5.4.2.7 The Role that Water Played in BA Treatment for Fiber Splitting

Based on the contrast of the benzoic acid treatments and the control experiments using pure water, it was found that water did play an important role in the fiber splitting of PP/PA6 meltblown web. Split fibers were also observed in the corresponding SEM pictures, although the numbers of the split fibers were not as many as those in the corresponding benzoic acid treated web, because the polar part in benzoic acid may bring more water molecules inside the PA part of the fiber. In addition, water treatment brought the changes in web structure and web properties as well, as mentioned above. Water molecules can enter into the amorphous region of PA part, and weaken the interaction among the PA molecules on the interface between PP and PA6 as what benzoic acid does. Thus, the internal stress on the interface started to increase until to overcome the

adhesion force between the two polymers; the two components began to separate into two parts, partially in general.

5.4.2.8 Changes in the Internal Structure after the Treatments

It is quite possible that the microstructure of the Bico MB fibers changed after treating with benzoic acid solution. The DSC curves were used to examine the structural change and the DSC curves for 50PP/50PA6 sample treated with Experiment 1, as well as the control sample, original sample, were shown together in Figure 5.16 (The heating ratio is 20 °C/min).

There is a small and broad endothermic peak starting at about 50 °C, ending at around 100 °C, on the left parts of the DSC curves of Control-1 sample and Experiment-1 sample. That is possibly the water effect due to the insufficient natural drying time (overnight). In the future, the sample should be dried out in the oven at a temperature below the lowest T_m among the three substances—PA6, PP and benzoic acid. In addition, the DSC experiments should be re-conducted in the process of heating-then-cooling, to reveal more information about the sample structure.

Since the benzoic acid was supposed to enter the PA parts of the 50PP/50PA6 sample, the attention was paid to the change in the T_m of PA6. It can be seen that the height of the endothermic peak increased after treating with water and benzoic acid solution; indicating that, more heat energy was required to heat the samples.

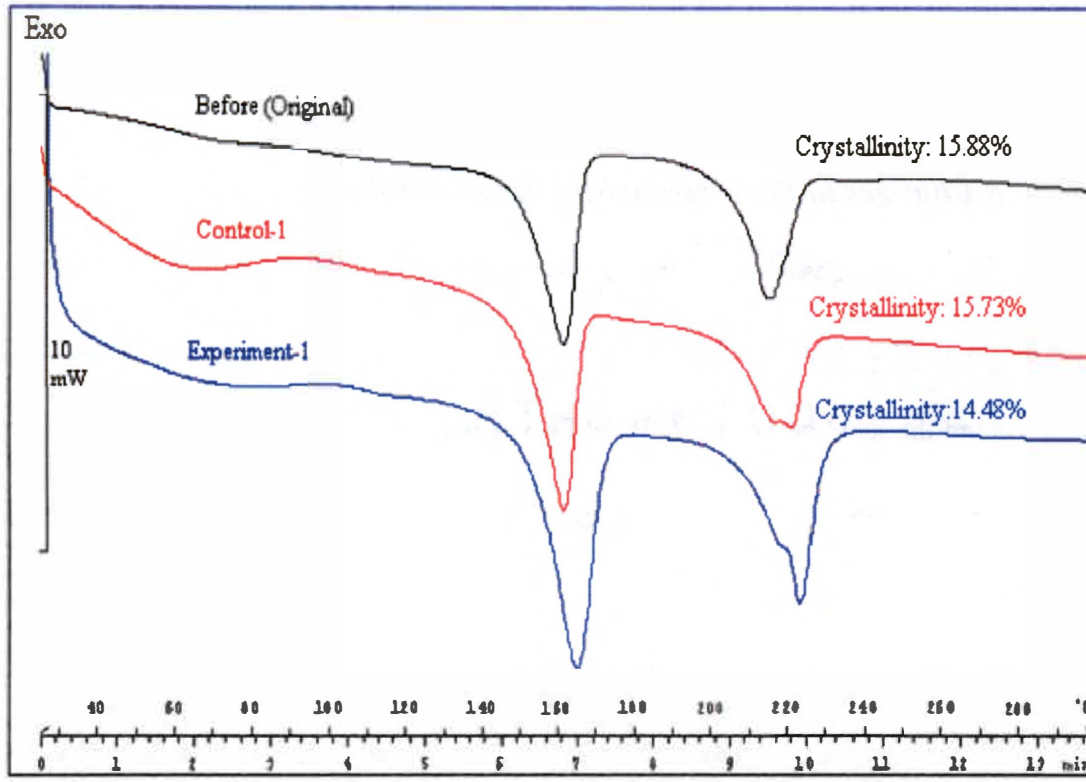

Figure 5.16 DSC curves of the original, Experiment-1 and Control samples.

In addition, the shape of the peak changed from single peak to dual peak after treating with pure water and benzoic acid solution, which is very interesting. Also, the T_m shifted to higher values after water treatment and benzoic acid treatment. The possible explanation is that the crystal form and molecular chain folding shape in the crystalline region of PA6 changed after the two treatments.

Nylon 6 is not centrosymmetric and is characterized by a directionality to the molecule (NH-CO or CO-NH) such that if a molecule is reversed end-for-end, it cannot be superimposed upon itself (Figure 5.17 (right)). The hydrogen-bonded sheets of the α form of nylon 6 involve adjacent molecules which have opposite directionality and are said to be antiparallel.

Arranged in this manner, all the H-bonds can be formed without strain and the packing is the most compact; the molecules are fully extended in this case [76].

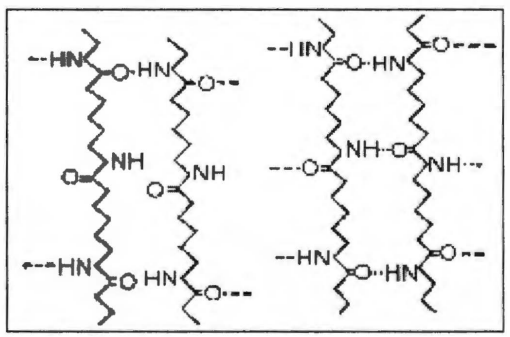

Figure 5.17 (left) γ form of PA6; (right) α form of PA6

If adjacent molecules were of the same direction (parallel), only half of the H-bonds could be formed, and the resultant crystal form is called γ form, as shown in Figure 5.17 (left), which is due to a parallel relative shifting of alternate chains in the H-bonded sheets by about one atom. This leads to a modified unit cell with poorer H-bonding and results in a molecular repeat distance which is shorter than that of the fully extended chains and a molecular packing which is pseudohexagonal. The γ form can be obtained by melt spinning. Since the H-bonds cannot be all effective under any condition, different crystal forms will be formed in different conditions of acting force, heat and moisture [76].

As we know, meltblowing technology is based on the melt-spinning technique. Therefore, during the meltblowing process of PP/PA6 bicomponent nonwoven web, the crystal form of PA6 is possibly dominant with γ form, because the fibers were not subject to enough post-drawing or setting during the production process, therefore, the γ form crystal in PA6 part could be formed easily and the resultant PA6 component has lower melting temperature, 215°C, as shown in Figure 5.16. After treating with water and benzoic acid solution, at temperature around 100°C, the melting temperature increased from the original value of 215°C, to 221°C and then finally to 223°C, based on the DSC results, indicating a gradual transition of the crystal form from the original unstable γ form to the stable α form. An alternative explanation is, the crystalline became perfect

after water treatment and BA treatment; the crystalline changed from small, fine shape into larger, integrated form, the melting temperature shifted to higher temperatures.

It also could be seen from the DSC curves that the crystallinity (by weight) decreased from the original sample (15.88%) to water treated (Control) sample (15.73%) and benzoic acid treated sample (14.48%). This was because more and more γ form crystals were gradually transited into α form crystals during treating with hot water and benzoic acid solution, and the molecular chains in γ form tend to be folded or compact [106], which resulted a higher crystallinity; the molecular chains in α form generally are fully extended [106], and hence a lower crystallinity will be exhibited.

5.5 Summary

Based on the two parts of investigation on fiber splitting in S/S Bico MB webs using BA solution, it was found that BA was an effective agent for fiber splitting in 50PA6/50PET and 50PA6/50PP S/S MB webs.

The achieved highest splitting ratio was approximately 47.5% for 50PET/50PA6 MB web; the corresponding fiber surface area was expected to increase by 30.25% theoretically, while the web strength increased and air permeability decreased after BA treatment, which may favor the application in filtration industry.

Benzoic acid was also an effective agent for fiber splitting in 50PP/50PA6 meltblown nonwoven web. After BA treatment with the condition of Experiment-1 (1:80,

8 g/l, 90-100 °C, 90 min), the initial dyeing ratio increased by 28.61%, while the corresponding control experiment (water treatment only increased initial dyeing ratio by 1.45%. After BA treatment with the condition Experiment-2, initial dyeing ratio increased by 44.08%, while the corresponding control treatment only increased initial dyeing ratio by 8.76%. Meanwhile, web property did not deteriorate noticeably.

Water also played an important role in the fiber splitting process using benzoic acid treatment. The fiber diameter decreased after treating with benzoic acid solution or water, but there was no much difference in diameter among the samples treated with benzoic acid or pure water. Although water may helped fiber splitting in 50PP/50PA6 meltblown web, its effect was not as great as that of benzoic acid, based on the experimental results above. Benzoic acid treatments brought out changes to web structure and properties as well. As a result, the web remained much of strength and elongation; fibers were not damaged obviously during the treatment, and the slight web shrinkage, increase in thickness, basis weight and fiber splitting facilitates the application of the treated web in filtration industry and adsorbent field.

Considering the four main parameters of the benzoic acid treatment, i.e., temperature, concentration, bath ratio and time, the optimal treating conditions were determined (110°C, 8g/l, 1:80 and 120 min), for the fiber splitting in 50PET/50PA6 meltblown nonwoven web.

In addition, DSC curves were used to analyze the structural change after water treatment (control experiment) and benzoic acid treatment. The results revealed that the crystal form and molecular chain packing form of PA6 possibly changed after water treatment and benzoic acid solution treatment at temperatures around 100°C.

The greatest increasing ratio of initial dyeing ratio for both 50PET/50PA6 and 50PA6/50PP Bico MB NW webs could achieve around 44% after BA treatment, indicating both the BA treated MB webs might have the similar increased fiber surface area, and thus they might have the similar adsorption property after BA treatment.

In a word, benzoic acid treatment could achieve a fairly good degree of fiber splitting without significant decrease in web property.

6 CONCLUSION

Finer fibers are increasingly desirable in nonwoven industry in many applications due to the increased specific surface area, and hence the correspondingly increased surface adsorption ability, as well as the improved filtration efficiency. Splitting bicomponent fibers to produce finer fibrous nonwoven webs, has become one of the hot topics in nonwoven industries, and this has been commercially achieved in bicomponent spunbond (SB) nonwoven webs. However, it has been more difficult for fiber splitting in bicomponent meltblown nonwoven webs, due to the lower-strength feature of meltblown fibers and webs; therefore, the known fiber splitting technologies which have been successfully applied to spunbond nonwoven fabrics may not suit for meltblown nonwoven webs.

Therefore, investigation of Bico fiber splitting mechanism and hence finding the proper ways to achieve fiber splitting in S/S Bico MB nonwoven webs is the key issue in this research. Based on the fiber splitting mechanism, incompatible polymer pairs were chosen and appropriate post-treating methods as well as the post-treating agents were selected to facilitate fiber splitting in S/S Bico MB nonwoven webs.

According to the traditional polymer adhesion theories, the diffusion theory and weak boundary theory may be used to study the Bico fiber splitting phenomenon in the

nonwoven webs. The Second Law of Thermodynamics was used to select the incompatible polymer pairs as the two components of Bico MB fibers in this research, which are polyolefin/polyamide, polyamide/polyester, and polyolefin/polyester.

Several post treatments were used to split side-by-side meltblown nonwoven fibers in this research, including hydroentanglement, heat-stretching, NaOH and benzoic acid treatment. In each post treatment method, the degree of fiber splitting was evaluated with SEM or laser-source microscope, and/or surface adsorption through the initial dyeing absorbency ratio of the webs. Fiber diameter, web structure and web properties were examined before and after the fiber-inducing treatment. The orthogonal experimental design method was applied to the experimental design, and the optimal experimental condition was decided based on the testing results and data analysis.

Hydroentanglement post treatment has been applied to S/S Bico MB nonwoven webs with the compositions of PA6/PE, PA6/PP and PA6/PET. Fiber diameter slightly decreased and fiber splitting was observed through the SEM results to a limited extent. The split fibers after hydroentangling exhibited flat-ribbon like cross-sectional configuration; however, pin holes were created during the hydroentangling treatment and they might deteriorate web structure and web property.

Heat-stretching post treatment was applied to S/S Bico MB nonwoven webs with the compositions of PA6/PE and PA6/PP. No split fibers were observed with the

heat-stretched samples; however, obvious changes in web structure and property were found after the post heat treatment. The heat-treated webs exhibited different properties along MD and CD, due to the treated webs being stretched along MD as they got shrunk along the CD. The flexural rigidity in the MD of the heat-stretched webs increased while the flexural rigidity in CD decreased after heat stretching treatment, due to the preferential fiber orientation along MD direction. The meltblown webs gained elasticity in CD after heat-stretching treatment.

The S/S Bico MB nonwoven webs with the compositions of 25PE/75PET, and 50PBT/50PP were treated with hydroxyl sodium at bath ratio of 1/20 and temperature of 100 °C using different concentration of NaOH and different treating time. Fiber splitting began when the treating time achieved 3 min. Some fibers began to dissolve partially with increasing NaOH concentration, and the webs lost strength and weight with longer treating time and higher NaOH concentration. It was found that NaOH treatment did not induce significant fiber splitting in 25PE/75PET and 50PBT/50PP S/S Bico MB webs.

Benzoic acid has been employed to split S/S Bico MB webs with the composition of 50PET/50PA6 and 50PP/50PA6. The 4-factor-3-level orthogonal experimental method was used to obtain the optimal treating conditions for each polymer pair. The factors included concentration, bath ratio, temperature and time; the levels might change with the different polymer pairs that were used.

The fiber diameter decreased due to fiber splitting, and the web shrank to some extent after benzoic acid treatment. Fiber splitting ratio was about 40% (for 50PA/PET S/S Bico MB web) and the surface adsorption was increased after the post treatment using benzoic acid. The crystallinity of the nylon 6 part of the 50PP/50PA6 MB fibers changed after benzoic acid treatment and water treatment, indicating the change in microstructure of the PA6 component. The crystal form of PA6 polymer possibly changed from unstable γ-form to stable α-form, during the post treatment at temperatures higher than the glass transition point of PA6. However, the web properties did not deteriorate significantly after treating with benzoic acid.

It was found that water played a role in splitting S/S Bico MB fibers through post treatment in aqueous medium, because water could diffuse into the amorphous region of hydrophilic polymer, such as nylon 6. The swelling of the hydrophilic part of the two components would result in the occurrence and build-up of internal stress at the interface between the two components, and the two components would separate eventually when the internal stress overcomes the interfacial strength on the interface between the two components. The reason for that benzoic acid could facilitate fiber splitting in Bico MB nonwoven webs was that the polar part in benzoic acid could bring about more water molecules into the amorphous region of nylon 6 polymer or PET polymer, and PA6/PET fiber, PA6/PP(PE) fiber or PP(PE)/PET(PBT) fiber might split

along the interface between the two components, due to increasingly grow-up and accumulation of internal stress on the interface, which was resulted from swelling of the hydrophilic polymer (PA6 or PET).

BA method could be an efficient way to split the S/S Bico MB fibers, compared to other three methods used in this research. The achieved fiber splitting ratio ranged from 28% to 47.5%, and the treated webs did not deteriorate in tensile property, while the barrier property increased after the post treatment with benzoic acid. Specific surface area of the BA treated fibers of both 50PA6/50PET and 50PA6/50PP S/S Bico MB webs might be increased by about 44%, compared to the untreated samples, which would favor the applications in adsorption, absorbency and filtration fields.

7 FUTURE WORK

Based on the diffusion theory of polymer adhesion theories, reduced contact time will facilitate subsequent Bico fiber splitting. Currently, the distance between die spinneret and cohanger of Reicofil® (Reifenhäuser, Gamany) Bico line at TANDEC is too long and not beneficial for S/S MB fiber splitting.

Machine modification is suggested to perform in the near future to facilitate fiber splitting by minimizing the contact time of the two components during the meltblowing process. The schematic of machine modification of the Bico line at TANDEC, UTK is shown in Figure 7.1.

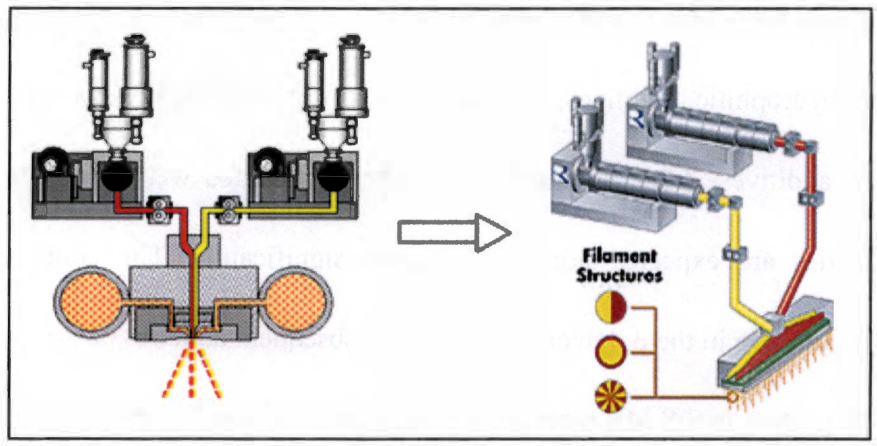

Figure 7.1 Machine modification at TANDEC, UTK in the future (Courtesy of Reifenhaüser, Germany)

In addition, hydrophilic/lubricant additive etc., can be meltblown together with one of the two polymers, therefore a weak boundary layer can be formed at the interface of the two components, which will promote the fiber splitting in the subsequent process of aqueous treatment. If the hydrophilic additive is added to the hydrophilic part of the two components, e.g., the PA part of Bico PP/PA fiber, then the incompatibility between the two components will be increased; the possibility of separation of the two components is hence increased too.

The 50PP/50PA6 S/S Bico MB webs with the PA6 polymer containing hydrophilic additives are going to be produced on the Reicofil® Bico MB line (from Reifenhaüser, Germany) at TANDEC, UTK, and the subsequent post treatments will be applied to the samples, including hydroentanglement, hot water treatment and benzoic acid treatment etc. More split fibers could be expected in the post-treated webs containing hydrophilic additives, compared to the post-treated webs containing no hydrophilic additives. After fiber splitting in the post-treated webs, web structure and web properties are expected not to deteriorate significantly. The combined use of hydrophilic additive in the polymer resin and the subsequent aqueous post-treatment may make fiber splitting in S/S MB nonwoven webs commercialized in the future.

The hydrophilicity and the degree of fiber splitting need to be examined after application of the hydrophilic additives and fiber splitting treatment. For the

measurement of splitting ratio of meltblown fibers, especially the meltblown fibers treated with chemicals for fiber splitting, the fibers may become too weak to be cut through embedding in wax, or using liquid nitrogen. However, other methods can be used to cut the specimen for the observation of fiber cross-sections, such as dyeing method, based on different absorbing ability to the dyestuff owing to the different structure and properties of the two components in the bicomponent meltblown fiber.

For the future research, more efficient post-treating chemicals should be selected to promote fiber splitting in S/S Bico MB NW webs. For example, to split fibers in PA6/PP or PA6/PET MB webs, the solvents such as formic acid (δ = 13.5 $(cal/cm^3)^{1/2}$), and ethanol (δ = 12.7 $(cal/cm^3)^{1/2}$), etc. may be considered as the post-treating agents, to swell the PA6 parts (δ = 13.0 $(cal/cm^3)^{1/2}$) in the Bico fibers, to achieve fiber splitting to a higher degree.

In addition, other technologies may be considered to split Bico MB fibers, such as molecular vibration method and lubricant additive method; also, one of the two components can contain branched side-group, so that the two components cannot well interdiffuse into each other, i.e., the two polymers do not match each other, they will tend to separate in the post treatment process, and hence fiber splitting will be easier to achieve in S/S MB nonwoven webs.

LIST OF REFERENCES

1. Holiday, T., *What are Nonwovens - Again?* Nonwoven Industry. **March**(1989): p. 31.

2. Charles B. Hassenboehler, J. and L.C. Wadsworth, *Electrically charged consolidated non-woven webs*. 1996, US Patent No. 5,486,411: USA.

3. Charles B. Hassenboehler, J. and L.C. Wadsworth, *Post treatment of nonwoven webs*. 1996, US Patent No. 5,244,482: USA.

4. Charles B. Hassenboehler, J. and L.C. Wadsworth, *Post-treatment of laminated nonwoven cellulosic fiber webs*. 1997, US Patent No. 5,599,366: USA.

5. Hassenboehler, C. *Technology for Stretchable Non-Elastic Nonwovens*. in *10th Annual International TANDEC Nonwovens Conference*. 2000. Knoxville, TN, USA.

6. Hassenboehler, C. *High Stretch Nonwoven Made from Your Hand Sample*. in *12th Annual International TANDEC Nonwovens Conference*. 2002. Knoxville, TN, USA.

7. Wadsworth, L.C. and J. Charles B. Hassenboehler, *Stretchable fabric technology options*. Nonwovens World. **Spring**(1994): p. 49.

8. Liu, Y., C.Q. Sun, and D. Zhang. *Changes in structure and properties of bicomponent meltblown nonwoven fabrics after hydroentanglement*. in *12th Annual International TANDEC Nonwoven Conference*. 2002. Knoxville, TN,

USA.

9. Liu, Y., D. Zhang, and C.Q. Sun. *Influence of heat-stretching treatment on the structure and properties of bico MB nonwoven webs*. in *13th Annual International TANDEC Nonwoven Conference*. 2003. Knoxville, TN, USA.

10. Liu, Y., D. Zhang, and C.Q. Sun. *Changes in Structure and Properties of Bicomponent Meltblown Nonwoven Fabrics after Post Treatment for Fiber Splitting*. in *13th Annual International TANDEC Nonwoven Conference*. 2003. Knoxville, TN, USA.

11. Liu, Y., D. Zhang, and C.Q. Sun. *Potential Possibilities of Splitting Bico MB Fibers - A Review*. in *Procedings of 13th Annual TANDEC International Nonwoven Conference Proceedings*. 2003. Knoxville, TN, USA.

12. Sun, C., D. Zhang, and Y. Liu. *Bi-component Fibers Meltblown Nonwovens and Potential Fiber Splitting*. in *Proceedings of TTSNA Conference*. 2004.

13. Sun, C.Q. and D. Zhang, *Bi-component Fiber Meltblown Nonwovens and Its Potential Applications*. Book of Papers, Since'01. 2001, Shanghai, China.

14. Sun, C.Q., D. Zhang, and Y. Liu, *Bicomponent Meltblown Nonwovens and Fiber Splitting*. Accepted by Journal of Industrial Textiles, April, 2004.

15. Sun, C.Q., D. Zhang, and Y. Liu, *Preliminary Study on Fiber Splitting of Bicomponent Meltblown Fibers fibers*. Accepted by Applied Polymer Science,

April, 2004.

16. Sun, C.Q., D. Zhang, and Y. Liu, *Preliminary Study on Fiber Splitting of Bicomponent Meltblown Fibers*. in *INTC 2003*. 2003. Baltimore, Maryland, USA.

17. Zhang, D., C. Sun, and Y. Liu. *Processing development and characterization of polyester-, polyolefin- and polyamide- based bicomponent Meltblown nonwovens*. in *Joint INDA-TAPPI Conference*. 2002. Atlanta, GA, USA.

18. Zhang, D., C. Sun, and L. Wadsworth. *Processing and Characterization of Mono- and Bi-component Fiber Meltblown Nonwovens*. in *9th International TANDEC Nonwoven Conference*. 1999. Knoxville, TN, USA.

19. Zhang, D., C. Sun, and L.C. Wadsworth, *Modeling of Mono- and Bi- Component Fiber Meltblown Process Using Surface Response Methodology*. Textile Research Journal, 2001. **71**(4): p. 301-308.

20. Zhang, D. and C.Q. Sun, *Development and Characterization of PTT-based Mono and Bi-component Meltblown Nonwovens*. Applied Polymer Science, 2002. **83**: p. 1280-1287.

21. Zhang, D., C.Q. Sun, and Y. Liu, *Influence of Heat-Stretching Treatment on the Structure And Properties of Bico MB Nonwoven Webs*. International Nonwovens Journal, 2004. **13**(1): p. 42.

22. Zhang, D., C.Q. Sun, and H. Song. *An Investigation of Fiber Splitting of*

Bicomponent Meltblown Microfiber Nonwovens by Water Treatment. in *INTC 2003*. 2003. Baltimore, Maryland, USA.

23. Bhat, G.S. *Bhat, Gajanan S.* in *PLACE Conference*. 2002. Boston, MA, USA.

24. Bhat, G.S., P.K. Jangala, and J.E. Spruiell, *Thermal bonding of polypropylene nonwovens: Effect of bonding variables on the structure and properties of the fabrics.* Journal of Applied Polymer Science, 2004. **92**(6): p. 3593-3600.

25. Bhat, G.S., P.K. Jangala, and J.E. Spruiell. *Effect of bonding variables in thermal bonding of polypropylene nonwovens*. in *Joint INDA-TAPPI Conference*. 2002. Atlanta, GA, United States.

26. Bhat, G.S. and H. Rong. *Biodegradable/compostable nonwovens form cotton-based compositions*. in *INTC 2003, International Nonwovens Technical Conference*. 2003. Baltimore, MD, United States.

27. Rong, H. and G.S. Bhat, *Binder fiber distribution and tensile properties of thermally point bonded cotton-based nonwovens.* Journal of Applied Polymer Science, 2004. **91**(5): p. 3148-3155.

28. Rong, H.M. and G. Bhat, *Preparation and Properties of Cotton-Eastar Nonwovens*. International Nonwovens Journal, 2003. **12**(2): p. 53-57.

29. Bresee, R.R. and T.S. Daniluk, *Characterizing Nonwoven Web Structure Using Image Analysis Technique, Part III: Web Uniformity Analysis.* INDA Journal of

Nonwovens Research, 1993. **5**(3): p. 28-38.

30. Bresee, R.R. and T.S. Daniluk, *Characterizing nonwoven web structure using image analysis techniques.* Tappi Journal, 1997. **80**(7): p. 133-138.

31. Bresee, R.R. and U.A. Qureshi, *Influence of Processing Conditions On Melt Blown Web Structure: Part 1. DCD.* International Nonwovens Journal, 2004. **13**(1): p. 49.

32. Huang, X. and R.R. Bresee, *Professional Image Analysis Software to Characterize Web tructure (WebPro User's Guide).* 1996.

33. Bresee, R.R. and W.-C. Ko, *Fiber formation during melt blowing.* International Nonwovens Journal, 2003. **12**(2): p. 21-28.

34. Zhao, R. and L.C. Wadsworth, *Study of polypropylene/poly(ethylene terephthalate) bicomponent melt-blowing process: The fiber temperature and elongational viscosity profiles of the spinline.* Journal of Applied Polymer Science, 2003. **89**(4): p. 1145-1150.

35. Zhao, R., et al., *Properties of PP/PET bicomponent melt blown microfiber nonwovens after heat-treatment.* Polymer International, 2003. **52**(1): p. 133-137.

36. Malkan, S.R., *Dissertation: Process-structure-property relationships in different molecular weight polypropylene melt blown webs.* 1990, The University of Tennessee: Knoxville.

37. Vargas, E., *Meltblown Technology Today*. 1989, San Francisco, CA: Miller Freeman Publications, Inc.

38. Marmon, S.E., B.P. Samuels, and E.S. Wazeerud-Din, *Entangled nonwoven fabrics and methods for forming the same from splittable multicomponent fibers*. 1998, Kimberly-Clark, USA: WO 9823804.

39. Buntin, R. and D.T. Lohkamp, *Melt blowing. A One Step process for New Nonwovens Products*. TAPPI, 1970. **56**(4): p. 74.

40. Haynes, B.D., B.D. Arnold, and J.M. Duellman, *Nonwoven composites comprising splittable thermoplastic bicomponent fibers or particles for absorbents with good durability and absorption properties and manufacture thereof*. 2000, Kimberly-Clark, USA: WO 2000029657.

41. Nishijima, M., *Process for producing nonwoven fabrics of ultrafine polyolefin fibers*. 1998, Chisso Corp., Japan: US 5,965,084.

42. Yu, J.-P., et al., *Splittable multicomponent elastomeric fibers*. 1999, Hills, Inc., USA: US99/23267.

43. Dugan, J.S., *Splittable multicomponent polyolefin fibers*. 2000, EP 1076121 A1: Fiber Innovation Technology, Inc.

44. Pike, R.D., *Superfine Microfiber Nonwoven Web*. 1996, Kimberly-Clark, USA: US96/18384.

45. Dugan, J.S., *Processing and applications of mechanically splittable multicomponent polyacrylonitrile/polyolefin fibers*. 1999, US 6,444,312: Fiber Innovation Technology, Inc.

46. Nagaoka, K., A. Matsunaga, and N. Yoshida, *Staple fiber nonwoven fabric and its production*. 2002, Japan: US 2002/0006502 A1.

47. Usui, Y. and H. Okaya, *Thermally splittable conjugated fibers and fiber aggregates*. 2001, Daiwa Spinning Co., Ltd., Japan: JP 2001279530 A2.

48. Bouchillon, R.E. *Bicomponent Fibers Worldwide*. in *INDA-TEC 92*. 1992. Cary, NC: April 7-10, P9-16.

49. Wang, Y.Z., *Application of Polymer Rheology in Melt Blowing Process and Online Rheological Sensor*, in *Chemical Engineering*. 2004, The University of Tennessee: Knoxville. p. 21.

50. Smith, J.A., *Microfibers: Functional Beauty*. 2004: http://ohioline.osu.edu/hyg-fact/5000/5546.html.

51. Works, T.H.R., *What is Microfiber, and what makes Wally Wipes so great...and all the tech stuff*. 2004: http://www.hotrodworks.net/wallywagsite/microfiber.html.

52. Bureau, A.F.M.A.F.E., *Microfiber*. 2004: http://www.fibersource.com/f-tutor/micro.htm.

53. Morton, W.E. and J.W.S. Hearle, *Physical Properties of Textile Fibers*. 2 ed. 1975,

New York: John Wiley & Sons. 156.

54. Wooliever, P., *Using Flat Mopping Systems in Hospitals*. 2004.

55. Unknown, *Microfiber*. 2004: http://www.fibersource.com/f-tutor/micro.htm.

56. Mansfield, R.G., *Covering Nonwovens*, http://www.textileworld.com/News.htm, Editor. 2001.

57. Pourdeyhimi, B., *New Directions in Nonwovens Technologies*. 2003: http://www.tx.ncsu edu/ncrc/presentations/directions_in_nonwovens_technology.pdf.

58. Kinloch, A.J. and J.G. Williams, *Crack blunting mechanisms in polymers*. Journal of Materials Science, 1980. **15**(4): p. 2141.

59. MITTAL, K.L., *The role of the interface in adhesion phenomena*. Polymer Engineering Science, 1977. **17**(7): p. 467.

60. Wu, S., *Polymer Interface and Adhesion*. 1982, New York and Basel: Marcel Dekker, INC.

61. SpecialChem, *Adhesion Guide*. 2004: www.specialchem4adhesives.com.

62. Voyutskii, S.S., *Autohesion and Adhesion of High Polymers*. Polymer Reviews. Vol. 4. 1963: Wiley, New York. 272.

63. Voyutskii, S.S. and V.L. Vakula, *The role of diffusion phenomena in polymer-to-polymer adhesion*. Journal of Applied Polymer Science, 1963. **7**: p.

475-91.

64. Voyutskii, S.S., *The diffusion theory of adhesion.* Rubber ChemIcal Technololy, 1960. **33**: p. 748.

65. Vasenin, R.M., *Adhesion of high polymers: I. The phenomenon of adhesion. II. Predicting adhesion.* Adhesives Age, 1965. **8**(5): p. 18-25.

66. Vasenin, R.M., *Adhesion pressure in the diffusion theory of adhesion.* Polymer Science USSR, 1961. **3**: p. 608.

67. Vasenin, R.M., *Adhesion of high polymers: I. The phenomenon of adhesion.* Adhesives Age, 1965. **8**(5): p. 18.

68. Vasenin, R.M., *Adhesion of high polymers: II. Predicting adhesion.* Adhesives Age, 1965. **8**(6): p. 30.

69. Wool, R.P., *Welding, Tack and Green Strength of Polymers*. Fundamentals of Adhesion, ed. L.H. Lee. 1990, New York: Plenum Press.

70. Jud, K., H.H. Kausch, and J.G. Williams, *Fracture Mechanics Studies of Crack Healing and Welding of Polymers.* Journal of Materials Science, 1981. **16**: p. 204.

71. Wool, R.P., *Welding of Polymer Interfaces.* Polymer Engieering Science, 1989. **29**: p. 1340.

72. Voyutskii, S.S. and B.V. Shtarkh, *The effect of molecular weight, molecular shape, and the presence of polar groups on autoadhesion of high polymers.* Rubber

Chemical Technology, 1957. **30**: p. 548.

73. Voyutskii, S.S., A.I. Shapovalova, and A.P. Pisarenko, *Adhesion of high polymers. III. Effect of the size, shape, and polarity of high-polymer molecules on the adhesion to cellophane.* Rubber ChemIcal Technology, 1957. **30**: p. 544.

74. Cassidy, P.E. and J.M.L. Johnson, Carl E., *Relation of glass transition temperature to adhesive strength.* Journal of Adhesion, 1972. **4**(3): p. 183.

75. Gardner, D.J., *Theories of Adhesion*, in *pdf.* 2004: http://www.umaine.edu/adhesion/gardner/5402002/theories%20of%20adhesion.

76. Zhao, H., et al., *Polymer Physics.* 1995, Beijing, China: China Textile Press. 49.

77. Ansarifar, M.A., K.N.G. Fuller, and G.J. Lake, *Adhesion of Unvulcanized Elastomers.* International Journal of Adhesion and Adhesives, 1993. **13**(2): p. 105.

78. Li, N. and X. Gao, *Relationship between Structure and Properties of Superfine Polyester/Polyamide Composite Fibers.* Synthetic Fibers, 1999. **7**: p. 8.

79. Bikerman, J.J., *The Science of Adhesive Joints.* 2 ed. 1968, New York: Academic. 349.

80. Bikerman, J.J., *The fundamentals of tackiness and adhesion.* Journal of Colloid Science, 1947. **2**: p. 163.

81. Bikerman, J.J., ed. *Recent Advances in Adhesion.* ed. L.H. Lee. 1973, Gordon &

Breach: New York.

82. Brewis, D.M. and I. Mathieson, *Adhesion and Bonding to Polyolefins (Rapra Review Report 143)*. International Journal of Adhesion and Adhesives, 2003. **23**(4): p. 339.

83. Dugan, J., *Synthetic split microfiber technology for filtration*. 2002: http://www.fitfibers.com/files/Microfibers%20for%20Filtration.doc.

84. Song, H., *Fiber Splitting of Bicomponent Meltblown Microfiber Nonwovens by Chemical and Water Treatment*, in *Textile Science and Engineering*. 2002, the University of Tennessee: Knoxville.

85. Akita, T., T. Ishikawa, and H. Sakakura, *Manufacture of ultrafine-denier polyester fibers*. 1994: Japan. p. 7.

86. Matsumoto, K., et al., *Multilobal polyester split fibers and their multifilament blend fibers, lightweight fabrics, and manufacture*. 1998: Japan. p. 9.

87. Ogawa, K., et al., *False-twisted splittable composite fibers for dry handle and silklike scroop and their manufacture*. 1998: Japan. p. 8.

88. Terao, H. and T. Nonaka, *Nubuck-like suedelike polyester fabrics with good softness and handle and manufacture thereof*. 1999: Japan. p. 6.

89. Koho, K.T., M. Kato, and T. Yamazaki, *Leather-like sheets with improved durability and their manufacture with less use of organic solvents*. 2002: Japan. p.

18.

90. White, C.F., *Hydroentanglement Technology Applied to Wet Formed and Other Precursor Webs.* TAPPI Journal, 1990. **73**(6): p. 187.

91. Drelich, A. *A Simplified Classification of Nonwoven Fabrics*. in *6th Annual TANDEC Internatioanl Conference*. 1988. Knoxville.

92. Heeler, J. *Hydroentanglement of short fibers*. in *11th Annual TANDEC International Nonwoven Conference*. 2001. Knoxville.

93. Watzl, A. *Spunbondin and Sponlacing: Two Leading Technologies Coming Together*. in *INTC 2000*. 2000. Dallas.

94. Vaidya, N., *Composites from Hydroentangled Webs*. 2002.

95. Ellison, M., *Improved Fiber Hydroentanglement Using Pulsed Elliptical Jets*. 2001: http://www.ntcresearch.org/pdf-rpts/Bref0601/F98-C04.pdf.

96. Nonwoven.co.uk. *High pressure hydroentanglement of cellulosic fibers*. in *EDANA Index 93 Conference*. 1993. Geneva: http://www.nonwoven.co.uk/reports/HPHE93.htm.

97. Kondo, R., S. Shoda, and H. Yokohama, *Manufacture of fine synthetic fibers by rapid process*. 1987: Japan.

98. Nakano, J., *Manufacture of nonwoven textiles*. 1996: Japan. p. 5.

99. Gu, Q., *Chapter 5*, in *Tables Used for Chemistry*. 1979, Jiangsu Science Press:

Nanjing. p. 26.

100. Lan, L., *Polymer Physics*. 1983, Xian: The Press of Northweat Polytechnic Uiversity. 235.

101. International-Adsorption-Society, *Adsorption Phenomena*, in *http://ias.vub.ac.be/General/Adsorption.html.* 2004: Belgium.

102. Ferrante, D., *Sorption Processes*, in *http://www.cee.vt.edu/program_areas/environmental/teach/gwprimer/sorp/sorp.html.* 1996: Virginia Tech.

103. United-Manufacturing-International, *1. Adsorption Properties:*, in *http://www.activatedcarbon.com/pdf%20forms/PrintQC.pdf.* 2004: Pleasanton, CA.

104. Piquero, T., Y. Pierre, and P. David, *Effects of carbon nanotubes treatments on their hydrogen adsorption capacity*, in *http://www.waterstof.org/20030725EHECP2-199.pdf.* 2004: France.

105. Skoog, D.A., *Principles of Instrumental Analysis*. Chapter 13: An Introduction to Ultraviolet/Visible Molecular Absorption Spectrometry, ed. 3. 1985, New York, NY: CBS College Publishing. 300.

106. Gao, X. and D. Wu, *Physics of Fiber Applications*. 2000, Beijing: China Textile Press.

VITA

Yanbo Liu was born in Jilin Province, People's Republic of China (P. R. China.) on October 17, 1965, and grew up there. She went to Tianjin Polytechnic University, Tianjin, P. R. China, in September, 1982 and got her Bachelor's Degree from the Department of Textile Engineering of this university in July, 1986.

After graduation with her Bachelor's Degree in textile engineering, Yanbo worked as a textile engineer for two years in Jilin City Wool Spinning and Weaving Factory, Jilin City, Jilin Province, P. R. China.

In September, 1988, Yanbo went back to Tianjin Polytechnic University for her graduate study, and acquired her Master's Degree in the Department of Textile and Engineering of this university in 1990.

After graduation with her Master's Degree, Yanbo worked at the College of Textile Engineering in Tianjin Polytechnic University as an assistant professor for 9 years. Then she went to the US and worked in the College of Textile Engineering, North Carolina State University, as a visiting scholar, sponsored by China government.

Yanbo transferred to the University of Tennessee at Knoxville (UTK) in January, 2001 and worked in TANDEC, for half a year, as a visiting scholar. She entered the graduate school in August 2001 and studied in the Department of Materials Science and Engineering, College of Engineering, UTK, for her Ph. D degree since then.

1624 4866 31
11/03/04 MAB